

**THE SWEET MODIFICATION OF NOD2, AN INNATE IMMUNE  
RECEPTOR INVOLVED IN CROHN'S DISEASE**

by

Ching-Wen Hou

A dissertation submitted to the Faculty of the University of Delaware in  
partial fulfillment of the requirements for the degree of Doctor of  
Philosophy in Chemistry and Biochemistry

Summer 2017

© 2017 Ching-Wen Hou  
All Rights Reserved

**THE SWEET MODIFICATION OF NOD2, AN INNATE IMMUNE  
RECEPTOR INVOLVED IN CROHN'S DISEASE**

by

Ching-Wen Hou

Approved:

---

Murray V. Johnston, Ph.D.  
Chair of the Department of Chemistry and Biochemistry

Approved:

---

George H. Watson, Ph.D.  
Dean of the College of Arts and Sciences

Approved:

---

Ann L. Ardis, Ph.D.  
Senior Vice Provost for Graduate and Professional Education

I certify that I have read this dissertation and that in my opinion it meets the academic and professional standard required by the University as a dissertation for the degree of Doctor of Philosophy.

Signed:

---

Catherine Leimkuhler Grimes, Ph.D.  
Professor in charge of dissertation

I certify that I have read this dissertation and that in my opinion it meets the academic and professional standard required by the University as a dissertation for the degree of Doctor of Philosophy.

Signed:

---

Brian Bahnson, Ph.D.  
Member of dissertation committee

I certify that I have read this dissertation and that in my opinion it meets the academic and professional standard required by the University as a dissertation for the degree of Doctor of Philosophy.

Signed:

---

John Koh, Ph.D.  
Member of dissertation committee

I certify that I have read this dissertation and that in my opinion it meets the academic and professional standard required by the University as a dissertation for the degree of Doctor of Philosophy.

Signed:

---

April Kloxin, Ph.D.  
Member of dissertation committee

## **ACKNOWLEDGMENTS**

I would like to express my sincere appreciation to my advisor Dr. Catherine Leimkuhler Grimes for giving me the opportunity to join this lab and collaborate on several projects. It was an honor to work with her. She not only fostered my development as an independent scientist but also raised my confidence level. She has been an inspiration as a person and as an advisor. Without her guidance and assistance, this dissertation would not have been possible.

I would like to thank my collaborator, Dr. Natasha E. Zachara from John Hopkins University, and my committee members, Dr. Brian Bahnson, Dr. John T. Koh, and Dr. April Kloxin for facilitating my dissertation and providing valuable comments and thoughtful insights on this project.

I also thank to Dr. Deni S. Galileo from the department of Biological Sciences for providing a key to access the dark room. Dr. John T. Koh for providing the tissue culture facility. In addition, thank to every staff from the department of Chemistry and Biochemistry. Special thanks to Susan Cheadle for all her assistance with my questions. Gary Lance and Karen Black from the department of Biological Sciences for helping me order everything with Fisher.

I am also thankful to each of my lab mates with whom I have had worked on different projects. Vishnu Mohanan for his mentorship and valuable suggestions, which is a big motivation that helps me to go through the beginning of my Ph.D. Yiben Wang for his kindness and friendship. He always helped me when I had a question, not only about research but also my personal life. Mackenzie Lauro for

helping me to get through the period of job searching and rough times. She always encouraged me in my life. I want to thank Lauren Genova for being the first person I met at Grime's lab. She is one of the sweetest people I have met, and we shared a lot of precious memories at UD. Hai Liang for being a very careful person in science which impressed me. I learned a lot of skills from him. I thank Kristen DeMeester for her smile and help. I am glad that we managed to work efficiently in a team with Hai to achieve our labeling work. Wally Drake for being a second reader for my dissertation and continuing my project. He is one of the smartest people I know. Elizabeth D'Ambrosio for being the kindest person. She always offers her help to me. Siavash Mashayekh for helping me to synthesize a compound and order anything I wanted. Junhui (Andrea) Zhou for being a model to me as an independent woman. Little Hannah Wastyk for being a good listener. She always encourages me to achieve my dream and goals. Klare Lazor and Ashley Brown for being patient and quick learners of experiments. Jenna Deibert for being a sweet person. Her words always can make me smile. Amy Schaefer and Jim Melnyk for being great team players in the MDP project. Additional thanks go to Yu Liu, Jason Burch, Matt Jensen, Ophelia Ukaegbu, Doug Kenny, Kathryn Hopkins, Zach Jones, Matt Hurlock and Leena Doolabh for being part of my lab life.

I thank all my friends I have made during my Ph.D. at UD. Special thanks to Yu-Ting (Sarah) Hung for being the honest person to me even sometimes too harsh. I appreciated that all the important moments we had at UD. I do not know how I would have survived here without her. Chia-Hung Tsai for being a coffee partner during my hard time. You are one of the most positive people I have met. I still remember your fox dancing. Maple Wang, Jing Zhang, Pan Teng for their friendship. I will never

forget the many girls nights and trips that we spent together. My thanks also go out to the other friends I met at UD: Peijun Tu, Meixi Chen, Yichen Duan, Baxter Abraham, Jing Zhao, Yue Wu, Tiantian Yu, Songnan Zhang, Zhengqi Zhang, Pengcheng Wu, Lan Wang, Xi Lin, Haoyu Wang, Lingxi Jiang, Ethan Zhang, Sam Kung, and Jia-Ming Lin for all the great time we spent together. I would like to thank my friends who came to USA as well to pursue a Ph.D. Special thanks to KC Chang for being my friend since we were in Taiwan. He is one of the hardest working people I know, and I am so lucky to have him as my close friend. Yu-Fan Chen for offering a place to me always when I was up in NJ. I miss the time we were together in NJ and NY with KC Chang and Tai-Yuan Yu.

I would also like to thank my fiancé, Jesus Nieto. You are an unexpected part of my life. Thank you for letting me be myself and always being there for me. You have made my life so beautiful. We have had adventures everywhere we go. I am so happy for the next adventures we are looking ahead.

Lastly, I thank my parents and my brother. They are my heart and inspiration. Even since I can remember they have told me I could do whatever I want. They always support every decision I made including came to the USA to pursue my Ph.D. I would not be here without their support, and I extend to them my deepest gratitude and love.

**I dedicate this dissertation to my parents Mr. Jun-Ming Hou  
and Mrs. Lu-Lan Wang**

**This thesis is largely adapted from the following publications:**

Hou C-W, Mohanan V, Zachara NE, Grimes CL. Identification and biological consequences of the *O*-GlcNAc modification of the human innate immune receptor, Nod2. *Glycobiology*. 2016;26(1):13-18. doi:10.1093/glycob/cwv076.

Hou C-W, Lauro ML, Grimes CL. Redefining the defensive line: critical components of the innate immune system. *ACS Infect. Dis.*, 2016; 2 (11): 746–748. doi: 10.1021/acsinfecdis.6b00174

Liang H, DeMeester KE, Hou C-W, Parent MA, Caplan JL, Grimes CL. Metabolic labelling of the carbohydrate core in bacterial peptidoglycan and its applications. *Nature Communications*. 2017; 8:15015. doi:10.1038/ncomms15015



## TABLE OF CONTENTS

LIST OF TABLES .....	xiii
LIST OF FIGURES .....	xiv
LIST OF ABBREVIATIONS .....	xxii
ABSTRACT .....	xxv

### Chapter

1	INTRODUCTION .....	1
1.1	Innate Immune System .....	1
1.2	Nod2 Signaling.....	4
1.3	Nod2 in Crohn's Disease .....	6
1.4	Post-translational Modification of Nod2 Signaling Cascade .....	7
1.5	<i>O</i> -GlcNAcylation .....	8
1.6	<i>O</i> -GlcNAc Transferase (OGT) .....	9
1.7	<i>O</i> -GlcNAcase (OGA) .....	11
1.8	Discussion.....	12
	REFERENCES .....	14
2	<i>O</i> -GLCNACYLATION OF WILD TYPE NOD2 AND ITS FUNCTION.....	23
2.1	Introduction .....	23
2.2	Materials and Method.....	24
2.2.1	Cell Culture .....	24
2.2.2	Antibodies and Materials .....	24
2.2.3	Co-Immunoprecipitation .....	25
2.2.4	Western Blot.....	25
2.2.5	Half-life Determination .....	26
2.2.6	Isolation of Polysome .....	27
2.2.7	Precipitation of Peptidyl-tRNA by CTAB .....	27
2.3	Results .....	28
2.3.1	<i>O</i> -GlcNAcylation of Nod2 .....	28
2.3.2	<i>O</i> -GlcNAcylation Level Regulate Nod2 Half-life in Cells .....	30

2.3.3	The Possible of Mechanism of Stabilization .....	31
2.4	Discussion.....	32
REFERENCES .....		34
3	INFLAMMATION AND <i>O</i> -GLCNACYLATION.....	37
3.1	Introduction .....	37
3.2	Materials and Methods .....	38
3.2.1	Cell Culture .....	38
3.2.2	Materials .....	38
3.2.3	Luciferase Reporter Assay .....	39
3.3	Results .....	39
3.3.1	Titration of <i>O</i> -GlcNAc Level by Thiamet-G in Cells .....	39
3.3.2	<i>O</i> -GlcNAcylation Regulates NF- $\kappa$ B Signaling .....	40
3.3.3	<i>O</i> -GlcNAcylation Regulates NF- $\kappa$ B Signaling through Nod2, Not through Other Downstream NF- $\kappa$ B Proteins.....	43
3.3.4	<i>O</i> -GlcNAcylation Is Not Increased upon MDP Treatment .....	44
3.4	Discussion.....	47
REFERENCES .....		48
4	<i>O</i> -GLCNACYLATION REGULATES THE STABILITY AND ACTIVITY OF NOD2 VARIANTS .....	52
4.1	Introduction .....	52
4.2	Materials and Methods .....	53
4.2.1	Cell Culture .....	53
4.2.2	Antibodies and Materials.....	53
4.2.3	Vector Construction.....	53
4.2.4	Cell transfection and Lentiviral Transduction .....	54
4.2.5	Cell Transfection and Retroviral Transduction .....	54
4.2.6	Co-Immunoprecipitation .....	55
4.2.7	Western Blot .....	56
4.2.8	Luciferase Reporter Assay .....	56
4.2.9	Half-life Determination .....	57
4.2.10	Cellular Thermal Shift Assay (CETSA).....	57
4.2.11	Site-directed Mutagenesis .....	58

4.3	Results .....	59
4.3.1	Construction of Nod2 Mutants Expressing Stable Cell Lines via Lentiviral System.....	59
4.3.2	<i>O</i> -GlcNAcylation of Nod2 Variants (R702W, G908R, and 1007fs).....	60
4.3.3	Construction of Doxycycline Regulated Nod2 Mutants Expressing Stable Cell Lines.....	61
4.3.4	Doxycycline Regulated Nod2 Mutants Expression.....	62
4.3.5	<i>O</i> -GlcNAcylation Regulated the Stability of Nod2 Variant (R702W).....	63
4.3.6	<i>O</i> -GlcNAcylation Regulated the Activity of Nod2 Variant (R702W).....	64
4.3.7	<i>O</i> -GlcNAcylation Did Not Regulate the Stability of Nod2 Variant (G908R).....	64
4.3.7.1	Cellular Thermal Shift Assay (CETSA).....	65
4.3.8	<i>O</i> -GlcNAcylation Did Not Regulate the Activity of Nod2 Variant (G908R).....	66
4.3.9	The Global <i>O</i> -GlcNAcylation in HEK293T-Nod2-G908R- Myc/Tet-op Cell Line.....	67
4.3.10	Construct a Point Mutation of Residue S933 of Full Length Nod2 .....	68
4.3.11	Create of Nod2 Mutants (S933A) Expressing Stable Cell Lines via Lentiviral System.....	69
4.3.12	<i>O</i> -GlcNAcylation of Nod2 Variants (S933A).....	69
4.3.13	<i>O</i> -GlcNAcylation Rescued the Stability and Activity of Nod2 Variant (1007fs).....	70
4.4	Discussion.....	72
	REFERENCES .....	74
5	NBD DOMAIN IS REQUIRED FOR <i>O</i> -GLCNACYLATION .....	77
5.1	Introduction .....	77
5.2	Materials and Methods .....	78
5.2.1	Cell Culture .....	78
5.2.2	Antibodies and Materials.....	78
5.2.3	Plasmid Construction.....	79
5.2.4	Site-directed Mutagenesis .....	80
5.2.5	Cell Transfection and Lentiviral Transduction.....	80

5.2.6	Protein Purification from HEK293T-Nod2Myc Cells .....	80
5.2.7	Co- Immunoprecipitation .....	81
5.2.8	Western Blot .....	82
5.2.9	Prediction of <i>O</i> -GlcNAc-modified Sites .....	83
5.3	Results .....	83
5.3.1	Purification of Nod2 from HEK293T-Nod2-Myc/K2605 Cells ..	83
5.3.2	Mapping of <i>O</i> -GlcNAc-modified Sites of Nod2 .....	84
5.3.3	Construction of Different Nod2 Domains Expressing Stable Cell Lines via Lentiviral System .....	84
5.3.4	Individual Nod2 Domain Is Not <i>O</i> -GlcNAcylated.....	85
5.3.5	Two Domains Combined of Nod2 Are <i>O</i> -GlcNAcylated .....	86
5.3.6	Prediction of <i>O</i> -GlcNAc- modified Sites Program .....	88
5.3.7	Mutation of T424A of Nod2.....	89
5.3.8	Nod2 Mutant (T424A) Is <i>O</i> -GlcNAcylated .....	90
5.4	Discussion.....	91
REFERENCES .....		93
6	CONCLUTIONS AND FUTURE DIRECTIONS.....	96
REFERENCES .....		99
Appendix		
A	METABOLIC LABELING OF THE CARBOHYDRATE CORE IN BACTERIAL PEPTIDOGLYCAN AND ITS APPLICATION.....	102
B	PERMISSION LETTERS .....	107

## LIST OF TABLES

<b>Table 1.1: Primer DNA sequences used for molecular cloning.....</b>	<b>79</b>
--	-----------

## LIST OF FIGURES

<b>Figure 1.1: Innate immune receptors.</b> These innate immune receptors will recognize unique structure from microorganism and then trigger the appropriate immune response.....	3
<b>Figure 1.2: Structure of Nod1 and Nod2.</b> Nod1 and Nod2 consist of a C-terminal leucine-rich repeat (LRR), a nucleotide binding and oligomerization domain (NOD) and caspase activating and recruiting domains (CARDs).....	4
<b>Figure 1.3: MDP and iE-DAP.</b> (A) MDP consists of <i>N</i> -acetylmuramic acid with a L-Ala-D-isoGln dipeptide chain. It is the ligand from peptidoglycan for Nod2. (B) iE-DAP is a dipeptide, a ligand from peptidoglycan for Nod1. ....	5
<b>Figure 1.4: NF-<math>\kappa</math>B pathway.</b> MDP activates Nod2 dependent NF- $\kappa$ B signaling. It will recruit RIP2 and then translate the signal to turn on NF- $\kappa$ B. stimulation of Nod2 leads to the recruitment of RIP2 which in turn translates the signal to turn on NF- $\kappa$ B.....	6
<b>Figure 1.5: <i>O</i>-GlcNAcylation.</b> The <i>O</i> -GlcNAc transferase (OGT) attaches <i>O</i> -GlcNAc to a protein at serine or threonine residues and <i>O</i> -GlcNAcase (OGA) removes <i>O</i> -GlcNAc from a target protein.....	8
<b>Figure 1.6: Hexosamine biosynthetic pathway (HBP).</b> UDP-GlcNAc is a metabolite of the hexosamine biosynthetic pathway(HBP), one endpoint of which is the modification and regulation of proteins by the <i>O</i> -GlcNAcylation in cells.....	9
<b>Figure 1.7: OGT and OGA.</b> (A) <i>O</i> -GlcNAc transferase (OGT) has three isoform, ncOGT, mOGT, and sOGT. (B) <i>O</i> -GlcNAcase (OGA) contains two isoform, OGA-L and OGA-S. ....	12
<b>Figure 2.1: UDP-GlcNAc.</b> UDP-GlcNAc is used a substrate for (A) the human enzyme, OGT and (B) the bacterial cell wall biosynthetic enzymes. (Reprinted with permission from Hou et. al., Copyright 2017, Glycobiology).....	23

- Figure 2.2: OGT modifies Nod2.** (A) Cell lysates were immunopurified with Myc antibody and blotted with Myc antibody; Control cells do not express Myc-Nod2. Thiamet-G inhibits OGA, elevating *O*-GlcNAcylation. (B) Cell lysates were immunopurified with Nod2 and blotted using CTD110.6. (C) Alternatively, the CTD110.6 was pre-incubated with free GlcNAc (Reprinted with permission from Hou et. al., Copyright 2017, Glycobiology)..... 29
- Figure 2.3: Reverse IP.** Co-IP were performed using 1 µl of anti-OGlcNAc (RL2 or CTD110.6) antibody per 200 µl of lysates (HEK293T/Nod2Myc cells) and probed for Myc using rabbit-Myc antibody (1:1000), anti-RL2 antibody (1:2000) and anti-CTD110.6 (1:1000) (Reprinted with permission from Hou et. al., Copyright 2017, Glycobiology). ..... 30
- Figure 2.4: *O*-GlcNAcylation regulates the half-life of Nod2 in cells.** (A) HEK293T-Nod2Myc/Tet-op cells were incubated with 1 µM Thiamet-G or DMSO for 4 h, prior to cycloheximide treatment (100 µg/ml) at the indicated time intervals. Nod2 was detected by anti-Myc western blotting. (B) Relative amount of Nod2 Myc to actin was plotted from three independent experiments as the means ± S.D. (C) The plot of the logarithm of Nod2 versus time for a first-order reaction. (Reprinted with permission from Hou et. al., Copyright 2017, Glycobiology). ..... 31
- Figure 2.5: Cotranslational *O*-GlcNAcylation of Nod2 in cells.** (A) *O*-GlcNAcylation also can occur during co-translation of proteins. (B) 5S-GlcNAc, OGT inhibitor, inhibits *O*-GlcNAcylation in cells. (C) Isolation of peptidyl-tRNA by CTAB from polysome fractions. (D) Nod2 was detected by anti-Myc western blotting. .... 32
- Figure 3.1: Titration of *O*-GlcNAcylation level in cells.** Western blot studies of HEK293T-Nod2Myc/Tet-op cells incubated with DMSO or different concentration of Thiamet-G for different periods of time. Global *O*-GlcNAc as detected by anti-CTD110.6 (1:1000) (upper) is increased. Actin (1:1000) was used as a loading control (lower)..... 40
- Figure 3.2: NF-κB activation of Nod2-transfected (HEK293T) cells line.** Dual-luciferase assay performed on stable expressed Nod2 (HEK293T-Nod2-Myc/Tet-op) cells in the presence of 100 nM Thiamet-G or DMSO for 4 h. After 4 h, cells were incubated with 20 µM MDP for 5 h, harvested, and tested for luciferase activity. \*  $p < 0.05$  was considered as significant. CMV (empty vector) was used as a control... 41

<b>Figure 3.3: NF-<math>\kappa</math>B activation of stable expressed Nod2 (HEK293T-Nod2-Myc/Tet-op) cells line.</b> Dual- luciferase assay performed on Nod2-transfected cells in the presence of 100 nM Thiamet-G or DMSO for 4 h. After 4 h, cells were incubated with 20 $\mu$ M MDP for 5 h, harvested, and tested for luciferase activity. * $p < 0.05$ was considered as significant. (Reprinted with permission from Hou et. al., Copyright 2017, Glycobiology).....	41
<b>Figure 3.4: NF-<math>\kappa</math>B activation of HCT-116 cells line.</b> Dual-luciferase assay performed on Nod2-transfected cells in the presence of 100 nM Thiamet-G or DMSO for 4 h. After 4 h, cells were incubated with 20 $\mu$ M MDP for 5 h, harvested, and tested for luciferase activity. * $p < 0.05$ was considered as significant. ....	42
<b>Figure 3.5: NF-<math>\kappa</math>B activation of stable expressed Nod2 (HEK293T-Nod2-Myc/Tet-op) cells line.</b> Dual- luciferase assay performed on Nod2-transfected cells in the presence of 200 nM TNF- $\alpha$ or DMSO for 4 h. After 4 h, cells were incubated with 20 $\mu$ M MDP for 5 h, harvested, and tested for luciferase activity. * $p < 0.05$ was considered as significant. (Reprinted with permission from Hou et. al., Copyright 2017, Glycobiology).....	44
<b>Figure 3.6: The cycling of <i>O</i>-GlcNAcylation.</b> The substrate of OGT, UDP-GlcNAc, is produced by hexosamine biosynthetic pathway (HBP), GlcNAc salvage pathway. In addition, free GlcNAc is taken by GlcNAc transporter and then converted to UDP-GlcNAc through HBP	45
<b>Figure 3.7: The structure of MDP and GlcNAc.</b> The structure of MDP shown in left. The structure of GlcNAc shown in right.....	46
<b>Figure 3.8: The level of <i>O</i>-GlcNAcylation in cells.</b> (A) HEK293T-Nod2-Myc/Tet-op cell lysates ( $\pm$ Thiamet-G (1 $\mu$ M, 4 h), $\pm$ MDP (20 $\mu$ M, 5h)) were immunopurified with Myc antibody and blotted with anti-CTD110.6 antibody; Control cells do not express Myc-Nod2. (B) Relative amount of CTD110.6 to Nod2 Myc was plotted from three independent experiments as the mean $\pm$ S.D. (Reprinted with permission from Hou et. al., Copyright 2017, Glycobiology) .....	46



**Figure 4.1: HEK293T stable cell lines expressing Nod2 mutants.** (A) HEK293T cells are used to produce lentiviral particles containing Nod2 mutants with helper plasmid (pCMVΔR8.2) and the envelope plasmid and then transduced into HEK293T cell. Stable cell lines were developed after puromycin selection. (B) Cell lysates from HEK293T-Nod2-R702W-Myc/K2605, HEK293T-Nod2-G908R-Myc/K2605, and HEK293T-Nod2-1007fs-Myc/K2605 were probed for Myc antibody (1:1000)..... 59

**Figure 4.2: OGT modifies Nod2 mutants.** (A) Cell lysates HEK293T-Nod2-R702W-Myc/K2605, HEK293T-Nod2-G908R-Myc/K2605, and HEK293T-Nod2-1007fs-Myc/K2605 cell lines were immunopurified with Myc antibody and blotted with CTD110.6. and Myc antibodies; Control cells do not express Myc-Nod2. Thiamet-G inhibits OGA, elevating *O*-GlcNAcylation..... 60

**Figure 4.3: Procedure of stable cell lines expressing doxycycline regulated Nod2 mutants.** (A) Phoenix-E cells are used to make retrovirus. First, retrovirus expressing containing RTRg and RTAb vectors is generated and transduced into HEK293T cells. (B) Second, retrovirus having HRSp-Nod2-R702W-Myc, HRSp-Nod2-G908R-Myc, or HRSp-Nod2-1007fs-Myc were generated by Phoenix-E cells individually and then transduced into HEK293T-RTRg/RTAb cells to create doxycycline regulated Nod2 mutants after puromycin..... 61

**Figure 4.4: Doxycycline regulated Nod2 mutants expression in HEK293T cells.** (A) Cell lysates from HEK293T-Nod2-R702W-Myc/Tet-op cell line induced at different concentration of doxycycline were probed for myc antibody (1:1000) to detect the amount of Nod2 expressed. Actin antibody (1:1000) was a loading control. (B) Cell lysates from HEK293T-Nod2-G908R-Myc/Tet-op cell line induced at different concentration of doxycycline were probed for myc antibody (1:1000) to detect the amount of Nod2 expressed. Actin antibody (1:1000) was a loading control. (C) Cell lysates from HEK293T-Nod2-1007fs-Myc/Tet-op cell line induced at different concentration of doxycycline were probed for myc antibody (1:1000) to detect the amount of Nod2 expressed. Actin antibody (1:1000) was a loading control. .... 62

- Figure 4.5: *O*-GlcNAcylation regulated the stability of Nod2 mutant (R702W) in cells.** (A) HEK293T-Nod2-R702W-Myc/Tet-op cells were incubated with 1  $\mu$ M Thiamet-G or DMSO for 4 h, and before cycloheximide treatment (100  $\mu$ g/ml) at the indicated time intervals. Nod2 was detected by anti-Myc western blotting. (B) Relative amount of Nod2 Myc to actin was plotted from three independent experiments as the means  $\pm$  S.D. (C) The plot of the logarithm of Nod2 versus time for a first-order reaction. (Reprinted with permission from Hou et. al., Copyright 2017, Glycobiology) ..... 63
- Figure 4.6: *O*-GlcNAcylation regulated the activity of Nod2 mutant (R702W) in cells.** Dual-luciferase assay performed on HEK293T transfected with 0.1ng 702 plasmid in the presence of 100 nM Thiamet-G or DMSO for 4 h. After 4 h cells were incubated with 20  $\mu$ M MDP for 5h, harvested, and tested for luciferase activity. \*  $p < 0.05$  was considered as significant. (Reprinted with permission from Hou et. al., Copyright 2017, Glycobiology) ..... 64
- Figure 4.7: *O*-GlcNAcylation did not affect the stability of Nod2 mutant (G908R) in cells.** (A) HEK293T-Nod2-G908R-Myc/Tet-op cells were incubated with 1  $\mu$ M Thiamet-G or DMSO for 4 h, and before cycloheximide treatment (100  $\mu$ g/ml) at the indicated time intervals. Nod2 was detected by anti-Myc western blotting. (B) Relative amount of Nod2 Myc to actin was plotted from three independent experiments as the means  $\pm$  S.D. .... 65
- Figure 4.8: *O*-GlcNAcylation did not affect the stability of Nod2 mutant (G908R) in cells using CETSA assay.** (A) HEK293T-Nod2-G908R-Myc/Tet-op cells were incubated with 1  $\mu$ M Thiamet-G or DMSO for 4 h, and performed CETSA assay and Western Blots (see materials and methods). Myc antibody (1:1000), SOD1 antibody (1:1000) (B) Relative amount of Nod2 Myc to SOD1 was plotted from three independent experiments as the means  $\pm$  S.D. by using GraphPad Prism (Boltzmann Sigmoidal model)..... 66
- Figure 4.9: *O*-GlcNAcylation did not regulate the activity of Nod2 mutant (G908R) in cells.** Dual-luciferase assay performed on HEK293T transfected with 0.1ng 908 plasmid in the presence of 100 nM Thiamet-G or DMSO for 4 h. After 4 h cells were incubated with 20  $\mu$ M MDP for 5h, harvested, and tested for luciferase activity. \*  $p < 0.05$  was considered as significant. .... 67

<b>Figure 4.10: Global <i>O</i>-GlcNAcylation in increased using Thiamet-G.</b> Cell lysates from HEK293T-Nod2-Myc/Tet-op cell line and HEK293T-Nod2-G908R-Myc/Tet-op cell line induced with Thiamet-G for 4 h and then were probed for CTD110.6 antibody (1:1000) to detect the global <i>O</i> -GlcNAcylation in cells. ....	68
<b>Figure 4.11: HEK293T stable cell lines expressing Nod2 mutants (S933A).</b> Cell lysates from Nod2-S933A-Myc/K2605 was probed for Myc antibody (1:1000). ....	69
<b>Figure 4.12: OGT modifies Nod2 mutant (S933A).</b> (A) Cell lysates from Nod2-S933A-Myc/K2605 cell line was immunopurified with Myc antibody and blotted with CTD110.6. and Myc antibodies; Control cells do not express Myc-Nod2. Thiamet-G inhibits OGA, elevating <i>O</i> -GlcNAcylation. ....	70
<b>Figure 4.13: <i>O</i>-GlcNAcylation affected the stability of Nod2 mutant (1007) in cells using CETSA assay.</b> (A) HEK293T-Nod2-1007fs-Myc/Tet-op cells were incubated with 1 $\mu$ M Thiamet-G or DMSO for 4 h, and performed CETSA assay and Western Blots (see materials and methods). Myc antibody (1:1000), SOD1 antibody (1:1000) (B) Relative amount of Nod2 Myc to SOD1 was plotted from three independent experiments as the means $\pm$ S.D. by using GraphPad Prism (Boltzmann Sigmoidal model). ....	71
<b>Figure 4.14: <i>O</i>-GlcNAcylation regulated the activity of Nod2 mutant (1007fs) in cells.</b> Dual-luciferase assay performed on HEK293T transfected with 0.1ng 1007fs plasmid in the presence of 100 nM Thiamet-G or DMSO for 4 h. After 4 h cells were incubated with 20 $\mu$ M MDP for 5h, harvested, and tested for luciferase activity. * $p < 0.05$ was considered as significant. ....	72
<b>Figure 5.1: SDS-Page analysis of Nod2 protein purification.</b> SDS-gel was stained using coomassie brilliant blue. Expected MW of Nod2 is 110 kDa. ....	83
<b>Figure 5.2: HEK293T stable cell lines expressing Nod2 domains.</b> (A) The constructs of Nod2: a) CARD b) NBD c) LRR d) CARD-NBD e) NBD-LRR. (B) Cell lysates from HEK293T-Nod2-CARD-Myc/K2605 cell, HEK293T-Nod2-NBD-Myc/K2605 cell, HEK293T-Nod2-LRR-Myc/K2605 cell, HEK293T-CARD-NBD-Myc/K2605 cell, and HEK293T-NBD-LRR-Myc/K2605 cells were probed for Myc antibody (1:1000). ....	85

- Figure 5.3: OGT did not modify Nod2 individual domain.** Cell lysates from HEK293T-Nod2-CARD-Myc/K2605 cell line, HEK293T-Nod2-NBD-Myc/K2605 cell line, and HEK293T-Nod2-LRR-Myc/K2605 cell lines were immunopurified with Myc antibody and blotted with (A) Myc and (B) CTD110.6 antibodies; Control cells do not express Myc-Nod2. Thiamet-G inhibits OGA, elevating *O*-GlcNAcylation. Boxed area in each lane is the different domain of Nod2. .... 86
- Figure 5.4: OGT modified two domains combined of Nod2.** Cell lysates from HEK293T-Nod2-CARD-NBD-Myc/K2605 cell and HEK293T-Nod2-NBD-LRR-Myc/K2605 cell lines were immunopurified with Myc antibody and blotted with (A) Myc and (B) CTD110.6 antibodies; Control cells do not express Myc-Nod2. Thiamet-G inhibits OGA, elevating *O*-GlcNAcylation. Boxed area in each lane is the two domains combined of Nod2. .... 87
- Figure 5.5: OGT modified two domains combined of Nod2.** Cell lysates from HEK293T-NOD2-CARD-NBD-Myc/K2605 cell and HEK293T-NOD2-NBD-LRR-Myc/K2605 cell lines were immunopurified with Myc antibody and blotted with (A) CTD110.6 and (B) CTD110.6 antibody that preincubated with free GlcNAc; Control cells do not express Myc-Nod2. Thiamet-G inhibits OGA, elevating *O*-GlcNAcylation. Boxed area in each lane is the two domains combined of Nod2..... 88
- Figure 5.6: Prediction of *O*-GlcNAc –modified sites of Nod2.** (A) The result of the *O*-GlcNAc prediction strength and the threshold. (B) The prediction indicated that residue T424 is highly recommended to be in *O*-GlcNAc-modified site. .... 89
- Figure 5.7: HEK293T stable cell lines expressing Nod2 mutant (T424A).** Cell lysates from HEK293T-Nod2-T424A-Myc/K2605 were probed for Myc antibody (1:1000). .... 90
- Figure 5.8: Nod2 mutant (T424A) is *O*-GlcNAcylated.** Cell lysates from HEK293T -Nod2-T424A-Myc/K2605 cell line was immunopurified with Myc antibody and blotted with Myc and CTD110.6 antibodies; Control cells do not express Myc-Nod2. Thiamet-G inhibits OGA, elevating *O*-GlcNAcylation..... 91

**Figure A.1: J774 mouse macrophage cells infected with labeled *E. coli*  $\Delta$ MurQ-KU cells.** (A) *E. coli*  $\Delta$ MurQ-KU cells pre-treated with **3** for 45 min were then used to infect J774 cells for 1 h. Cells were fixed and Az488 was clicked into remodeled bacterial peptidoglycan (green). Whole bacterial cells were visualized as shown with white arrows. Cellular DNA was labeled with DAPI (blue) (scale bar, 10  $\mu$ m). (B) Cells treated as in (a) in which deformed bacterial cells with released fluorescent fragments were visualized as shown with white arrows. Fluorescent images are maximum intensity projections of z-stacks. Three-dimensional renderings are provided in Supplementary Videos S6 and S8. Images are representative of a minimum of 3 fields viewed per replicate with at least 2 technical replicates and infection experiments were conducted in at least 3 biological replicates. (Reprinted with permission from Liang and DeMeester et. al., Copyright 2017, Nature Communications) ..... 105

**Figure A.2: Time course study of J774 macrophage invasion.** *E. coli*  $\Delta$ MurQ KU cells pre-treated with **3** for 45 min were then used to infect J774 cells for 20, 40, 60 or 80 minutes. Macrophage cells were treated with gentamycin for an additional 30 min. then collected at total time points 50, 70, 90 and 110 min post infection (p.i.). Cells were fixed and Az488 was clicked into remodeled bacterial peptidoglycan (green). DAPI (blue) was used for cellular DNA staining. Three-dimensional SIM imaging (top) and DIC + 3-D SIM overlay (bottom) are shown. Arrowheads point to corresponding labeled bacterial cells or fragments. Images shown are one representative field for each time point (scale bars, 10  $\mu$ m). Fluorescent images are maximum intensity projections of z-stacks. Images are representative of a minimum of 3 fields viewed per replicate with at least 2 technical replicates and the experiment was conducted in at least 3 biological replicates. (Reprinted with permission from Liang and DeMeester et. al., Copyright 2017, Nature Communications) ..... 106

## LIST OF ABBREVIATIONS

A	Alanine
ATCC	American type culture collection
BME	$\beta$ -mercaptoethanol
CaCl <sub>2</sub>	Calcium chloride
CARD	Caspase recruitment domain
CO <sub>2</sub>	Carbon dioxide
CTAB	Cetyltrimethylammonium bromide
DMEM	Dulbecco's Modified Eagle's Medium
DNA	Deoxyribonucleic acid
EDTA	Ethylenediaminetetraacetic acid
ETD	Electron transfer dissociation
FBS	Fetal bovine serum
FS	Frame shift
G	Glycine
GlcNAc	N-acetylglucosamine
HAT	Histone acetyl transferase
HBP	Hexosamine biosynthetic pathway
HCF	Host cell factor
HEK	Human embryonic kidney
HRP	Horseradish peroxidase

Hsp70	Heat shock protein 70
iE-DAP	D-glutamyl-meso-diaminopimelic acid
IκB	Inhibitor of κB
IKKγ	IκB kinase γ
IP	Immunoprecipitation
KCl	Potassium chloride
LPS	Lipopolysaccharide
LRR	Leucine rich repeat
mAb	Monoclonal antibody
MAMPs	Microorganism-associated molecular patterns
MES	2- Morpholinoethanesulfonic acid
MDP	Muramyl dipeptide
MgCl <sub>2</sub>	Magnesium chloride
NaCl	Sodium chloride
NaF	Sodium fluoride
NLR	Nod-like receptors
Na <sub>3</sub> VO <sub>4</sub>	Trisodium phosphate
NBD	Nucleotide binding domain
NOD2	Nucleotide binding oligomerization domain-containing protein 2
OGA	<i>O</i> -GlcNAcase
OGT	<i>O</i> -GlcNAc transferase
PBS	Phosphate buffered saline
PCR	Polymerase chain reaction
PRR	Pattern recognition receptors

PAMPs	Pathogen-associated molecular patterns
R	Arginine
RNA	Ribonucleic acid
RelA	Nuclear factor-kappaB p65
RIP2	Receptor-interacting serine/threonine- protein kinase 2
RTAb	Transactivator
RTRg	Transrepressor
S	Serine
SDS	Sodium dodecyl sulfate
SDS-PAGE	Sodium Dodecyl Sulfate--Polyacrylamide Gel Electrophoresis
SOD1	Superoxide dismutase 1
SPR	Surface plasmon resonance
TBS	Tris buffered saline
TBST	TBS + Tween 20 solution (0.05%)
TLR	Toll like receptor
TNF- $\alpha$	tumor necrosis factor- $\alpha$
TPR	Tetratricopeptide repeat
t-RNA	Transfer RNA
UDP-GlcNAc	Uridine Diphosphate N-acetylglucosamine
W	Tryptophan
WT	Wild type



## ABSTRACT

The innate immune system, the first line of defense against pathogens, utilizes a series of receptors, including Toll-like receptors and Nod-like receptors, to generate the proper immune response.

Nucleotide-binding oligomerization domain 2 (Nod2) is one of Nod-like receptors that can sense the bacterial peptidoglycan component, muramyl dipeptide (MDP). Upon activation Nod2 induces the production of various inflammatory molecules such as cytokines and chemokines. Genetic linkage analysis identified and revealed that three major mutations in Nod2 associated with the development of Crohn's disease are R702W, G908R, and 1007fs. In addition, previous studies have shown these Nod2 variants have lower NF- $\kappa$ B activation in response to MDP compared to wild type Nod2.

The objective of this dissertation is to further characterize Nod2 and determine if it is post-translationally modified by *O*-GlcNAc. *O*-GlcNAcylation is one type of post-translational modification in which the *O*-GlcNAc transferase (OGT) transfers *N*-acetylglucosamine (GlcNAc) from UDP-GlcNAc to selected serine and threonine residues of intracellular proteins. As GlcNAc is a major component of peptidoglycan of the bacterial cell wall and a large amount of GlcNAc is released from bacterial cell wall during cell wall remodeling, we hypothesized that Nod2 could be *O*-

GlcNAcylated.

We found that wild type Nod2 and Nod2 Crohn's-associated variants are *O*-GlcNAcylated. This modification affects both wild type and Nod2 mutants stability and ability to signal via the NF- $\kappa$ B pathways.

Finally, in order to identify the peptidoglycan fragments that are generated inside the cellular environment, we have developed a new labelling approach to study peptidoglycan degradation process in vivo. Ultimately, we will utilize this approach to identify peptidoglycan fragments that effect the level of *O*-GlcNAcylation and OGT activity.

## **Chapter 1**

### **INTRODUCTION**

#### **1.1 Innate Immune System**

Nearly 100 years ago, Sir Alexander Fleming revealed to the world that our bodies produce an enzyme called lysozyme which functions as an antibiotic by destroying the cell walls of many bacterial cells (1). Today, we recognize that lysozyme is just one of the many mechanisms that our bodies have to protect ourselves against infectious diseases as part of our innate immune system. This seemingly simple “first line of defense” has proven to be much more sophisticated than was originally suggested. Janeway and Medzhitov initially proposed the idea that our bodies contain innate immune receptors that specifically recognize unique structures from microbes; but more importantly they hypothesized that these receptors subsequently informed the adaptive immune response (2-5). Seminal work by Beutler and Hoffman identified the first of these receptors, the Toll- like receptors (TLRs). In his Nobel winning work, Hoffman demonstrated that the TLRs were responsible for sensing a fungal infection in *Drosophila* (6) and shortly after, Beutler published his Nobel manuscript, describing that TLR4 is responsible for sensing lipopolysaccharide (LPS) from bacteria (7). The past twenty years has seen the field of innate immunity explode and we now know that there are many different types of innate immune receptors responsible for pathogen sensing including TLRs, Nod-like receptors (NLRs), C-type lectin receptors, RIG-1 like receptors, and DNA sensors (8, 9). These innate immune receptors recognize conserved structures in a pathogen,

pathogen-associated molecular patterns (PAMPs), and induce inflammatory and antimicrobial responses. Recognition also leads to the expression of protective proteins, including chemokines, cytokines, defensins, immunoreceptors, and cell adhesion molecules, to help us to defend against infection and send signals to the adaptive immune system (9) (Figure 1.1). However, PAMPs do not only exist in pathogens, they are generally in all microorganisms, including the ones in the microbiome. Thus, these molecules have been renamed to microorganism-associated molecular patterns (MAMPs) (10).

There are two main types of innate immune receptors, Toll-like receptors (TLRs) that recognize microbial structure at the cell membrane (11), and nucleotide-binding oligomerization domain (NOD)-like receptors (NLRs) that recognize microbial fragments in the cytoplasm (12).

The NLR family plays an important role in recognizing MAMPs in the innate immune system. There are 23 NLR proteins in humans (13, 14). They have a similar structure consisting of a variable N-terminal domain, a central nucleotide-binding domain (NBD), and a C-terminal leucine-rich repeat (LRR) domain. There are four subfamilies of the NLR family based on their N-terminal domain: NLRC, NLRA, NLRP and NLRB. These subfamilies have either a caspase recruitment domain (CARD), an acidic transactivation domain, a pyrin domain or a baculovirus inhibitor repeat respectively (15). The NBD domain is involved in oligomerization and activating downstream signaling of receptor-interacting protein 2 (RIP2) (16). The LRR domains of NODs have been proposed to recognize ligands (17, 18).

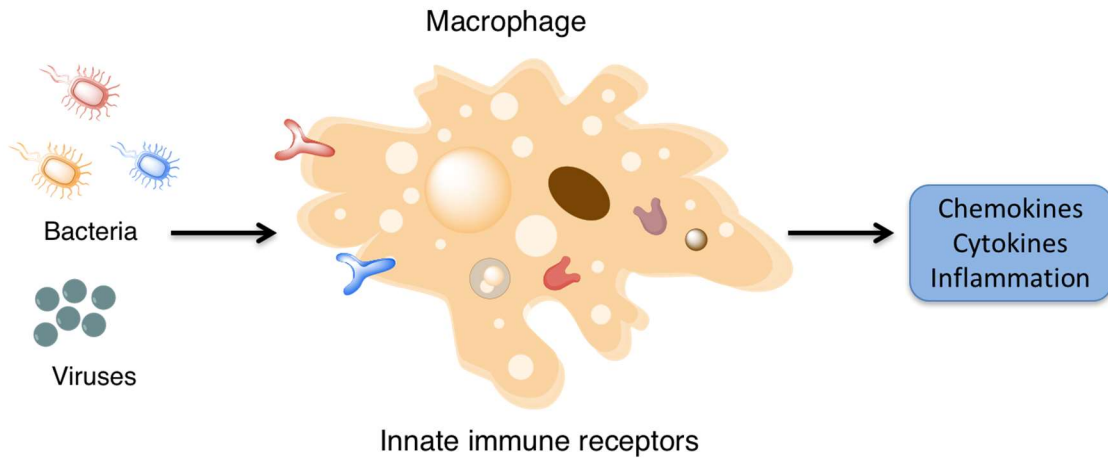


**Figure 1.1: Innate immune receptors.** These innate immune receptors will recognize unique structure from microorganism and then trigger the appropriate immune response.

Nod1 and Nod2 are well characterized receptors since they were the first of the NLRs to be identified (19-21). They both contain CARD domains, an NBD domain and an LRR domain, except Nod2 has an additional CARD domain while Nod1 has only one (Figure 1.2). Nod1 can detect D-glutamyl-meso-diaminopimelic acid (iE-DAP) that presents in a peptidoglycan from Gram-negative bacteria and some of Gram-positive bacteria. By contrast, Nod2 can recognize muramyl dipeptide (MDP) that presents in all Gram-negative and Gram-positive bacteria (Figure 1.3).

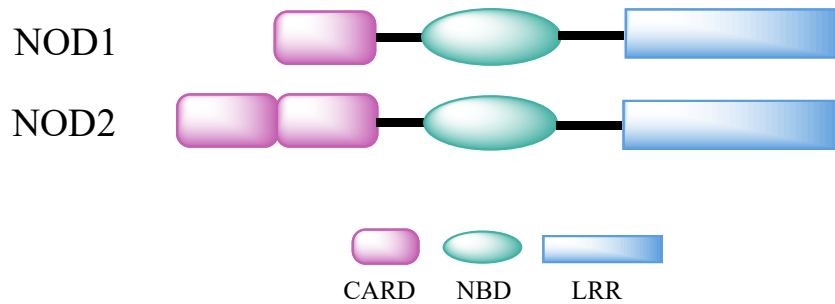


**Figure 1.2: Structure of Nod1 and Nod2.** Nod1 and Nod2 consist of a C-terminal leucine-rich repeat (LRR), a nucleotide binding and oligomerization domain (NOD) and caspase activating and recruiting domains (CARDs).

## 1.2 Nod2 Signaling

Nod2 is a 110 kDa protein (1040 amino acids) and highly expressed in dendritic cells, macrophages and Paneth cells in the ileum (22, 23). Nod2 can recognize the bacterial cell wall fragment, MDP (Figure 1.3) (24, 25). Also, it has already been shown that MDP can directly bind to NOD2 through its LRR domain by using surface plasmon resonance (SPR) and fluorescent polarization (26, 27).

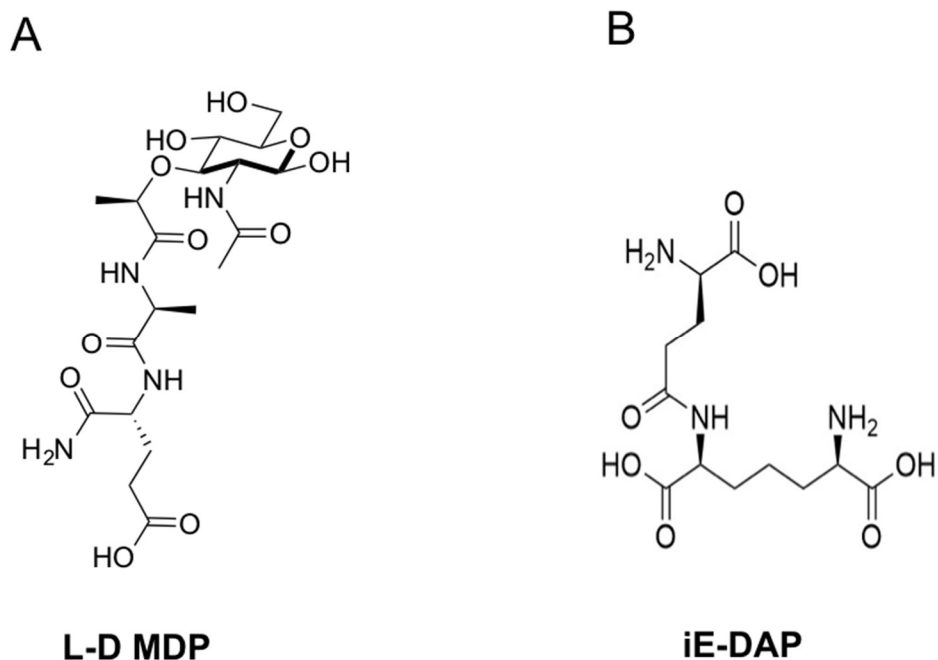


**Figure 1.3: MDP and iE-DAP.** (A) MDP consists of *N*-acetylmuramic acid with a L-Ala-D-isoGln dipeptide chain. It is the ligand from peptidoglycan for Nod2. (B) iE-DAP is a dipeptide, a ligand from peptidoglycan for Nod1.

Once Nod2 binds to MDP, it promotes oligomerization of Nod2 and then recruit receptor-interacting serine/threonine-protein kinase 2 (RIP2) by CARD-CARD interaction (28). This interaction mediates polyubiquitination of NF- $\kappa$ B inhibitor – I $\kappa$ B kinase  $\gamma$  (IKK $\gamma$ ) (29). This allows NF- $\kappa$ B to translocate to the nucleus to turn on the transcription of various inflammatory molecules (30, 31) (Figure 1.4).

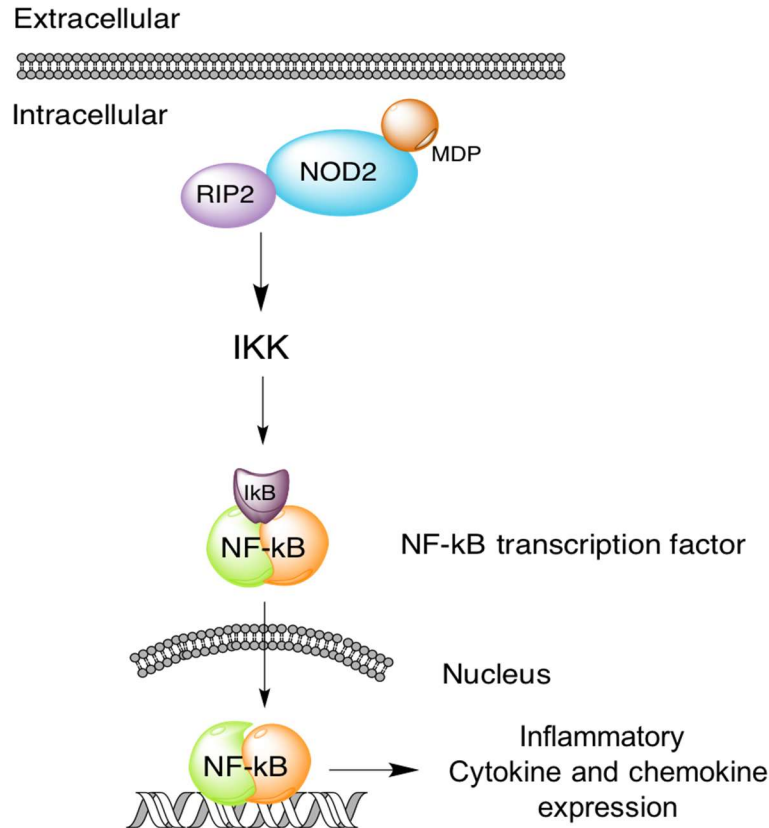


**Figure 1.4: NF-κB pathway.** MDP activates Nod2 dependent NF-κB signaling. It will recruit RIP2 and then translate the signal to turn on NF-κB. stimulation of Nod2 leads to the recruitment of RIP2 which in turn translates the signal to turn on NF-κB.

### 1.3 Nod2 in Crohn's Disease

Crohn's disease is a chronic inflammatory disorder of the entire gastrointestinal tract from mouth to anus. It can affect 700,000 people in the United States. There is no cure for Crohn's disease; most patients require constant medication or surgery (32). Genome-wide association studies (GWAS) identified 30 susceptibility loci for Crohn's disease (33). Nod2 was the first gene linked to the development of Crohn's disease (34, 35). There are three common Nod2 variants (R702W, G908R,



and 1007fs) in the LRR region linked to the development of Crohn's disease (Figure 1.2) (34-36). Individual Nod2 variants exhibit a slightly increased risk of developing Crohn's disease. However, Nod2 variants with homozygous or compound heterozygous have a 20-40-fold increased risk (37).

Previous studies have shown these Nod2 variants have lower NF- $\kappa$ B activation in response to MDP compared to wild type Nod2 (25). Briefly, it was shown in a transfection based assay that Nod2 mutations cause a reduction and/or elimination of this activity. Different amounts of DNA of Nod2 were transfected into HEK293T cells. After transfection, cells were treated with different concentrations of MDP. The data indicated that 1007fs mutant did not have ability to respond at all different treatment of Nod2 and MDP; however, other two mutants had reduced level of NF- $\kappa$ B activation to MDP (25).

#### **1.4 Post-translational Modification of Nod2 Signaling Cascade**

In order to increase functional diversity to response signaling, cells will increase proteins diversity from 20,000 protein-coding genes to over 1 million proteins through post-translational modifications that add functional group, degrade proteins, or cleave subunits (38, 39).

A variety of post-translational modifications are reported to regulate Nod2 signaling. Ubiquitination is a well-known post-translational modification modulating the signaling cascade of Nod2. For example, P62 is a scaffold protein involved in autophagy that interacts with Nod2. This interaction was shown to inhibit the polyubiquitin-ligase activity to protect Nod2 from degradation by the proteasome (40).

Phosphorylation is another known post-translational modification that regulates Nod2 mediated NF- $\kappa$ B activation. RIP2, a kinase, is recruited and interacts

with Nod2 upon MDP stimulation and then activates NF- $\kappa$ B signaling (Figure 1.4). Interesting, RIP2 has been reported to autophosphorylate on S176 and Y474, which increases NF- $\kappa$ B activation (41).

These previous studies suggest that post-translational modifications of Nod2 interacting proteins regulate the Nod2 signaling cascade. I sought to determine if any post-translational modifications, *O*-GlcNAcylation, occur on Nod2 itself.

### 1.5 *O*-GlcNAcylation

*O*-GlcNAcylation was first described by Torres and Hart in 1984 (42). It is a dynamic post translational modification in which the *O*-GlcNAc transferase (OGT) transfers GlcNAc from UDP-GlcNAc to selected serine and threonine residues, while *O*-GlcNAcase (OGA) removes *O*-GlcNAc from target proteins (Figure 1.5). This differs from phosphorylation, which is mediated by numerous kinases and phosphatases, whereas the *O*-GlcNAc modification is controlled by two enzymes alone (42-46).

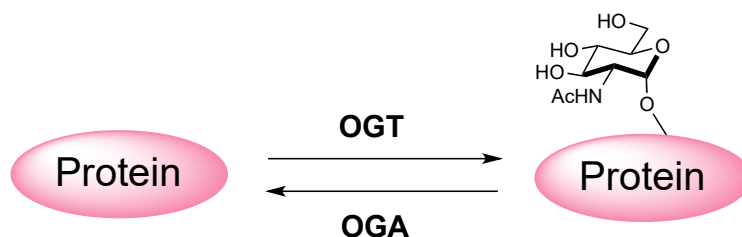


**Figure 1.5: *O*-GlcNAcylation.** The *O*-GlcNAc transferase (OGT) attaches *O*-GlcNAc to a protein at serine or threonine residues and *O*-GlcNAcase (OGA) removes *O*-GlcNAc from a target protein.

This modification is different from traditional protein glycosylation. It is found on nuclear, mitochondrial and cytoplasmic proteins modified with a single  $\beta$ -N-acetylglucosamine monosaccharide moiety. In contrast, protein glycosylation attaches complex oligosaccharides to a protein. The substrate (UDP-GlcNAc) for *O*-GlcNAcylation is a product of the hexosamine biosynthetic pathway (HBP) (Figure 1.6), which regulates glucose, amino acid, nucleotide and fatty acid metabolism in cells. *O*-GlcNAcylation has been proposed to regulate cellular nutrition and stress in order to respond to cell signals and metabolism (47). Further, misregulation of *O*-GlcNAcylation has been linked to several human diseases, including Alzheimer's disease, obesity, diabetes and cancer (48, 49).

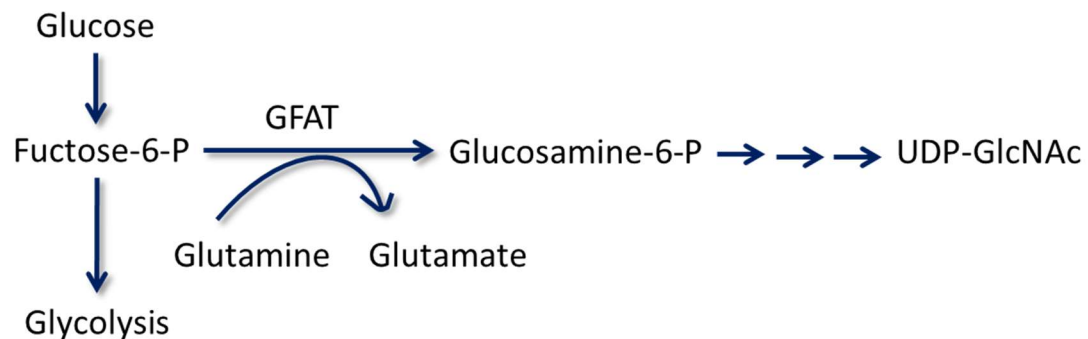


**Figure 1.6: Hexosamine biosynthetic pathway (HBP).** UDP-GlcNAc is a metabolite of the hexosamine biosynthetic pathway(HBP), one endpoint of which is the modification and regulation of proteins by the *O*-GlcNAcylation in cells

## 1.6 *O*-GlcNAc Transferase (OGT)

OGT is expressed in all tissues, particularly the brain, pancreas, heart and skeletal muscle. OGT has two domains, an N-terminal tetratricopeptide repeat (TPR)

domain, and a C-terminal catalytic domain. OGT encodes three splice variants that depend on the numbers of TPR in the N-terminal. Nucleocytoplasmic OGT (ncOGT) is the longest isoform containing 13 TPRs and is localized in the nucleus and cytoplasm (50, 51). The second-longest isoform, having 9 TPRs, is a mitochondrial OGT (mOGT) with a mitochondrial targeting sequence in the N-terminus (52). The shortest isoform containing 3 TPRs is sOGT (53) (Figure 1.7A).

The TPR domain of OGT regulates the substrate recognition of a broad range of target proteins, especially TPRs 1-6 which are required for glycosylation of the substrate (54, 55). In addition, TPRs 12 and 13 of ncOGT are believed to regulate target proteins to the OGT substrate-binding cleft (45). There is no conserved sequence in target proteins that represents an OGT substrate consensus motif, however, several literatures indicated that *O*-GlcNAc modification occurs on the P/V-P/V-V-gS/T-S/T sequence (56-58). The crystal structure of ncOGT with UDP and the casein kinase II-peptide substrate shows that the enzyme and substrate peptide is enforced by the presence of prolines and amino acids around the Ser/Thr residues of the target protein (45). In addition, another study indicates *O*-GlcNAc modification tends to happen on disordered protein regions, which are also the same sites for phosphorylation (59).

Interestingly, OGT reveals endopeptidase activity to divide the substrate, the host cell factor (HCF-1), into N- and C- terminal fragments. HCF-1 is a transcriptional coregulatory protein involved in cell cycle progress (60). There is a series of six 26-residue amino acids (HCF-1<sub>PRO</sub>), which is the cleaved site of proteolytic maturation process, between N and C- terminus of HCF-1. The HCF-1<sub>N</sub> subunit regulates cells passing through the G1 phase (61, 62) and the HCF-1<sub>C</sub> subunit controls mitosis and

cytokinesis in M phase (63). In 2001, Dr. Herr's lab demonstrated that OGT can recognize the HCF-1<sub>PRO</sub> repeat and cleave it. Those results showed that OGT plays a role in HCF-1 proteolytic maturation (64).

### **1.7 *O*-GlcNAcase (OGA)**

OGA is expressed in all the same tissues as OGT, particularly the brain, pancreas and skeletal muscle. OGA has two splice variants, OGA-L and OGA-S. OGA-L is the longest isoform and is localized in the cytosol and nucleus (43, 65, 66). OGA-L contains an N-terminal catalytic domain and a C-terminal pseudo-histone acetyltransferase (HAT) domain (67). The short isoform, OGA-S, has a unique 15-amino acid C-terminal extension without the pseudo-HAT domain. OGA-S exists in lipid droplets (68) (Figure 1.7B).

There is no crystal structure of human OGA; however, GH84 glycoside hydrolases from bacteria have provided structural information (69, 70). A high sequence similarity between human OGT and its bacterial homolog's catalytic domains implies a conserved enzymatic mechanism (69).

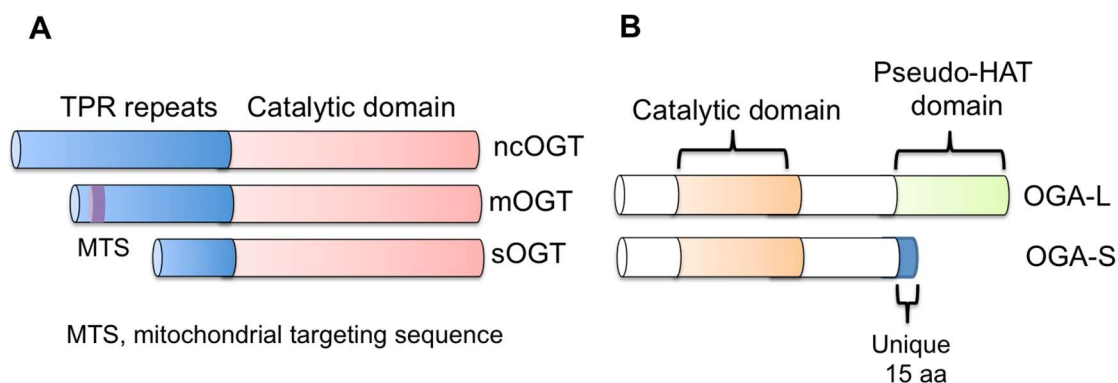


**Figure 1.7: OGT and OGA.** (A) *O*-GlcNAc transferase (OGT) has three isoforms, ncOGT, mOGT, and sOGT. (B) *O*-GlcNAcase (OGA) contains two isoform, OGA-L and OGA-S.

## 1.8 Discussion

Nod2 is an innate immune receptor that recognizes bacterial cell wall fragments and triggers an inflammatory response. In 2001, genetic linkage analysis showed that Nod2 mutation is associated with an incidence of occurrence for Crohn's disease (21, 34). Crohn's disease is a chronic inflammatory disorder that affects 750,000 people in the United States. Further studies showed that Nod2 mutations linked to Crohn's disease is a loss of function mutation that lacks the ability to respond to bacterial invasion, which is predicted to be the cause for the chronic inflammation associated with the disease. Currently, there is no cure for this disease.

Recently we have shown that Nod2 is an unstable protein and the Crohn's-associated mutants are even more unstable. We have shown that overexpression of the molecular chaperone HSP70 restores the stability and the proper signaling to the Crohn's mutants (71). We were interested in to investigate if Nod2 is *O*-GlcNAc modified by OGT since UDP-GlcNAc, the substrate of OGT, is a component of bacterial cell wall. Previous studies have shown *O*-GlcNAcylation can increase

stability of proteins. We were wondering if this modification can regulate the stability of Nod2 and mutants. We proposed that targeting the stabilization of Nod2 mutants may rescue their activity by allowing the proper protein level to be maintained. In this dissertation, we showed a novel method that could be implemented to stabilize Nod2 mutants thus rescuing their activity. Chapter 2 will discover that Nod2 is *O*-GlcNAcylated and this modification will regulate the half-life of Nod2. Chapter 3 will describe that this modification also affects Nod2 mediated NF- $\kappa$ B activation through stabilization of Nod2. Chapter 4 will discuss the application of this modification on Crohn's-associated Nod2 variants. In chapter 5 will reveal that the NBD domain of Nod2 is important for *O*-GlcNAcylation. Finally, chapter 6 will be the conclusion and future direction of this dissertation.

## REFERENCES

1. Fleming A. On a remarkable bacteriolytic element found in tissues and secretions. *Proceedings of the Royal Society of London Series B-Containing Papers of a Biological Character*. 1922;93(653):306-17. doi: 10.1098/rspb.1922.0023. PubMed PMID: WOS:000200332800001.
2. Janeway CA. APPROACHING THE ASYMPTOTE - EVOLUTION AND REVOLUTION IN IMMUNOLOGY. *Cold Spring Harbor Symposia on Quantitative Biology*. 1989;54:1-13. PubMed PMID: WOS:A1989JX74500001.
3. Medzhitov R, Janeway CA. On the semantics of immune recognition. *Research in Immunology*. 1996;147(4):208-14. doi: 10.1016/0923-2494(96)87222-1. PubMed PMID: WOS:A1996VA74700004.
4. Medzhitov R, PrestonHurlburt P, Janeway CA. A human homologue of the *Drosophila* Toll protein signals activation of adaptive immunity. *Nature*. 1997;388(6640):394-7. PubMed PMID: WOS:A1997XM52800055.
5. Medzhitov R. Approaching the asymptote: 20 years later. *Immunity*. 2009;30(6):766-75. Epub 2009/06/23. doi: 10.1016/j.immuni.2009.06.004. PubMed PMID: 19538928.
6. Lemaitre B, Nicolas E, Michaut L, Reichhart JM, Hoffmann JA. The dorsoventral regulatory gene cassette *spatzle/Toll/cactus* controls the potent antifungal response in *Drosophila* adults. *Cell*. 1996;86(6):973-83. doi: 10.1016/s0092-8674(00)80172-5. PubMed PMID: WOS:A1996VJ44300015.
7. Poltorak A, Smirnova I, He XL, Liu MY, Van Huffel C, Birdwell D, Alejos E, Silva M, Du X, Thompson P, Chan EKL, Ledesma J, Roe B, Clifton S, Vogel S, Beutler B. Genetic and physical mapping of the *Lps* locus: Identification of the Toll-4 receptor as a candidate gene in the critical region. *Blood Cells Molecules and Diseases*. 1998;24(17):340-55. doi: 10.1006/bcmd.1998.0201. PubMed PMID: WOS:000075927100001.
8. Brubaker SW, Bonham KS, Zanoni I, Kagan JC. Innate immune pattern recognition: a cell biological perspective. *Annual review of immunology*.



2015;33:257-90. Epub 2015/01/13. doi: 10.1146/annurev-immunol-032414-112240. PubMed PMID: 25581309.

9. Akira S, Uematsu S, Takeuchi O. Pathogen recognition and innate immunity. *Cell*. 2006;124(4):783-801. Epub 2006/02/25. doi: 10.1016/j.cell.2006.02.015. PubMed PMID: 16497588.

10. Mackey D, McFall AJ. MAMPs and MIMPs: proposed classifications for inducers of innate immunity. *Molecular microbiology*. 2006;61(6):1365-71. Epub 2006/08/11. doi: 10.1111/j.1365-2958.2006.05311.x. PubMed PMID: 16899081.

11. Takeda K, Akira S. Roles of Toll-like receptors in innate immune responses. *Genes Cells*. 2001;6(9):733-42. PubMed PMID: 11554921.

12. Franchi L, Warner N, Viani K, Nunez G. Function of Nod-like receptors in microbial recognition and host defense. *Immunol Rev*. 2009;227(1):106-28. PubMed PMID: 19120480.

13. Biswas A, Kobayashi KS. Regulation of intestinal microbiota by the NLR protein family. *International immunology*. 2013;25(4):207-14. Epub 2013/01/18. doi: 10.1093/intimm/dxs116. PubMed PMID: 23325116; PMCID: 3597849.

14. Feerick CL, McKernan DP. Understanding the regulation of pattern recognition receptors in inflammatory diseases - a 'Nod' in the right direction. *Immunology*. 2016. Epub 2016/10/06. doi: 10.1111/imm.12677. PubMed PMID: 27706808.

15. Ting JP, Duncan JA, Lei Y. How the noninflammasome NLRs function in the innate immune system. *Science*. 2010;327(5963):286-90. PubMed PMID: 20075243.

16. Abbott DW, Wilkins A, Asara JM, Cantley LC. The Crohn's disease protein, NOD2, requires RIP2 in order to induce ubiquitylation of a novel site on NEMO. *Current biology : CB*. 2004;14(24):2217-27. Epub 2004/12/29. doi: 10.1016/j.cub.2004.12.032. PubMed PMID: 15620648.

17. Girardin SE, Jehanno M, Mengin-Lecreulx D, Sansonetti PJ, Alzari PM, Philpott DJ. Identification of the critical residues involved in peptidoglycan detection by Nod1. *The Journal of biological chemistry*. 2005;280(46):38648-56. doi: 10.1074/jbc.M509537200. PubMed PMID: 16172124.

18. Tanabe T, Chamaillard M, Ogura Y, Zhu L, Qiu S, Masumoto J, Ghosh P, Moran A, Predergast MM, Tromp G, Williams CJ, Inohara N, Nunez G. Regulatory

regions and critical residues of NOD2 involved in muramyl dipeptide recognition. *Embo J.* 2004;23(7):1587-97. PubMed PMID: 15044951.

19. Bertin J, Nir WJ, Fischer CM, Tayber OV, Errada PR, Grant JR, Keilty JJ, Gosselin ML, Robison KE, Wong GH, Glucksmann MA, DiStefano PS. Human CARD4 protein is a novel CED-4/Apaf-1 cell death family member that activates NF-kappaB. *The Journal of biological chemistry.* 1999;274(19):12955-8. Epub 1999/05/01. PubMed PMID: 10224040.

20. Inohara N, Ogura Y, Chen FF, Muto A, Nunez G. Human Nod1 confers responsiveness to bacterial lipopolysaccharides. *The Journal of biological chemistry.* 2001;276(4):2551-4. Epub 2000/11/04. doi: 10.1074/jbc.M009728200. PubMed PMID: 11058605.

21. Ogura Y, Inohara N, Benito A, Chen FF, Yamaoka S, Nunez G. Nod2, a Nod1/Apaf-1 family member that is restricted to monocytes and activates NF-kappaB. *The Journal of biological chemistry.* 2001;276(7):4812-8. doi: 10.1074/jbc.M008072200. PubMed PMID: 11087742.

22. Gutierrez O, Pipaon C, Inohara N, Fontalba A, Ogura Y, Prosper F, Nunez G, Fernandez-Luna JL. Induction of Nod2 in myelomonocytic and intestinal epithelial cells via nuclear factor-kappa B activation. *The Journal of biological chemistry.* 2002;277(44):41701-5. PubMed PMID: 12194982.

23. Ogura Y, Lala S, Xin W, Smith E, Dowds TA, Chen FF, Zimmermann E, Tretiakova M, Cho JH, Hart J, Greenson JK, Keshav S, Nunez G. Expression of NOD2 in Paneth cells: a possible link to Crohn's ileitis. *Gut.* 2003;52(11):1591-7. Epub 2003/10/23. PubMed PMID: 14570728; PMCID: 1773866.

24. Girardin SE, Boneca IG, Viala J, Chamaillard M, Labigne A, Thomas G, Philpott DJ, Sansonetti PJ. Nod2 is a general sensor of peptidoglycan through muramyl dipeptide (MDP) detection. *The Journal of biological chemistry.* 2003;278(11):8869-72. PubMed PMID: 12527755.

25. Inohara N, Ogura Y, Fontalba A, Gutierrez O, Pons F, Crespo J, Fukase K, Inamura S, Kusumoto S, Hashimoto M, Foster SJ, Moran AP, Fernandez-Luna JL, Nunez G. Host recognition of bacterial muramyl dipeptide mediated through NOD2. Implications for Crohn's disease. *The Journal of biological chemistry.* 2003;278(8):5509-12. PubMed PMID: 12514169.

26. Grimes CL, Ariyananda Lde Z, Melnyk JE, O'Shea EK. The Innate Immune Protein Nod2 Binds Directly to MDP, a Bacterial Cell Wall Fragment. *Journal of the*

American Chemical Society. 2012;134(33):13535-7. Epub 2012/08/04. doi: 10.1021/ja303883c. PubMed PMID: 22857257; PMCID: 3424850.

27. Mo J, Boyle JP, Howard CB, Monie TP, Davis BK, Duncan JA. Pathogen sensing by nucleotide-binding oligomerization domain-containing protein 2 (NOD2) is mediated by direct binding to muramyl dipeptide and ATP. *The Journal of biological chemistry*. 2012;287(27):23057-67. Epub 2012/05/03. doi: 10.1074/jbc.M112.344283. PubMed PMID: 22549783; PMCID: 3391102.

28. McCarthy JV, Ni J, Dixit VM. RIP2 is a novel NF-kappa B-activating and cell death-inducing kinase. *Journal of Biological Chemistry*. 1998;273(27):16968-75. doi: DOI 10.1074/jbc.273.27.16968. PubMed PMID: WOS:000074545200050.

29. Kobayashi K, Inohara N, Hernandez LD, Galan JE, Nunez G, Janeway CA, Medzhitov R, Flavell RA. RICK/Rip2/CARDIAK mediates signalling for receptors of the innate and adaptive immune systems. *Nature*. 2002;416(6877):194-9. PubMed PMID: 11894098.

30. McCarthy JV, Ni J, Dixit VM. RIP2 is a novel NF-kappaB-activating and cell death-inducing kinase. *The Journal of biological chemistry*. 1998;273(27):16968-75. PubMed PMID: 9642260.

31. Nembrini C, Kisielow J, Shamshiev AT, Tortola L, Coyle AJ, Kopf M, Marsland BJ. The kinase activity of Rip2 determines its stability and consequently Nod1- and Nod2-mediated immune responses. *The Journal of biological chemistry*. 2009;284(29):19183-8. Epub 2009/05/29. doi: 10.1074/jbc.M109.006353. PubMed PMID: 19473975; PMCID: 2740541.

32. Dignass A, Van Assche G, Lindsay JO, Lemann M, Soderholm J, Colombel JF, Danese S, D'Hoore A, Gassull M, Gomollon F, Hommes DW, Michetti P, O'Morain C, Oresland T, Windsor A, Stange EF, Travis SP, European Cs, Colitis O. The second European evidence-based Consensus on the diagnosis and management of Crohn's disease: Current management. *Journal of Crohn's & colitis*. 2010;4(1):28-62. Epub 2010/12/03. doi: 10.1016/j.crohns.2009.12.002. PubMed PMID: 21122489.

33. Jostins L, Ripke S, Weersma RK, Duerr RH, McGovern DP, Hui KY, Lee JC, Schumm LP, Sharma Y, Anderson CA, Essers J, Mitrovic M, Ning K, Cleynen I, Theatre E, Spain SL, Raychaudhuri S, Goyette P, Wei Z, Abraham C, Achkar JP, Ahmad T, Amininejad L, Ananthakrishnan AN, Andersen V, Andrews JM, Baidoo L, Balschun T, Bampton PA, Bitton A, Boucher G, Brand S, Buning C, Cohain A, Cichon S, D'Amato M, De Jong D, Devaney KL, Dubinsky M, Edwards C, Ellinghaus D, Ferguson LR, Franchimont D, Fransen K, Gearry R, Georges M, Gieger C, Glas J, Haritunians T, Hart A, Hawkey C, Hedl M, Hu X, Karlsen TH, Kupcinskis L,

Kugathasan S, Latiano A, Laukens D, Lawrance IC, Lees CW, Louis E, Mahy G, Mansfield J, Morgan AR, Mowat C, Newman W, Palmieri O, Ponsioen CY, Potocnik U, Prescott NJ, Regueiro M, Rotter JI, Russell RK, Sanderson JD, Sans M, Satsangi J, Schreiber S, Simms LA, Sventoraityte J, Targan SR, Taylor KD, Tremelling M, Verspaget HW, De Vos M, Wijmenga C, Wilson DC, Winkelmann J, Xavier RJ, Zeissig S, Zhang B, Zhang CK, Zhao H, International IBDGC, Silverberg MS, Annese V, Hakonarson H, Brant SR, Radford-Smith G, Mathew CG, Rioux JD, Schadt EE, Daly MJ, Franke A, Parkes M, Vermeire S, Barrett JC, Cho JH. Host-microbe interactions have shaped the genetic architecture of inflammatory bowel disease. *Nature*. 2012;491(7422):119-24. Epub 2012/11/07. doi: 10.1038/nature11582. PubMed PMID: 23128233; PMCID: 3491803.

34. Ogura Y, Bonen DK, Inohara N, Nicolae DL, Chen FF, Ramos R, Britton H, Moran T, Karaliuskas R, Duerr RH, Achkar JP, Brant SR, Bayless TM, Kirschner BS, Hanauer SB, Nunez G, Cho JH. A frameshift mutation in NOD2 associated with susceptibility to Crohn's disease. *Nature*. 2001;411(6837):603-6. PubMed PMID: 11385577.

35. Hugot JP, Chamaillard M, Zouali H, Lesage S, Cezard JP, Belaiche J, Almer S, Tysk C, O'Morain CA, Gassull M, Binder V, Finkel Y, Cortot A, Modigliani R, Laurent-Puig P, Gower-Rousseau C, Macry J, Colombel JF, Sahbatou M, Thomas G. Association of NOD2 leucine-rich repeat variants with susceptibility to Crohn's disease. *Nature*. 2001;411(6837):599-603. Epub 2001/06/01. doi: 10.1038/35079107. PubMed PMID: 11385576.

36. Lesage S, Zouali H, Cezard JP, Colombel JF, Belaiche J, Almer S, Tysk C, O'Morain C, Gassull M, Binder V, Finkel Y, Modigliani R, Gower-Rousseau C, Macry J, Merlin F, Chamaillard M, Jannot AS, Thomas G, Hugot JP, Group E-I, Group E, Group G. CARD15/NOD2 mutational analysis and genotype-phenotype correlation in 612 patients with inflammatory bowel disease. *American journal of human genetics*. 2002;70(4):845-57. Epub 2002/03/05. doi: 10.1086/339432. PubMed PMID: 11875755; PMCID: 379113.

37. Hugot JP, Zaccaria I, Cavanaugh J, Yang H, Vermeire S, Lappalainen M, Schreiber S, Annese V, Jewell DP, Fowler EV, Brant SR, Silverberg MS, Cho J, Rioux JD, Satsangi J, Parkes M, Consortium IBDIG. Prevalence of CARD15/NOD2 mutations in Caucasian healthy people. *The American journal of gastroenterology*. 2007;102(6):1259-67. Epub 2007/02/27. doi: 10.1111/j.1572-0241.2007.01149.x. PubMed PMID: 17319929.

38. International Human Genome Sequencing C. Finishing the euchromatic sequence of the human genome. *Nature*. 2004;431(7011):931-45. doi: 10.1038/nature03001. PubMed PMID: 15496913.

39. Jensen ON. Modification-specific proteomics: characterization of post-translational modifications by mass spectrometry. *Curr Opin Chem Biol.* 2004;8(1):33-41. doi: 10.1016/j.cbpa.2003.12.009. PubMed PMID: 15036154.
40. Park S, Ha SD, Coleman M, Meshkibaf S, Kim SO. p62/SQSTM1 enhances NOD2-mediated signaling and cytokine production through stabilizing NOD2 oligomerization. *PloS one.* 2013;8(2):e57138. doi: 10.1371/journal.pone.0057138. PubMed PMID: 23437331; PMCID: PMC3577775.
41. Dorsch M, Wang A, Cheng H, Lu C, Bielecki A, Charron K, Clauser K, Ren H, Polakiewicz RD, Parsons T, Li P, Ocain T, Xu Y. Identification of a regulatory autophosphorylation site in the serine-threonine kinase RIP2. *Cell Signal.* 2006;18(12):2223-9. doi: 10.1016/j.cellsig.2006.05.005. PubMed PMID: 16824733.
42. Torres CR, Hart GW. Topography and polypeptide distribution of terminal N-acetylglucosamine residues on the surfaces of intact lymphocytes. Evidence for O-linked GlcNAc. *The Journal of biological chemistry.* 1984;259(5):3308-17. Epub 1984/03/10. PubMed PMID: 6421821.
43. Dong DL, Hart GW. Purification and characterization of an O-GlcNAc selective N-acetyl-beta-D-glucosaminidase from rat spleen cytosol. *The Journal of biological chemistry.* 1994;269(30):19321-30. PubMed PMID: 8034696.
44. Wells L, Vosseller K, Hart GW. Glycosylation of nucleocytoplasmic proteins: signal transduction and O-GlcNAc. *Science.* 2001;291(5512):2376-8. Epub 2001/03/28. PubMed PMID: 11269319.
45. Lazarus MB, Nam Y, Jiang J, Sliz P, Walker S. Structure of human O-GlcNAc transferase and its complex with a peptide substrate. *Nature.* 2011;469(7331):564-7. doi: 10.1038/nature09638. PubMed PMID: 21240259; PMCID: PMC3064491.
46. Andres LM, Blong IW, Evans AC, Rumachik NG, Yamaguchi T, Pham ND, Thompson P, Kohler JJ, Bertozzi CR. Chemical Modulation of Protein O-GlcNAcylation via OGT Inhibition Promotes Human Neural Cell Differentiation. *ACS Chem Biol.* 2017. doi: 10.1021/acscchembio.7b00232. PubMed PMID: 28541657.
47. Hart GW, Housley MP, Slawson C. Cycling of O-linked beta-N-acetylglucosamine on nucleocytoplasmic proteins. *Nature.* 2007;446(7139):1017-22. Epub 2007/04/27. doi: 10.1038/nature05815. PubMed PMID: 17460662.
48. Yang YR, Suh PG. O-GlcNAcylation in cellular functions and human diseases. *Advances in biological regulation.* 2014;54:68-73. Epub 2013/11/05. doi: 10.1016/j.jbior.2013.09.007. PubMed PMID: 24184094.

49. Groves JA, Lee A, Yildirim G, Zachara NE. Dynamic O-GlcNAcylation and its roles in the cellular stress response and homeostasis. *Cell stress & chaperones*. 2013;18(5):535-58. Epub 2013/04/27. doi: 10.1007/s12192-013-0426-y. PubMed PMID: 23620203; PMCID: 3745259.
50. Lubas WA, Frank DW, Krause M, Hanover JA. O-Linked GlcNAc transferase is a conserved nucleocytoplasmic protein containing tetratricopeptide repeats. *The Journal of biological chemistry*. 1997;272(14):9316-24. Epub 1997/04/04. PubMed PMID: 9083068.
51. Kreppel LK, Blomberg MA, Hart GW. Dynamic glycosylation of nuclear and cytosolic proteins. Cloning and characterization of a unique O-GlcNAc transferase with multiple tetratricopeptide repeats. *The Journal of biological chemistry*. 1997;272(14):9308-15. Epub 1997/04/04. PubMed PMID: 9083067.
52. Hanover JA, Yu S, Lubas WB, Shin SH, Ragano-Caracciola M, Kochran J, Love DC. Mitochondrial and nucleocytoplasmic isoforms of O-linked GlcNAc transferase encoded by a single mammalian gene. *Archives of biochemistry and biophysics*. 2003;409(2):287-97. Epub 2002/12/31. PubMed PMID: 12504895.
53. Love DC, Kochan J, Cathey RL, Shin SH, Hanover JA. Mitochondrial and nucleocytoplasmic targeting of O-linked GlcNAc transferase. *Journal of cell science*. 2003;116(Pt 4):647-54. Epub 2003/01/23. PubMed PMID: 12538765.
54. Lubas WA, Hanover JA. Functional expression of O-linked GlcNAc transferase. Domain structure and substrate specificity. *The Journal of biological chemistry*. 2000;275(15):10983-8. PubMed PMID: 10753899.
55. Jinek M, Rehwinkel J, Lazarus BD, Izaurralde E, Hanover JA, Conti E. The superhelical TPR-repeat domain of O-linked GlcNAc transferase exhibits structural similarities to importin alpha. *Nat Struct Mol Biol*. 2004;11(10):1001-7. doi: 10.1038/nsmb833. PubMed PMID: 15361863.
56. Alfaro JF, Gong CX, Monroe ME, Aldrich JT, Clauss TR, Purvine SO, Wang Z, Camp DG, 2nd, Shabanowitz J, Stanley P, Hart GW, Hunt DF, Yang F, Smith RD. Tandem mass spectrometry identifies many mouse brain O-GlcNAcylated proteins including EGF domain-specific O-GlcNAc transferase targets. *Proc Natl Acad Sci U S A*. 2012;109(19):7280-5. doi: 10.1073/pnas.1200425109. PubMed PMID: 22517741; PMCID: PMC3358849.
57. Vosseller K, Trinidad JC, Chalkley RJ, Specht CG, Thalhhammer A, Lynn AJ, Snedecor JO, Guan S, Medzihradszky KF, Maltby DA, Schoepfer R, Burlingame AL. O-linked N-acetylglucosamine proteomics of postsynaptic density preparations using

lectin weak affinity chromatography and mass spectrometry. *Mol Cell Proteomics*. 2006;5(5):923-34. doi: 10.1074/mcp.T500040-MCP200. PubMed PMID: 16452088.

58. Wang Z, Udeshi ND, Slawson C, Compton PD, Sakabe K, Cheung WD, Shabanowitz J, Hunt DF, Hart GW. Extensive crosstalk between O-GlcNAcylation and phosphorylation regulates cytokinesis. *Sci Signal*. 2010;3(104):ra2. doi: 10.1126/scisignal.2000526. PubMed PMID: 20068230; PMCID: PMC2866299.

59. Trinidad JC, Barkan DT, Gulledge BF, Thalhammer A, Sali A, Schoepfer R, Burlingame AL. Global identification and characterization of both O-GlcNAcylation and phosphorylation at the murine synapse. *Mol Cell Proteomics*. 2012;11(8):215-29. doi: 10.1074/mcp.O112.018366. PubMed PMID: 22645316; PMCID: PMC3412957.

60. Zargar Z, Tyagi S. Role of host cell factor-1 in cell cycle regulation. *Transcription*. 2012;3(4):187-92. doi: 10.4161/trns.20711. PubMed PMID: 22771988; PMCID: PMC3654768.

61. Goto H, Motomura S, Wilson AC, Freiman RN, Nakabeppu Y, Fukushima K, Fujishima M, Herr W, Nishimoto T. A single-point mutation in HCF causes temperature-sensitive cell-cycle arrest and disrupts VP16 function. *Genes Dev*. 1997;11(6):726-37. PubMed PMID: 9087427.

62. Tyagi S, Herr W. E2F1 mediates DNA damage and apoptosis through HCF-1 and the MLL family of histone methyltransferases. *EMBO J*. 2009;28(20):3185-95. doi: 10.1038/emboj.2009.258. PubMed PMID: 19763085; PMCID: PMC2771094.

63. Julien E, Herr W. Proteolytic processing is necessary to separate and ensure proper cell growth and cytokinesis functions of HCF-1. *EMBO J*. 2003;22(10):2360-9. doi: 10.1093/emboj/cdg242. PubMed PMID: 12743030; PMCID: PMC156000.

64. Capotosti F, Guernier S, Lammers F, Waridel P, Cai Y, Jin J, Conaway JW, Conaway RC, Herr W. O-GlcNAc transferase catalyzes site-specific proteolysis of HCF-1. *Cell*. 2011;144(3):376-88. doi: 10.1016/j.cell.2010.12.030. PubMed PMID: 21295698.

65. Gao Y, Wells L, Comer FI, Parker GJ, Hart GW. Dynamic O-glycosylation of nuclear and cytosolic proteins: cloning and characterization of a neutral, cytosolic beta-N-acetylglucosaminidase from human brain. *The Journal of biological chemistry*. 2001;276(13):9838-45. Epub 2001/01/20. doi: 10.1074/jbc.M010420200. PubMed PMID: 11148210.

66. Comtesse N, Maldener E, Meese E. Identification of a nuclear variant of MGEA5, a cytoplasmic hyaluronidase and a beta-N-acetylglucosaminidase.

Biochemical and biophysical research communications. 2001;283(3):634-40. doi: 10.1006/bbrc.2001.4815. PubMed PMID: 11341771.

67. He Y, Roth C, Turkenburg JP, Davies GJ. Three-dimensional structure of a *Streptomyces svaceus* GNAT acetyltransferase with similarity to the C-terminal domain of the human GH84 O-GlcNAcase. *Acta crystallographica Section D, Biological crystallography*. 2014;70(Pt 1):186-95. Epub 2014/01/15. doi: 10.1107/S1399004713029155. PubMed PMID: 24419391; PMCID: 3919268.

68. Keembiyehetty CN, Krzeslak A, Love DC, Hanover JA. A lipid-droplet-targeted O-GlcNAcase isoform is a key regulator of the proteasome. *Journal of cell science*. 2011;124(Pt 16):2851-60. Epub 2011/08/03. doi: 10.1242/jcs.083287. PubMed PMID: 21807949; PMCID: 3148132.

69. Dennis RJ, Taylor EJ, Macauley MS, Stubbs KA, Turkenburg JP, Hart SJ, Black GN, Vocadlo DJ, Davies GJ. Structure and mechanism of a bacterial beta-glucosaminidase having O-GlcNAcase activity. *Nat Struct Mol Biol*. 2006;13(4):365-71. doi: 10.1038/nsmb1079. PubMed PMID: 16565725.

70. Rao FV, Dorfmueller HC, Villa F, Allwood M, Eggleston IM, van Aalten DM. Structural insights into the mechanism and inhibition of eukaryotic O-GlcNAc hydrolysis. *EMBO J*. 2006;25(7):1569-78. doi: 10.1038/sj.emboj.7601026. PubMed PMID: 16541109; PMCID: PMC1440316.

71. Mohanan V, Grimes CL. The molecular chaperone HSP70 binds to and stabilizes NOD2, an important protein involved in Crohn disease. *The Journal of biological chemistry*. 2014;289(27):18987-98. Epub 2014/05/03. doi: 10.1074/jbc.M114.557686. PubMed PMID: 24790089; PMCID: 4081938.



## Chapter 2

### *O*-GLCNACYLATION OF WILD TYPE NOD2 AND ITS FUNCTION

#### 2.1 Introduction

Bacterial cell wall, peptidoglycan, is a highly-conserved structure found in all bacteria. Peptidoglycan contains a repetition of carbohydrates, N-acetylglucosamine (GlcNAc) and *N*-acetylmuramic acid (Figure 2.1) cross-linked by short chains of peptides to form a lattice surrounding the entire cell (1, 2). Large amounts of GlcNAc and other bacterial cell wall building blocks, such as UDP-GlcNAc, are released during bacterial growth, division and bacterial host invasion (3, 4). GlcNAc is not only important in bacterial cell wall but also serves as a metabolite of the hexosamine biosynthetic pathway (HBP), one endpoint of which is the modification and regulation of proteins by *O*-GlcNAcylation (5).

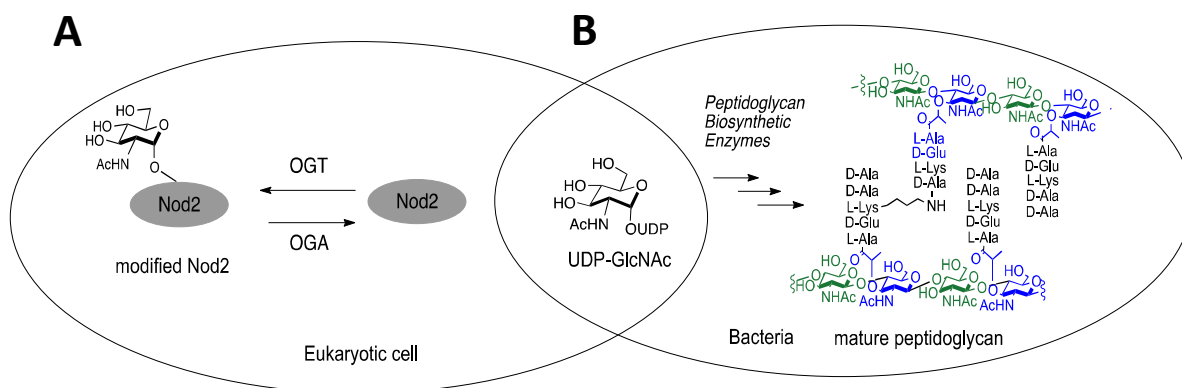


**Figure 2.1: UDP-GlcNAc.** UDP-GlcNAc is used as a substrate for (A) the human enzyme, OGT and (B) the bacterial cell wall biosynthetic enzymes. (Reprinted with permission from Hou et. al., Copyright 2017, Glycobiology)

*O*-GlcNAcylation is a dynamic post translational modification in which the *O*-GlcNAc transferase (OGT) transfers GlcNAc from UDP-GlcNAc to selected serine and threonine residues; whereas *O*-GlcNAcase (OGA) removes *O*-GlcNAc from target proteins (6-8) (Figure 1.5). This modification is found on nuclear, mitochondrial and cytoplasmic proteins(9, 10). *O*-GlcNAc is thought to regulate proteins in a manner analogous to protein phosphorylation, and like phosphorylation the levels of *O*-GlcNAc responds to numerous extra-and intracellular signals, including those that simulate an immune response in lymphocytes such as lipid polysaccharide (LPS) (11) . However, the relationship between GlcNAc, bacterial cell wall fragments and cytoplasmic innate immune receptors, such as Nod2 is still unclear. Here, we define the role of *O*-GlcNAcylation on regulation the stability of Nod2.

## **2.2 Materials and Method**

### **2.2.1 Cell Culture**

HEK293T cell was obtained from the American Type Culture Collection (ATCC, Manassas, VA). HEK293T-Nod2-Myc/K2605 cell is previously described (12). Cells were cultured in DMEM, 10% FBS (Atlantic Biologicals), 2 mM l-glutamine, penicillin-streptomycin and grown in a humidified incubator at 37 °C and 5% CO<sub>2</sub>.

### **2.2.2 Antibodies and Materials**

The mouse monoclonal anti-*O*-GlcNAc antibody, CTD110.6 and RL-2 were produced and purified by Core C4 (Dept. Biological Chemistry, JHU). All other antibodies were purchased from Cell Signaling Technology. Thiamet-G was

purchased from Sigma-Adrich. MDP was purchased from Bachem. 10 X PBS was purchased from Lonza (cat, no: 17-517Q).

### **2.2.3 Co-Immunoprecipitation**

Cells were rinsed with 1X PBS and the lysates were collected using freshly prepared lysis buffer (1% triton X-100, 2 mM EDTA, 4 mM Na<sub>3</sub>PO<sub>4</sub>, 100 mM NaCl, 10 mM MES pH 5.8, 10 mM NaF, 1 protease inhibitor cocktail tablet (Roche)) and lysed by passing through a 20-gauge needle. Aliquots of 1.2 mg of lysates were mixed with 2 µl of antibody and incubated overnight at 4 °C. Lysate-antibody mixture was incubated with 40 µl of Dynabeads protein A (Life Technologies) beads (prewashed in 0.1M sodium phosphate pH8.0 and lysis buffer) for 3 h at 4 °C. After 3 h, lysate-antibody-bead mixture was washed four times using 200 µL of lysis buffer containing varying concentrations of NaCl as follows: Wash 1– 100 mM NaCl, wash 2- 300 mM NaCl, wash 3-500 mM NaCl, wash 4-100 mM NaCl. Proteins were eluted at 100 °C for 5 min with 2X reaction buffer (100 mM TrisHCl pH 6.8, 4% SDS, 12% Glycerol, 0.008% bromophenol blue, 2% BME (β-mercaptoethanol)).

### **2.2.4 Western Blot**

Cells were rinsed with 1X PBS and appropriate amount of lysis buffer (1% triton X-100, 2 mM EDTA, 4 mM Na<sub>3</sub>PO<sub>4</sub>, 100 mM NaCl, 10 mM MES pH 5.8, 10 mM NaF, 1 protease inhibitor tablet) was added and lysed using a 20-gauge needle. Protein quantification was performed by a Bradford assay using Bio-Rad Protein Assay Dye Reagent Concentrate according to the manufacturer's instruction. Samples were prepared using 5X loading buffer (250 mM TrisHCl pH 6.8, 10% SDS, 30% Glycerol 0.02% bromophenol blue, 5% BME) and boiled for 5 min. The samples

were electrophoresed in 7.5% polyacrylamide gels containing 0.1% sodium dodecyl sulfate. Western transfer onto nitrocellulose membrane was carried out using semi-dry transfer at 25 V for 1 h. 10% nonfat dry milk in TBS-Tween (T) was used to block the membrane for 1 h and washed in TBS-T three times for 5 min each. The blots were incubated overnight at 4 °C with the appropriate amount of antibodies prepared in 1% milk (1:1000). After three washes, the membrane was incubated with HRP-conjugated secondary antibody for 60 min at room temperature. Following secondary incubation, the blot was washed three times in TBS-T and incubated with the substrate (Bio-Rad) according to the manufacturer's instruction. The blots were exposed to Fuji Super RX-U Half Speed Blue films (Brandywine Imaging Inc) in the dark room. All western blots were performed at least three times independently. Using the replicates, the data were analyzed using Image Lab<sup>TM</sup>. This analysis is reported alongside all western blot images.

### **2.2.5 Half-life Determination**

Cycloheximide was used at a concentration of 100 µg/ml, and the lysates were collected every 4 h. Thiamet-G (1 µM) was incubated 4 h prior to the addition of cycloheximide. Cells were treated, lysed, quantified for protein content and analyzed by Western blot.

The protein bands for Nod2 and Actin were quantified using Image Lab 5.0. Actin is used as the loading control and the ratio of the intensity of Nod2 to actin bands ( $I_r$ ) were used to analyze the half-life values as previously described (13). Briefly, relative Nod2 band intensities were plotted against time assuming first-order decay ( $\ln(I_r)$  vs. time). The rate constant was calculated using the negative slope of the line ( $k = -\text{slope}$ ), and the corresponding half-life was calculated ( $T_{1/2} = \ln(2)/k$ ). Each

condition was performed in duplicates and the Student's t-tests were used to determine statistical significance.  $P < 0.05$  was considered as statistically significant.

#### **2.2.6 Isolation of Polysomes**

HEK293T-Nod2-Myc cells were seeded in 150 mm dish ( $5 \times 10^6$ ). The next day, cells were treated with 5S-GlcNAc or methanol overnight. 20  $\mu$ l of cycloheximide (100 mg/ml) was added into cells for 5 min before isolation of polysomes. Cells were rinsed with 2 ml of cold PBS twice and lysed in 1.5 ml of old polysomes lysis buffer (100 mM Tris (pH 7.4), 50 mM KCl, 25 mM  $MgCl_2$ , 100  $\mu$ g/ml cycloheximide, 1 mM DTT, 100  $\mu$ M PMSF, 200  $\mu$ g/ml heparin, 50  $\mu$ M N-ethylmaleimide (NEM), 40 U/ml RNase inhibitor, 1 % Triton X-100 and cOmplete mini protease inhibitor) and vortexed for 5 s. Lysates were centrifuged at 17,000 g for 12 min at 4 °C. The supernatants were added on the top of a 1.5 ml of cold 35 % sucrose cushion in buffer (10 mM Tris pH 7.4, 85 mM KCl, and 5 mM  $MgCl_2$ ). After ultracentrifugation of the samples for 2 h at 55,300 rpm in a Beckman Type 60 Ti rotor at 4 °C, the pellets containing polysomes were resuspended in 200  $\mu$ L, pH 7.4, resuspension buffer (50 mM Tris, 100 mM NaCl, 2 mM EDTA, 1% SDS and cOmplete mini protease inhibitor) (14).

#### **2.2.7 Precipitation of Peptidyl-tRNA by CTAB**

50  $\mu$ l of polysomes fraction was mixed with 500  $\mu$ l of 2 % (w/v) cetyltrimethylammonium bromide (CTAB) and vortexed for 5 s. 500  $\mu$ l of 0.5 M sodium acetate (pH 5.4) and 100  $\mu$ g of yeast tRNA were added to induce the precipitation of peptidyl-tRNA at 4 °C for 10 min. Sample was incubated at 30 °C for 10 min and then was collected by centrifugation at 17,000 g for 10 min at room

temperature. Precipitates were washed with 1 % CTAB and 0.25 M sodium acetate at room temperature and then pellet was resuspended in 200 µl resuspension buffer (50 mM Tris, 100 mM NaCl, 2 mM EDTA, 1% SDS and cOmplete mini protease inhibitor) after centrifugation at 17,000 g for 10 min at room temperature (14).

## **2.3 Results**

### **2.3.1 *O*-GlcNAcylation of Nod2**

Nod2 was assayed for the *O*-GlcNAc modification using the GlcNAc-specific antibody, CTD110.6. Briefly, Hek293T cells that stably expresses Nod2 with a Myc epitope tag on the N-terminus (Nod2Myc) (12) were treated with or without the *O*-GlcNAcase inhibitor, Thiamet-G (1 µM, 4 h). Nod2 was immunoprecipitated from cell lysates with an anti-Myc antibody and detected with CTD110.6 (Figure 2.2 A-B). In order to ensure that the antibody, CTD110.6, was truly detecting the *O*-GlcNAcylation modification, the CTD110.6 antibody was preincubated with free GlcNAc and then used in the western blot analysis (Figure 2.2 B-C). When the inhibitor of OGA is present, the level of *O*-GlcNAcylation increases (Figure 2.2 B). When the free GlcNAc is used in the experiment, the band for *O*-GlcNAcylation is no longer present (Figure 2.2 C).

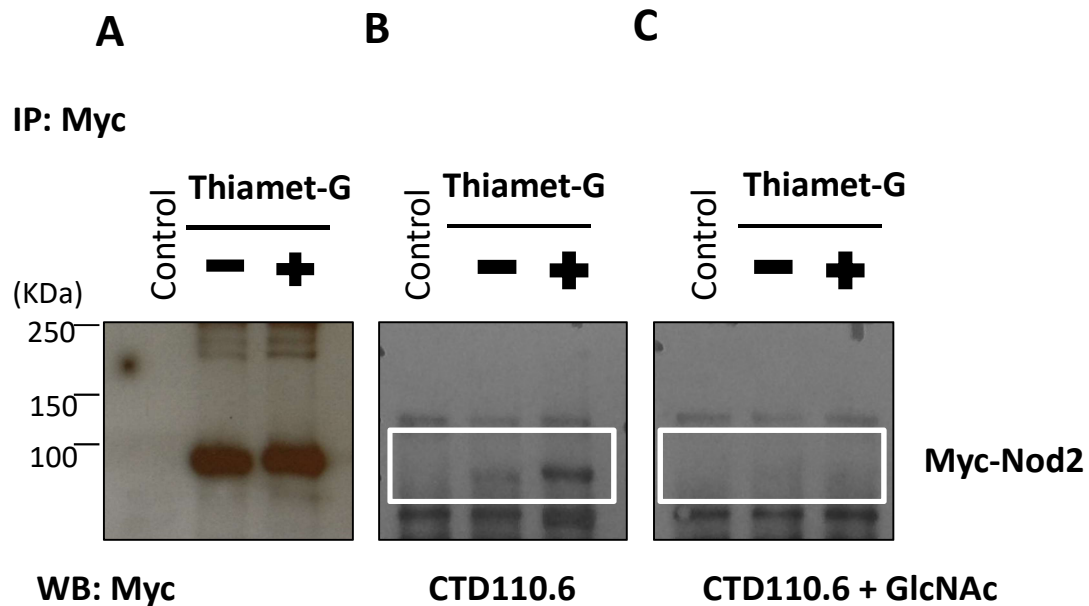


**Figure 2.2: OGT modifies Nod2.** (A) Cell lysates were immunopurified with Myc antibody and blotted with Myc antibody; Control cells do not express Myc-Nod2. Thiamet-G inhibits OGA, elevating *O*-GlcNAcylation. (B) Cell lysates were immunopurified with Nod2 and blotted using CTD110.6. (C) Alternatively, the CTD110.6 was pre-incubated with free GlcNAc (Reprinted with permission from Hou et. al., Copyright 2017, Glycobiology).

Next, the reverse assay was performed using the antibodies (CTD110.6 and RL2) for the *O*-GlcNAc modification and assayed for the presence of Nod2. Nod2 was immunoprecipitated (Figure 2.3). Together these, data demonstrate that Nod2 is post-translationally modified by OGT.

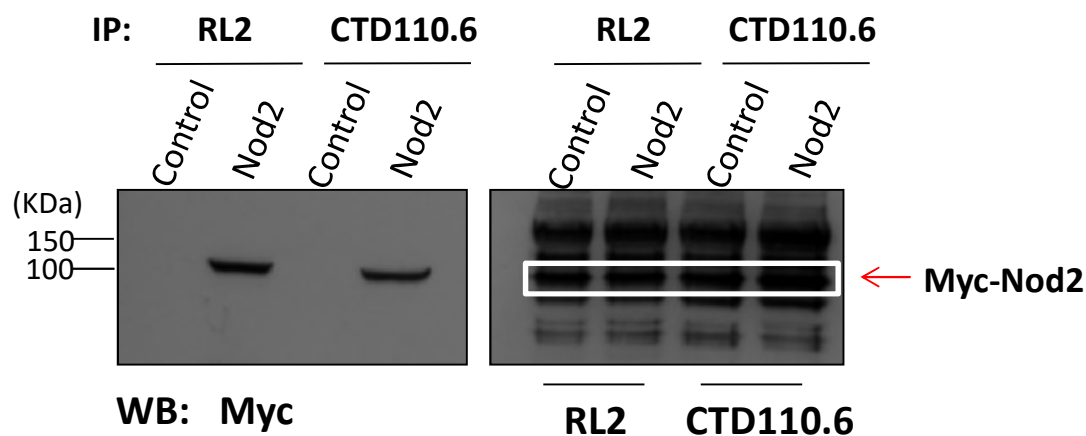


**Figure 2.3: Reverse IP.** Co-IP were performed using 1  $\mu$ l of anti-*O*-GlcNAc (RL2 or CTD110.6) antibody per 200  $\mu$ l of lysates (HEK293T/Nod2Myc cells) and probed for Myc using rabbit-Myc antibody (1:1000), anti-RL2 antibody (1:2000) and anti-CTD110.6 (1:1000) (Reprinted with permission from Hou et. al., Copyright 2017, Glycobiology).

### 2.3.2 *O*-GlcNAcylation Level Regulate Nod2 Half-life in Cells

Previous studies demonstrated that *O*-GlcNAcylation can regulate protein stability and function (15). We hypothesized that this modification could affect Nod2 stability, as it has previously been shown that Nod2 is inheritably unstable. In order to test this, the classical protein half-life experiment using cycloheximide (100  $\mu$ g/ml), a translational inhibitor, was performed (16). When Nod2 is not treated with Thiamet-G, the half-life is  $10.6 \pm 2.4$  h. However, when cells are treated with Thiamet-G (1  $\mu$ M, 4 h), the half-life is  $17.3 \pm 4.5$  h (Figure 2.4 A-C), suggesting that the modification alters the stability of Nod2.



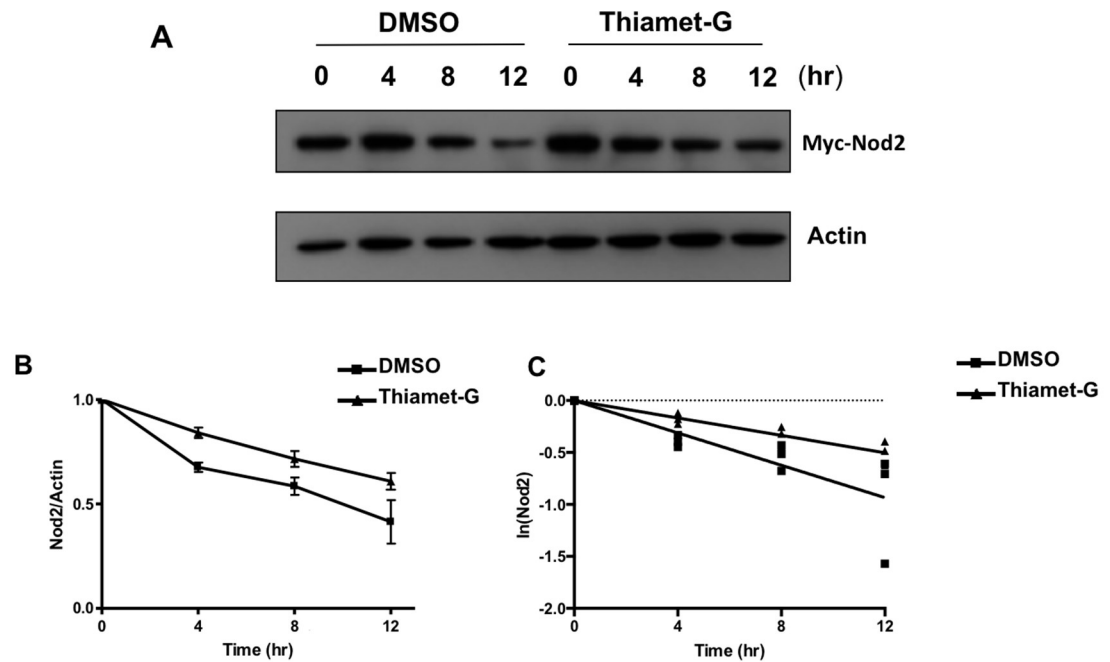


**Figure 2.4: *O*-GlcNAcylation regulates the half-life of Nod2 in cells.** (A) HEK293T-Nod2Myc/Tet-op cells were incubated with 1  $\mu$ M Thiamet-G or DMSO for 4 h, prior to cycloheximide treatment (100  $\mu$ g/ml) at the indicated time intervals. Nod2 was detected by anti-Myc western blotting. (B) Relative amount of Nod2 Myc to actin was plotted from three independent experiments as the means  $\pm$  S.D. (C) The plot of the logarithm of Nod2 versus time for a first-order reaction. (Reprinted with permission from Hou et. al., Copyright 2017, Glycobiology).

### 2.3.3 The Possible of Mechanism of Stabilization

In 2015, Dr. Vocadlo's lab reported that *O*-GlcNAcylation could also occur during nascent protein translation (Figure 2.5A) to prevent proteins from degradation via the ubiquitin- proteasome pathway (14). To test the hypothesis that *O*-GlcNAcylation modulates the stability of Nod2 through this mechanism as well, we isolated polysomes from HEK293T-Nod2-Myc cells after treating with OGT inhibitor, 5S-GlcNAc, overnight (Figure 2.5 B) and then extraction of peptidyl-tRNA by CTAB

(Figure 2.5 C). I found that when 5S-GlcNAc was present, the level of *O*-GlcNAcylation decreases in Nod2 nascent chains (peptidyl-tRNA) from polysomes fractions (Figure 2.5 C-D). This data indicated that Nod2 may utilize *O*-GlcNAcylation to stabilize nascent chains of Nod2 to prevent proteins from degradation via ubiquitin-proteasome pathway. Further experiments are needed to confirm this mechanism.

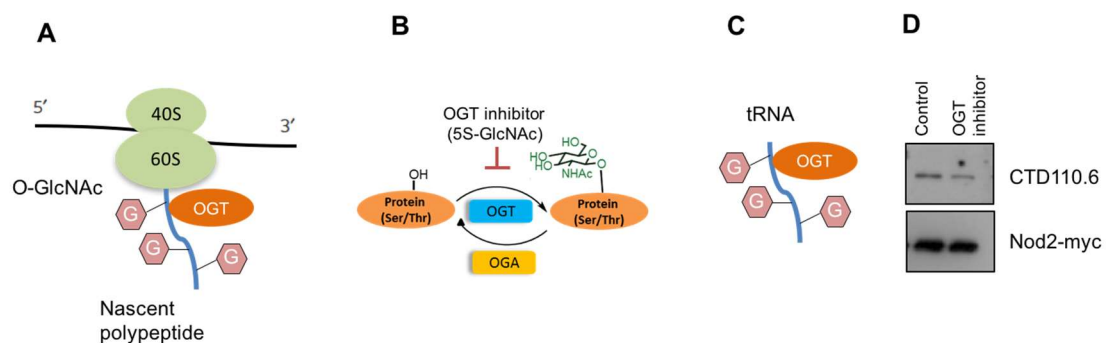


**Figure 2.5: Cotranslational *O*-GlcNAcylation of Nod2 in cells.** (A) *O*-GlcNAcylation also can occur during co-translation of proteins. (B) 5S-GlcNAc, OGT inhibitor, inhibits *O*-GlcNAcylation in cells. (C) Isolation of peptidyl-tRNA by CTAB from polysomes fractions. (D) Nod2 was detected by anti-Myc western blotting.

## 2.4 Discussion

*O*-GlcNAcylation is a dynamic and reversible modification in the cytosol and nucleus (7, 17). OGT catalyzes the *O*-GlcNAcylation of proteins at the serine or threonine residues and OGA removes the *O*-GlcNAc group from proteins (6, 18-20). Previous studies showed that this modification could compete with phosphorylation at the same residues (21), affect protein-protein interactions (22), induce a conformational change of proteins (23), and regulate protein stability (24).

Here, I reported that Nod2 is *O*-GlcNAcylated by OGT via co-IP assay (Figure 2.2-2.3). In addition, using a cycloheximide assay I confirmed that this modification can regulate Nod2 stability and increase the half-life (Figure 2.4). The possible mechanism of this stabilization is that *O*-GlcNAcylation stabilizes nascent polypeptide chains of Nod2 from degradation via ubiquitin- proteasome (Figure 2.5) (14). Next I proposed that by increasing the stability of Nod2 would lead to an increase the activity of Nod2 NF- $\kappa$ B activation? Thus, the following chapter will explain how *O*-GlcNAcylation affects the activity of Nod2.

## REFERENCES

1. van Heijenoort J. Formation of the glycan chains in the synthesis of bacterial peptidoglycan. *Glycobiology*. 2001;11(3):25R-36R. Epub 2001/04/26. PubMed PMID: 11320055.
2. Lovering AL, Safadi SS, Strynadka NC. Structural perspective of peptidoglycan biosynthesis and assembly. *Annual review of biochemistry*. 2012;81:451-78. doi: 10.1146/annurev-biochem-061809-112742. PubMed PMID: 22663080.
3. Park JT, Uehara T. How bacteria consume their own exoskeletons (turnover and recycling of cell wall peptidoglycan). *Microbiology and molecular biology reviews* : MMBR. 2008;72(2):211-27, table of contents. Epub 2008/06/07. doi: 10.1128/MMBR.00027-07. PubMed PMID: 18535144; PMCID: 2415748.
4. Naseem S, Parrino SM, Buenten DM, Konopka JB. Novel roles for GlcNAc in cell signaling. *Communicative & integrative biology*. 2012;5(2):156-9. Epub 2012/07/19. doi: 10.4161/cib.19034. PubMed PMID: 22808320; PMCID: 3376051.
5. Groves JA, Lee A, Yildirim G, Zachara NE. Dynamic O-GlcNAcylation and its roles in the cellular stress response and homeostasis. *Cell stress & chaperones*. 2013;18(5):535-58. Epub 2013/04/27. doi: 10.1007/s12192-013-0426-y. PubMed PMID: 23620203; PMCID: 3745259.
6. Dong DL, Hart GW. Purification and characterization of an O-GlcNAc selective N-acetyl-beta-D-glucosaminidase from rat spleen cytosol. *The Journal of biological chemistry*. 1994;269(30):19321-30. Epub 1994/07/29. PubMed PMID: 8034696.
7. Torres CR, Hart GW. Topography and polypeptide distribution of terminal N-acetylglucosamine residues on the surfaces of intact lymphocytes. Evidence for O-linked GlcNAc. *The Journal of biological chemistry*. 1984;259(5):3308-17. Epub 1984/03/10. PubMed PMID: 6421821.
8. Wells L, Vosseller K, Hart GW. Glycosylation of nucleocytoplasmic proteins: signal transduction and O-GlcNAc. *Science*. 2001;291(5512):2376-8. Epub 2001/03/28. PubMed PMID: 11269319.

9. Holt GD, Haltiwanger RS, Torres CR, Hart GW. Erythrocytes contain cytoplasmic glycoproteins. O-linked GlcNAc on Band 4.1. *The Journal of biological chemistry*. 1987;262(31):14847-50. Epub 1987/11/05. PubMed PMID: 3117790.
10. Hart GW, Housley MP, Slawson C. Cycling of O-linked beta-N-acetylglucosamine on nucleocytoplasmic proteins. *Nature*. 2007;446(7139):1017-22. Epub 2007/04/27. doi: 10.1038/nature05815. PubMed PMID: 17460662.
11. Raetz CR, Whitfield C. Lipopolysaccharide endotoxins. *Annual review of biochemistry*. 2002;71:635-700. Epub 2002/06/05. doi: 10.1146/annurev.biochem.71.110601.135414. PubMed PMID: 12045108; PMCID: 2569852.
12. Mohanan V, Grimes CL. The molecular chaperone HSP70 binds to and stabilizes NOD2, an important protein involved in Crohn disease. *The Journal of biological chemistry*. 2014;289(27):18987-98. Epub 2014/05/03. doi: 10.1074/jbc.M114.557686. PubMed PMID: 24790089; PMCID: 4081938.
13. Belle A, Tanay A, Bitincka L, Shamir R, O'Shea EK. Quantification of protein half-lives in the budding yeast proteome. *Proc Natl Acad Sci U S A*. 2006;103(35):13004-9. Epub 2006/08/19. doi: 10.1073/pnas.0605420103. PubMed PMID: 16916930; PMCID: 1550773.
14. Zhu Y, Liu TW, Cecioni S, Eskandari R, Zandberg WF, Vocadlo DJ. O-GlcNAc occurs cotranslationally to stabilize nascent polypeptide chains. *Nature chemical biology*. 2015;11(5):319-25. Epub 2015/03/17. doi: 10.1038/nchembio.1774. PubMed PMID: 25774941.
15. Chu CS, Lo PW, Yeh YH, Hsu PH, Peng SH, Teng YC, Kang ML, Wong CH, Juan LJ. O-GlcNAcylation regulates EZH2 protein stability and function. *P Natl Acad Sci USA*. 2014;111(4):1355-60. doi: DOI 10.1073/pnas.1323226111. PubMed PMID: ISI:000330231100042.
16. Schneider-Poetsch T, Ju J, Eyler DE, Dang Y, Bhat S, Merrick WC, Green R, Shen B, Liu JO. Inhibition of eukaryotic translation elongation by cycloheximide and lactimidomycin. *Nature chemical biology*. 2010;6(3):209-17. Epub 2010/02/02. doi: 10.1038/nchembio.304. PubMed PMID: 20118940; PMCID: 2831214.
17. Holt GD, Hart GW. The subcellular distribution of terminal N-acetylglucosamine moieties. Localization of a novel protein-saccharide linkage, O-linked GlcNAc. *The Journal of biological chemistry*. 1986;261(17):8049-57. PubMed PMID: 3086323.

18. Haltiwanger RS, Holt GD, Hart GW. Enzymatic addition of O-GlcNAc to nuclear and cytoplasmic proteins. Identification of a uridine diphospho-N-acetylglucosamine:peptide beta-N-acetylglucosaminyltransferase. *The Journal of biological chemistry*. 1990;265(5):2563-8. PubMed PMID: 2137449.
19. Kreppel LK, Blomberg MA, Hart GW. Dynamic glycosylation of nuclear and cytosolic proteins. Cloning and characterization of a unique O-GlcNAc transferase with multiple tetratricopeptide repeats. *The Journal of biological chemistry*. 1997;272(14):9308-15. Epub 1997/04/04. PubMed PMID: 9083067.
20. Vocadlo DJ. O-GlcNAc processing enzymes: catalytic mechanisms, substrate specificity, and enzyme regulation. *Curr Opin Chem Biol*. 2012;16(5-6):488-97. doi: 10.1016/j.cbpa.2012.10.021. PubMed PMID: 23146438.
21. Hart GW, Slawson C, Ramirez-Correa G, Lagerlof O. Cross talk between O-GlcNAcylation and phosphorylation: roles in signaling, transcription, and chronic disease. *Annual review of biochemistry*. 2011;80:825-58. doi: 10.1146/annurev-biochem-060608-102511. PubMed PMID: 21391816; PMCID: PMC3294376.
22. Yang X, Su K, Roos MD, Chang Q, Paterson AJ, Kudlow JE. O-linkage of N-acetylglucosamine to Sp1 activation domain inhibits its transcriptional capability. *Proc Natl Acad Sci U S A*. 2001;98(12):6611-6. doi: 10.1073/pnas.111099998. PubMed PMID: 11371615; PMCID: PMC34401.
23. Simanek EE, Huang DH, Pasternack L, Machajewski TD, Seitz O, Millar DS, Dyson HJ, Wong CH. Glycosylation of threonine of the repeating unit of RNA polymerase II with beta-linked N-acetylglucosamine leads to a turnlike structure. *Journal of the American Chemical Society*. 1998;120(45):11567-75. doi: DOI 10.1021/ja982312w. PubMed PMID: WOS:000077119600005.
24. Yang WH, Kim JE, Nam HW, Ju JW, Kim HS, Kim YS, Cho JW. Modification of p53 with O-linked N-acetylglucosamine regulates p53 activity and stability. *Nat Cell Biol*. 2006;8(10):1074-83. doi: 10.1038/ncb1470. PubMed PMID: 16964247.

## Chapter 3

### INFLAMMATION AND *O*-GLCNACYLATION

#### 3.1 Introduction

The inflammatory response uses a variety of signaling pathways that control expression of both pro- and anti- inflammatory mediators in cells. The NF- $\kappa$ B pathway is one of these signaling pathways (1). NF- $\kappa$ B, a transcription factor, is involved in many biological pathways, for example, inflammation, cell survival, immune response, growth and development (2-3). There are five NF- $\kappa$ B transcription factor families identified: p65 (RelA), RelB, c-Rel, p105/p50 and p100/p52 (4-6). Regulation of the NF- $\kappa$ B pathway is crucial in inflammation and misregulation of this pathway has been linked to chronic inflammation, autoimmunity, and cancers (2, 7).

Post-translational modifications, such as phosphorylation and ubiquitination, are involved in activation of NF- $\kappa$ B. In non- stimulated cells, NF- $\kappa$ B is inhibited by inhibitor of  $\kappa$ B (I $\kappa$ B) in the cytosol. After stimulation, I $\kappa$ B is phosphorylated by the I $\kappa$ B kinase (IKK). It leads to degradation of I $\kappa$ B by ubiquitination and free NF- $\kappa$ B translocates into the nucleus to activate NF- $\kappa$ B pathways (Figure 1.4) (8).

Several studies also show that *O*-GlcNAcylation plays a role in the activation of NF- $\kappa$ B by regulation of IKK $\beta$  activity, inhibition of the interaction of NF- $\kappa$ B with I $\kappa$ B, and promotion of NF- $\kappa$ B acetylation (9-11). For example, RelA (NF- $\kappa$ B p65) is *O*-GlcNAcylated on T532 which decreases its affinity for I $\kappa$ B and lead to translocation of RelA into the nucleus (11).

In contrast, other manuscripts indicate that *O*-GlcNAcylation decreases the activation of NF- $\kappa$ B. *O*-GlcNAcylation of p65 NF- $\kappa$ B decreases NF- $\kappa$ B activation by increasing association of the NF- $\kappa$ B with I $\kappa$ B (12). Therefore, *O*-GlcNAcylation has distinctive effects on the NF- $\kappa$ B pathway.

Here I used the dual luciferase assay (13) to investigate NF- $\kappa$ B activation of Nod2 upon MDP stimulation in cells. MDP is a well-known fragment from both Gram-negative and Gram-positive bacteria that can activate the NF- $\kappa$ B and MAP kinase pathways in a Nod2 dependent manner (14-17). Using this established NF- $\kappa$ B luciferase reporter assay, I have shown *O*-GlcNAcylation can regulate Nod2- induced NF- $\kappa$ B activity.

## **3.2 Materials and Methods**

### **3.2.1 Cell Culture**

HEK293T, a human embryonic kidney cell line, and HCT116, a human colon epithelial cell line, cells were obtained from the American Type Culture Collection (ATCC, Manassas, VA). HEK293T-Nod2-Myc/Tet-op cell is previously described (13) . Cells were cultured in DMEM, 10% FBS (Atlantic Biologicals), 2 mM l-glutamine, penicillin-streptomycin and grown in a humidified incubator at 37 °C and 5% CO<sub>2</sub>.

### **3.2.2 Materials**

Thiamet-G was purchased from Sigma-Adrich. MDP was purchased from Bachem. Dual-luciferase reporter assay kit was purchased from Promega. Lipofectamine LTX was purchased from ThermoFisher. 10 X PBS was purchased from Lonza (cat, no: 17-517Q).



### 3.2.3 Luciferase Reporter Assay

An aliquot of 10 ng pGL4.32 (luc2P/NF- $\kappa$ B-RE/Hygro), 1 ng pRL *Renilla* luciferase reporter vector, 0.1 ng of Nod2-CMV vector were transfected to cells (seeding density =  $5 \times 10^4$ ) in a 24 well dish using Lipofectamine LTX. Cells were pre-incubated with Thiamet-G for 4 h and then incubated with stimuli for 5 h, and the lysates were collected to perform the Dual-Luciferase Reporter Assay (Promega) and were normalized to *Renilla* activity. Relative luciferase activity of firefly to *Renilla* is plotted. Results shown are the means  $\pm$  S.D. of experiments.

## 3.3 Results

### 3.3.1 Titration of *O*-GlcNAc Level by Thiamet-G in Cells

To evaluate the effect of concentration of Thiamet-G, an OGA inhibitor ( $K_i$  = 20 nM for human OGA) (18), in cells, I treated cells with different concentrations of Thiamet-G at different times. Thiamet-G inhibits that *O*-GlcNAc is removed by OGA and leads to an increased amount of *O*-GlcNAcylation in cells (18). As expected, Thiamet-G induction for at least 2 h and 100 nM increased *O*-GlcNAcylation levels in cells. It reached a maximum after 4 h of treatment (100 nM) and remained at this level for 6 h (Figure 3.1). There is no huge difference of band intensity between 100 nM and 200 nM of Thiamet-G. Therefore, 100 nM of Thiamet-G will be performed in luciferase reporter assay.

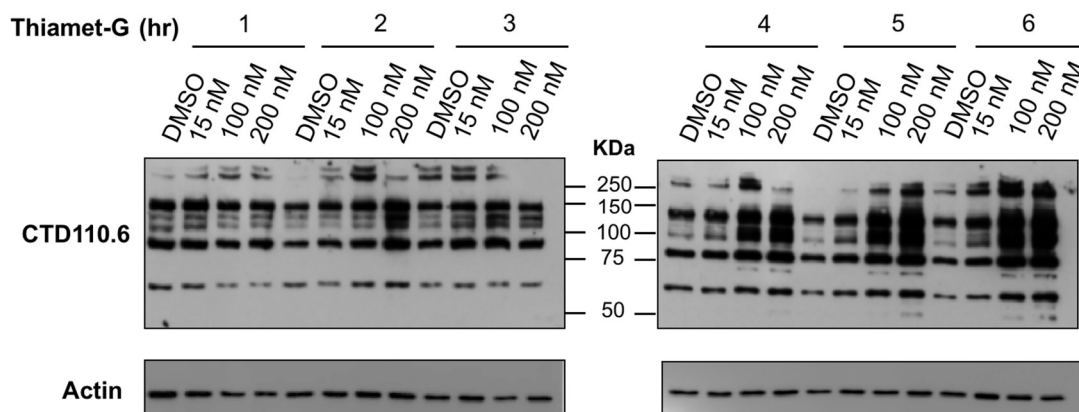


**Figure 3.1: Titration of *O*-GlcNAcylation level in cells.** Western blot studies of HEK293T-Nod2Myc/Tet-op cells incubated with DMSO or different concentration of Thiamet-G for different periods of time. Global *O*-GlcNAc as detected by anti-CTD110.6 (1:1000) (upper) is increased. Actin (1:1000) was used as a loading control (lower).

### 3.3.2 *O*-GlcNAcylation Regulates NF- $\kappa$ B Signaling

Nod2 is known to activate the NF- $\kappa$ B pathway upon stimulation by MDP, triggering an inflammatory response. In order to determine the impact of *O*-GlcNAcylation on Nod2 dependent NF- $\kappa$ B signaling, an established NF- $\kappa$ B luciferase reporter assay was employed (13). The data show that Nod2 increased NF- $\kappa$ B activation when *O*-GlcNAcylation levels were increased in both Nod2-transfected (HEK293T) (Figure 3.2) and stable expressed Nod2 (HEK293T-Nod2-Myc/Tet-op) cells (Figure 3.3), and increased *O*-GlcNAcylation does not generally activate NF- $\kappa$ B.

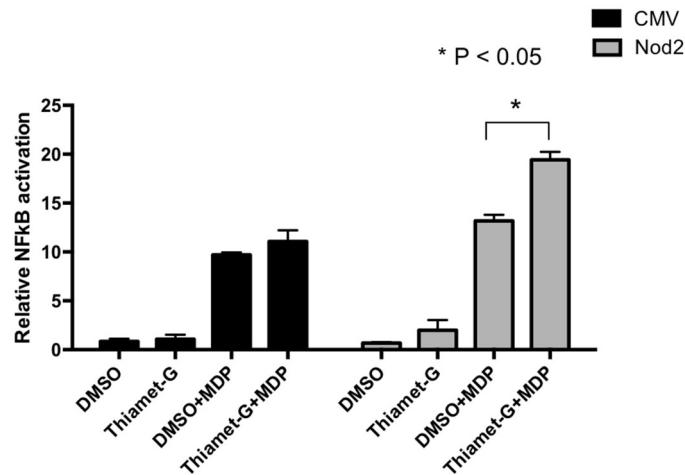


**Figure 3.2: NF-κB activation of Nod2-transfected (HEK293T) cells line.** Dual-luciferase assay performed on stable expressed Nod2 (HEK293T-Nod2-Myc/Tet-op) cells in the presence of 100 nM Thiamet-G or DMSO for 4 h. After 4 h, cells were incubated with 20 μM MDP for 5 h, harvested, and tested for luciferase activity. \*  $p < 0.05$  was considered as significant. CMV (empty vector) was used as a control.

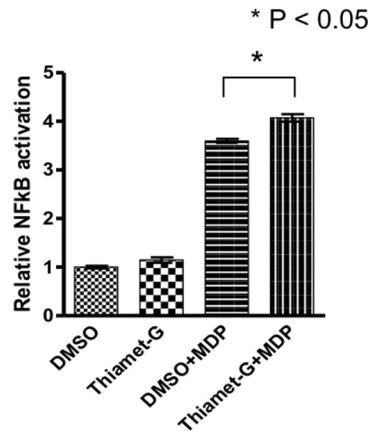


**Figure 3.3: NF-κB activation of stable expressed Nod2 (HEK293T-Nod2-Myc/Tet-op) cells line.** Dual-luciferase assay performed on Nod2-transfected cells in the presence of 100 nM Thiamet-G or DMSO for 4 h. After 4 h, cells were incubated with 20 μM MDP for 5 h, harvested, and tested for luciferase activity. \*  $p < 0.05$  was considered as significant. (Reprinted with permission from Hou et. al., Copyright 2017, Glycobiology)

In order to detect if endogenous Nod2 also has the same effect of NF- $\kappa$ B activation upon Thiamet-G treatment, HCT-116 cells were tested. HCT-116 is an intestinal epithelial that has been shown to endogenously express Nod2. Our results showed that Nod2 increased NF- $\kappa$ B activation when *O*-GlcNAcylation level was increased using Thiamet-G in cells. The same trend was observed in endogenous Nod2 (HCT-116) cells line (Figure 3.4).

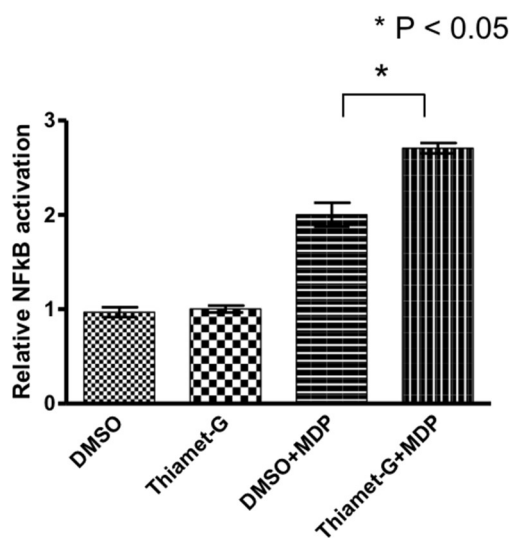


**Figure 3.4: NF- $\kappa$ B activation of HCT-116 cells line.** Dual- luciferase assay performed on Nod2-transfected cells in the presence of 100 nM Thiamet-G or DMSO for 4 h. After 4 h, cells were incubated with 20  $\mu$ M MDP for 5 h, harvested, and tested for luciferase activity. \*  $p < 0.05$  was considered as significant.

### **3.3.3 *O*-GlcNAcylation Regulates NF- $\kappa$ B Signaling through Nod2, Not through Other Downstream NF- $\kappa$ B Proteins**

In addition, to determine if this was an effect primarily on Nod2 or other downstream NF- $\kappa$ B proteins, Tumor necrosis factor- $\alpha$  (TNF- $\alpha$ ), which is not dependent on Nod2, was used. TNF- $\alpha$  is a member of a super family of tumor necrosis factors (TNFs) involved in inflammation and it signals through two transmembrane receptors, TNFR1 and TNFR2 (19). TNF- $\alpha$  can bind to both TNFR1 and TNFR2 to respond to different signals. Activation of TNFR1 is the major cause for inflammatory responses (20, 21). Once TNF- $\alpha$  binds to TNFR1, it leads to silencer of death domain (SODD) released from TNFR1 and dimerizes TNFR1. The dimerized TNFR1 then binds to TNF receptor-associated death domain (TRADD), which recruits receptor interacting protein-1 (RIP-1), TNFR-associated factor 2 (TRAF2), and a serine/threonine kinase (IKK). IKK then mediates polyubiquitination of NF- $\kappa$ B inhibitor, IKK $\gamma$ , and activate NF- $\kappa$ B pathway (22-24). TNF- $\alpha$  is induced upon inflammatory stimulation such as lipopolysaccharide (LPS), other bacterial fragments, and interleukin (IL-1)(25). We found that Thiamet-G did not potentiate TNF- $\alpha$  dependent activation of NF- $\kappa$ B, suggesting that in the context of MDP activation, *O*-GlcNAc is acting on directly Nod2 (Figure 3.5)

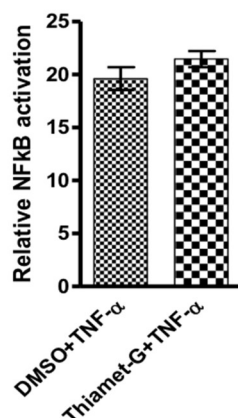


**Figure 3.5: NF-κB activation of stable expressed Nod2 (HEK293T-Nod2-Myc/Tet-op) cells line.** Dual-luciferase assay performed on Nod2-transfected cells in the presence of 200 nM TNF-α or DMSO for 4 h. After 4 h, cells were incubated with 20 μM MDP for 5 h, harvested, and tested for luciferase activity. \*  $p < 0.05$  was considered as significant. (Reprinted with permission from Hou et. al., Copyright 2017, Glycobiology)

### 3.3.4 O-GlcNAcylation Is Not Increased upon MDP Treatment

*N*-Acetylglucosamine (GlcNAc), an important structure of bacterial cell wall peptidoglycan, and fungal cell wall chitin, is involved in cell signaling in bacteria and fungi. Human fungal pathogen *Candida albicans* changes its morphology from budding yeast cells to long filamentous hyphal after GlcNAc stimulation(26). In addition, GlcNAc also regulates cell signals of pathogenic *E. coli*. GlcNAc reduced production of CURLI (27). CURLI fibers are required for pathogenic *E. coli* to attach host cells through biofilm formation, adhesion, and the internalization (28). Interestingly, previous studies also showed that GlcNAc is involved in cell signaling in mammalian cells through *O*-GlcNAcylation. There are many mechanisms to convert GlcNAc to UDP-GlcNAc in cells. For example, GlcNAc can be converted to GlcNAc-6-phosphatate (GlcNAc-6-P) by GlcNAc kinase (NAGK) through the

GlcNAc salvage pathway. It then enters HBP pathway to be processed to UDP-GlcNAc (29, 30). Besides, exogenous GlcNAc can be taken up by a glucose transporter and then is processed to UDP-GlcNAc (31) (Figure 3.6).

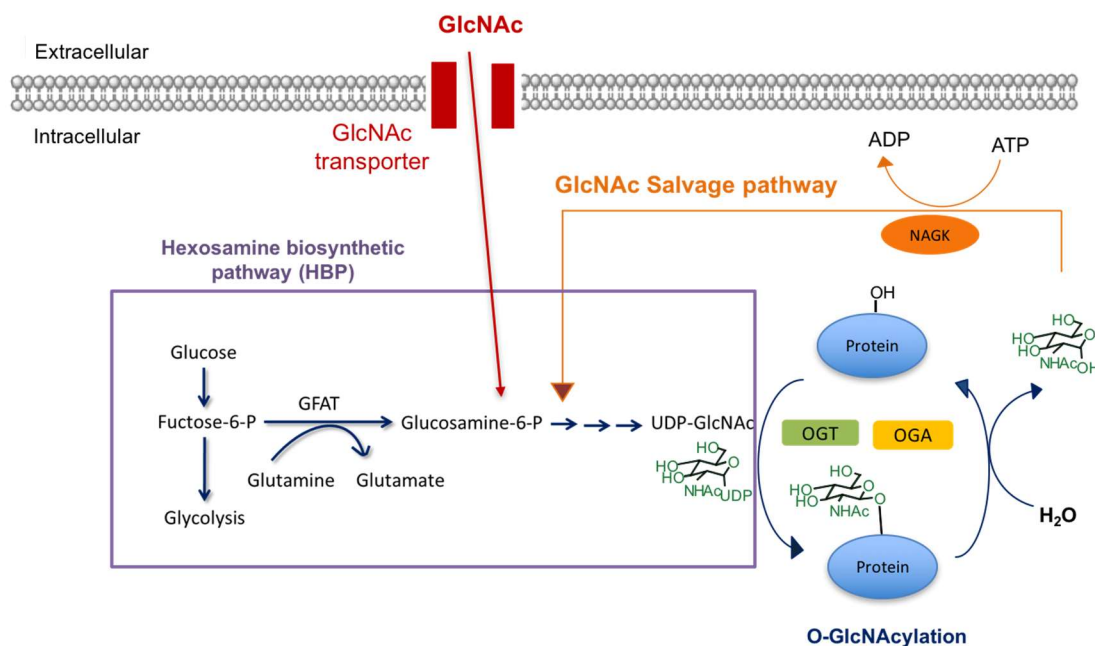


**Figure 3.6: The cycling of *O*-GlcNAcylation.** The substrate of OGT, UDP-GlcNAc, is produced by hexosamine biosynthetic pathway (HBP), GlcNAc salvage pathway. In addition, free GlcNAc is taken by GlcNAc transporter and then converted to UDP-GlcNAc through HBP

MDP is structurally similar to GlcNAc (Figure 3.7), both contain sugar structures (GlcNAc) and they differ only through the attachment of a lactic acid moiety at the 3 position of the carbohydrate. We assayed the ability of Nod2 GlcNAcylation levels to increase in the presence of MDP. There was no difference in *O*-GlcNAcylation levels upon MDP treatment in the presence or absence of Thiamet-

G (Figures 3.8). This suggests that the increase in NF- $\kappa$ B activity when treated with Thiamet-G is a result of increased stability of Nod2, either by modification with GlcNAc or other mechanisms.

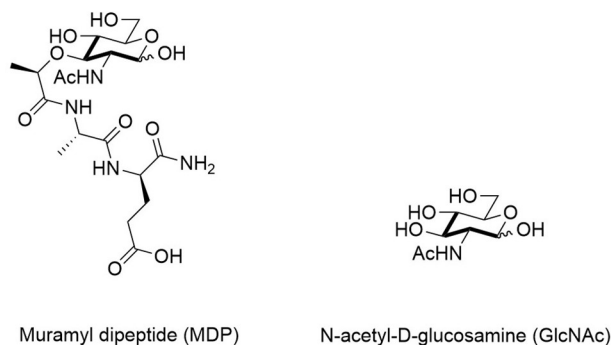


**Figure 3.7: The structure of MDP and GlcNAc.** The structure of MDP shown in left. The structure of GlcNAc shown in right.

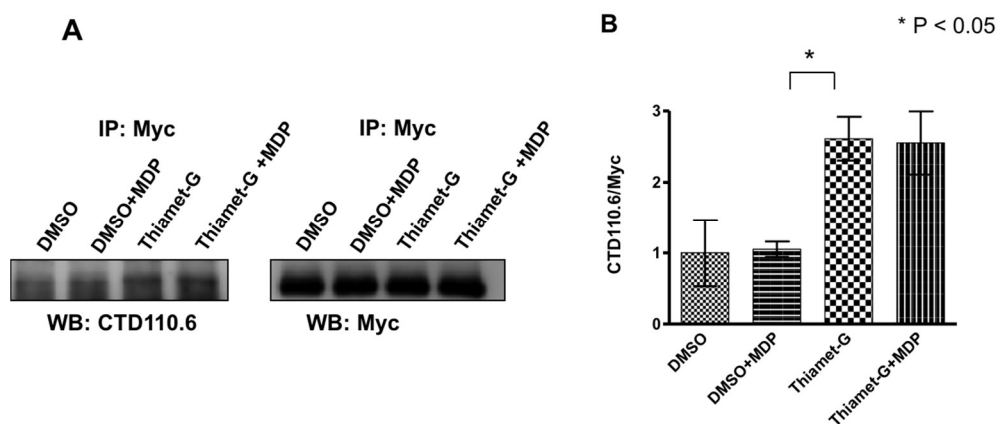


**Figure 3.8: The level of *O*-GlcNAcylation in cells.** (A) HEK293T-Nod2-Myc/Tet-op cell lysates ( $\pm$ Thiamet-G (1  $\mu$ M, 4 h),  $\pm$ MDP (20  $\mu$ M, 5h)) were immunopurified with Myc antibody and blotted with anti-CTD110.6 antibody; Control cells do not express Myc-Nod2. (B) Relative amount of CTD110.6 to Nod2 Myc was plotted from three independent experiments as the mean  $\pm$ S.D. (Reprinted with permission from Hou et. al., Copyright 2017, Glycobiology)



### 3.4 Discussion

The nuclear factor NF- $\kappa$ B pathway plays an important role in inflammation by promoting the expression of inflammatory genes including cytokines, adhesion molecules, and chemokines upon cellular stimulation, such as stress or pathogens (3). MDP, a fragment from the bacterial cell wall, is well known to activate NF- $\kappa$ B pathway through Nod2 signaling (32). However, the luciferase reporter assay that detects NF- $\kappa$ B activation is easy to influence. For example, increasing the amount of Nod2 DNA or the concentration of MDP can induce huge activation levels of NF- $\kappa$ B (33). Therefore, the luciferase reporter assay need to be performed properly (34).

In order to exclude this influence, we inputted empty vector (CMV) as a control for background activation. We could detect significant activation of NF- $\kappa$ B through Nod2, but not empty vector, upon treatment of Thiamet-G plus MDP (Figure 3.2). Besides using empty vector as a control, I also precisely control how much of Nod2 DNA (0.1  $\mu$ g) is used in experiment to avoid high background activation. Thus, I will perform same transfection conditions for Nod2 variants to investigate the function of this modification in the following chapters.

## REFERENCES

1. Akira S, Uematsu S, Takeuchi O. Pathogen recognition and innate immunity. *Cell*. 2006;124(4):783-801. PubMed PMID: 16497588.
2. Hoesel B, Schmid JA. The complexity of NF-kappaB signaling in inflammation and cancer. *Mol Cancer*. 2013;12:86. doi: 10.1186/1476-4598-12-86. PubMed PMID: 23915189; PMCID: PMC3750319.
3. Baldwin AS, Jr. The NF-kappa B and I kappa B proteins: new discoveries and insights. *Annual review of immunology*. 1996;14:649-83. doi: 10.1146/annurev.immunol.14.1.649. PubMed PMID: 8717528.
4. Sen R, Baltimore D. Inducibility of kappa immunoglobulin enhancer-binding protein NF-kappa B by a posttranslational mechanism. *Cell*. 1986;47(6):921-8. PubMed PMID: 3096580.
5. Oeckinghaus A, Ghosh S. The NF-kappaB family of transcription factors and its regulation. *Cold Spring Harb Perspect Biol*. 2009;1(4):a000034. doi: 10.1101/cshperspect.a000034. PubMed PMID: 20066092; PMCID: PMC2773619.
6. Sen R, Baltimore D. Multiple nuclear factors interact with the immunoglobulin enhancer sequences. *Cell*. 1986;46(5):705-16. PubMed PMID: 3091258.
7. Napetschnig J, Wu H. Molecular basis of NF-kappaB signaling. *Annu Rev Biophys*. 2013;42:443-68. doi: 10.1146/annurev-biophys-083012-130338. PubMed PMID: 23495970; PMCID: PMC3678348.
8. Lawrence T. The nuclear factor NF-kappaB pathway in inflammation. *Cold Spring Harb Perspect Biol*. 2009;1(6):a001651. doi: 10.1101/cshperspect.a001651. PubMed PMID: 20457564; PMCID: PMC2882124.
9. Kawauchi K, Araki K, Tobiume K, Tanaka N. Loss of p53 enhances catalytic activity of IKKbeta through O-linked beta-N-acetyl glucosamine modification. *Proc Natl Acad Sci U S A*. 2009;106(9):3431-6. doi: 10.1073/pnas.0813210106. PubMed PMID: 19202066; PMCID: PMC2651314.

10. Allison DF, Wamsley JJ, Kumar M, Li D, Gray LG, Hart GW, Jones DR, Mayo MW. Modification of RelA by O-linked N-acetylglucosamine links glucose metabolism to NF-kappaB acetylation and transcription. *Proc Natl Acad Sci U S A*. 2012;109(42):16888-93. doi: 10.1073/pnas.1208468109. PubMed PMID: 23027940; PMCID: PMC3479489.
11. Yang WH, Park SY, Nam HW, Kim DH, Kang JG, Kang ES, Kim YS, Lee HC, Kim KS, Cho JW. NFkappaB activation is associated with its O-GlcNAcylation state under hyperglycemic conditions. *Proc Natl Acad Sci U S A*. 2008;105(45):17345-50. doi: 10.1073/pnas.0806198105. PubMed PMID: 18988733; PMCID: PMC2582288.
12. Xing D, Gong K, Feng W, Nozell SE, Chen YF, Chatham JC, Oparil S. O-GlcNAc modification of NFkappaB p65 inhibits TNF-alpha-induced inflammatory mediator expression in rat aortic smooth muscle cells. *PloS one*. 2011;6(8):e24021. doi: 10.1371/journal.pone.0024021. PubMed PMID: 21904602; PMCID: PMC3164132.
13. Mohanan V, Grimes CL. The molecular chaperone HSP70 binds to and stabilizes NOD2, an important protein involved in Crohn disease. *The Journal of biological chemistry*. 2014;289(27):18987-98. Epub 2014/05/03. doi: 10.1074/jbc.M114.557686. PubMed PMID: 24790089; PMCID: 4081938.
14. Kobayashi KS, Chamaillard M, Ogura Y, Henegariu O, Inohara N, Nunez G, Flavell RA. Nod2-dependent regulation of innate and adaptive immunity in the intestinal tract. *Science*. 2005;307(5710):731-4. PubMed PMID: 15692051.
15. Girardin SE, Travassos LH, Herve M, Blanot D, Boneca IG, Philpott DJ, Sansonetti PJ, Mengin-Lecreulx D. Peptidoglycan molecular requirements allowing detection by Nod1 and Nod2. *The Journal of biological chemistry*. 2003;278(43):41702-8. PubMed PMID: 12871942.
16. Girardin SE, Boneca IG, Viala J, Chamaillard M, Labigne A, Thomas G, Philpott DJ, Sansonetti PJ. Nod2 is a general sensor of peptidoglycan through muramyl dipeptide (MDP) detection. *The Journal of biological chemistry*. 2003;278(11):8869-72. PubMed PMID: 12527755.
17. Ting JP, Duncan JA, Lei Y. How the noninflammasome NLRs function in the innate immune system. *Science*. 2010;327(5963):286-90. Epub 2010/01/16. doi: 10.1126/science.1184004. PubMed PMID: 20075243.
18. Yuzwa SA, Shan X, Macauley MS, Clark T, Skorobogatko Y, Vosseller K, Vocadlo DJ. Increasing O-GlcNAc slows neurodegeneration and stabilizes tau against

aggregation. *Nature chemical biology*. 2012;8(4):393-9. doi: 10.1038/nchembio.797. PubMed PMID: 22366723.

19. Banner DW, D'Arcy A, Janes W, Gentz R, Schoenfeld HJ, Broger C, Loetscher H, Lesslauer W. Crystal structure of the soluble human 55 kd TNF receptor-human TNF beta complex: implications for TNF receptor activation. *Cell*. 1993;73(3):431-45. PubMed PMID: 8387891.

20. Shalaby MR, Sundan A, Loetscher H, Brockhaus M, Lesslauer W, Espevik T. Binding and regulation of cellular functions by monoclonal antibodies against human tumor necrosis factor receptors. *The Journal of experimental medicine*. 1990;172(5):1517-20. PubMed PMID: 2172437; PMCID: PMC2188665.

21. Sheehan KC, Pinckard JK, Arthur CD, Dehner LP, Goeddel DV, Schreiber RD. Monoclonal antibodies specific for murine p55 and p75 tumor necrosis factor receptors: identification of a novel in vivo role for p75. *The Journal of experimental medicine*. 1995;181(2):607-17. PubMed PMID: 7836916; PMCID: PMC2191879.

22. Hsu H, Xiong J, Goeddel DV. The TNF receptor 1-associated protein TRADD signals cell death and NF-kappa B activation. *Cell*. 1995;81(4):495-504. PubMed PMID: 7758105.

23. Hsu H, Huang J, Shu HB, Baichwal V, Goeddel DV. TNF-dependent recruitment of the protein kinase RIP to the TNF receptor-1 signaling complex. *Immunity*. 1996;4(4):387-96. PubMed PMID: 8612133.

24. Takeuchi M, Rothe M, Goeddel DV. Anatomy of TRAF2. Distinct domains for nuclear factor-kappaB activation and association with tumor necrosis factor signaling proteins. *The Journal of biological chemistry*. 1996;271(33):19935-42. PubMed PMID: 8702708.

25. Walsh LJ, Trinchieri G, Waldorf HA, Whitaker D, Murphy GF. Human dermal mast cells contain and release tumor necrosis factor alpha, which induces endothelial leukocyte adhesion molecule 1. *Proc Natl Acad Sci U S A*. 1991;88(10):4220-4. PubMed PMID: 1709737; PMCID: PMC51630.

26. Naseem S, Parrino SM, Buenten DM, Konopka JB. Novel roles for GlcNAc in cell signaling. *Communicative & integrative biology*. 2012;5(2):156-9. Epub 2012/07/19. doi: 10.4161/cib.19034. PubMed PMID: 22808320; PMCID: 3376051.

27. Barnhart MM, Lynem J, Chapman MR. GlcNAc-6P levels modulate the expression of Curli fibers by *Escherichia coli*. *Journal of bacteriology*.

2006;188(14):5212-9. doi: 10.1128/JB.00234-06. PubMed PMID: 16816193; PMCID: PMC1539958.

28. Barnhart MM, Chapman MR. Curli biogenesis and function. *Annu Rev Microbiol.* 2006;60:131-47. doi: 10.1146/annurev.micro.60.080805.142106. PubMed PMID: 16704339; PMCID: PMC2838481.

29. Bueding E, Mackinnon JA. Hexokinases of *Schistosoma mansoni*. *The Journal of biological chemistry.* 1955;215(2):495-506. PubMed PMID: 13242546.

30. Hinderlich S, Berger M, Schwarzkopf M, Effertz K, Reutter W. Molecular cloning and characterization of murine and human N-acetylglucosamine kinase. *Eur J Biochem.* 2000;267(11):3301-8. PubMed PMID: 10824116.

31. Schleicher ED, Weigert C. Role of the hexosamine biosynthetic pathway in diabetic nephropathy. *Kidney Int Suppl.* 2000;77:S13-8. PubMed PMID: 10997685.

32. Inohara N, Ogura Y, Chen FF, Muto A, Nunez G. Human Nod1 confers responsiveness to bacterial lipopolysaccharides. *The Journal of biological chemistry.* 2001;276(4):2551-4. Epub 2000/11/04. doi: 10.1074/jbc.M009728200. PubMed PMID: 11058605.

33. Murray PJ. NOD proteins: an intracellular pathogen-recognition system or signal transduction modifiers? *Curr Opin Immunol.* 2005;17(4):352-8. doi: 10.1016/j.coi.2005.05.006. PubMed PMID: 15950446.

34. Beutler B. Autoimmunity and apoptosis: the Crohn's connection. *Immunity.* 2001;15(1):5-14. PubMed PMID: 11485733.

## Chapter 4

### ***O*-GLCNACYLATION REGULATES THE STABILITY AND ACTIVITY OF NOD2 VARIANTS**

#### **4.1 Introduction**

Crohn's disease (CD) is one of the major chronic inflammatory bowel disorders that affects 700,000 people in the United States. The causes of CD were unknown until 1996, when Hugot discovered that a sensitivity locus for CD on chromosome 16 (1). In 2001, he identified three independent associations for CD: two point mutations of Nod2 (R702W and G908W) and a frameshift variant (1007fs) (2).

It has been shown that the Nod2 Crohn's mutants are defective in their abilities to signal the presence of bacterial cell wall fragments (3). Moreover, it has been shown that stabilization of Nod2 via over-expression of HSP70 restores the ability for the mutants to signal (4). Therefore, the Nod2 Crohn's mutants are less stable, leading to decreased protein levels and ability to activate NF- $\kappa$ B. We considered that the Nod2 Crohn's mutants could be modified by OGT and the *O*-GlcNAc modification of Nod2 could affect the ability of the mutants stability and ability to signal.

In order to determine this hypothesis, we designed a lentiviral system that would allow cells to over-express Nod2 variants, so that this modification could be detected using antibody (CTD110.6). Using this system, I have discovered that three Nod2 mutants correlated to Crohn's disease are *O*-GlcNAcylated.

We also utilized another viral system, a tetracycline inducible retroviral system, that was developed by Dr. Blau's laboratory (5). These cells were used for stability

and activity assays. This inducible system would allow us to control the expression of protein in cells. I found that *O*-GlcNAcylation can regulate Nod2 stability and activity.

## **4.2 Materials and Methods**

### **4.2.1 Cell Culture**

HEK293T cell was obtained from the American Type Culture Collection (ATCC, Manassas, VA). Cells were cultured in DMEM, 10% FBS (Atlantic Biologicals), 2 mM l-glutamine, penicillin-streptomycin and grown in a humidified incubator at 37 °C and 5% CO<sub>2</sub>.

### **4.2.2 Antibodies and Materials**

The mouse monoclonal anti-*O*-GlcNAc antibody, CTD110.6 was produced and purified by Core C4 (Dept. Biological Chemistry, JHU). All other antibodies were purchased from Cell Signaling Technology. Thiamet-G was purchased from Sigma-Adrich. MDP was purchased from Bachem. Lipofectamine LTX was purchased from ThermoFisher. 10 X PBS was purchased from Lonza (cat, no: 17-517Q). Liquid nitrogen was purchased from local provider.

### **4.2.3 Vector Construction**

K2605-Nod2-R702W-Myc, K2605-Nod2G908R-Myc, and K2605-Nod2-1007fs-Myc were constructed by digestion with *Bam*H1 and *Xho*1 from pBKCMV vectors containing the various Nod2 variants and ligated into K2605 lentiviral vector. The ligated products were transformed into DH5 $\alpha$  competent cells.

HRSp- Nod2-R702W-Myc, HRSp-Nod2-G908R-Myc, and HRSp-Nod2-1007fs-Myc were constructed by digestion with *Bgl*II and *Asc*I from pBKCMV

vectors containing the various Nod2 variants and ligated into HRSp retroviral vectors. The ligated products were transformed into HB101 competent cells.

#### **4.2.4 Cell transfection and Lentiviral Transduction**

HEK293T cells were seeded in a 6-well plate (seeding density =  $5 \times 10^5$ ). The next day, cells were transfected with K2605-Nod2-R702W-Myc, K2605-Nod2-G908R-Myc, and K2605-Nod2-1007fs-Myc lentiviral vectors individually along with helper plasmid (pCMV $\Delta$ R8.2) and the envelope plasmid in the proportion of 4:3:1 (2: 1.5: 0.5  $\mu$ g for cells in a 6-well plate). DNA was transfected into cells using Lipofectamine LTX (500  $\mu$ l of Opti-MEM and 6  $\mu$ l of LTX). Medium was changed the next day after transfection. After 8 h, medium containing the viral vector particles were collected and then filtered (0.45  $\mu$ M). The packaged vectors were added to the cell line to be stably transduced along with polybrene (10  $\mu$ g/ml final concentration). The vector transduced cells were selected by puromycin (12  $\mu$ g/ml final concentration).

#### **4.2.5 Cell Transfection and Retroviral Transduction**

There are two steps to make stable Nod2 mutants via retroviral system:

(1) Making stable cell lines having transactivator (RTAb) and transrepressor (RTRg): Phoenix-E cells were seeded in a 6-well plate (seeding density =  $5 \times 10^5$ ). The next day, 2  $\mu$ g of retroviral RTAb and RTRg DNA were transfected into cells using Lipofectamine LTX (500  $\mu$ l of Opti-MEM and 5  $\mu$ l of LTX). Medium was changed the next day after transfection. After 8 h, medium containing the viral vector particles was collected and then filtered (0.45  $\mu$ M). The packaged vectors were added to the



cell line (HEK293T) to be stably transduced along with polybrene (10 µg/ml final concentration).

(2) Making Nod2 variants in RTRb/RTAg stable cell lines: Phoenix-E cells were seeded in a 6-well plate (seeding density =  $5 \times 10^5$ ). The next day, 2 µg of HRSp-Nod2-R702W-Myc, HRSp-Nod2-G908R-Myc, and HRSp-Nod2-1007fs-Myc DNA were transfected into cells individually using Lipofectamine LTX (500 µl of Opti-MEM and 5 µl of LTX). Medium was changed the next day after transfection. After 8 h, medium containing the viral vector particles was collected and then filtered (0.45 µM). The packaged vectors were added to the cell line (RTRb/RTAg) to be stably transduced along with polybrene (10 µg/ml final concentration).

#### **4.2.6 Co-Immunoprecipitation**

Cells were rinsed with 1X PBS and the lysates were collected using freshly prepared lysis buffer (1% triton X-100, 2 mM EDTA, 4 mM Na<sub>3</sub>PO<sub>4</sub>, 100 mM NaCl, 10 mM MES pH 5.8, 10 mM NaF, 1 protease inhibitor cocktail tablet (Roche)) and lysed by passing through a 20-gauge needle. 1.2 mg of lysates were mixed with 2 µl of antibody and incubated overnight at 4 °C. Lysate-antibody mixture was incubated with 40 µl of Dynabeads protein A (Life Technologies) beads (prewashed in 0.1M sodium phosphate pH8.0 and lysis buffer) for 3 h at 4 °C. After 3 h, lysate-antibody-bead mixture was washed four times using 200 µL of lysis buffer containing varying concentrations of NaCl as follows: Wash 1– 100 mM NaCl, wash 2- 300 mM NaCl, wash 3- 500 mM NaCl, wash 4- 100 mM NaCl. Proteins were eluted at 100 °C for 5 min with 2X reaction buffer (100 mM TrisHCl pH 6.8, 4% SDS, 12% Glycerol, 0.008% bromophenol blue, 2% BME (β-mercaptoethanol)).

#### **4.2.7 Western Blot**

Cells were rinsed with 1X PBS and appropriate amount of lysis buffer (1% triton X-100, 2 mM EDTA, 4 mM Na<sub>3</sub>PO<sub>4</sub>, 100 mM NaCl, 10 mM MES pH 5.8, 10 mM NaF, 1 protease inhibitor tablet) was added and lysed using a 20-gauge needle. Protein quantification was performed by a Bradford assay using Bio-Rad Protein Assay Dye Reagent Concentrate according to the manufacturer's instruction. Samples were prepared using 5X loading buffer (250 mM TrisHCl pH 6.8, 10% SDS, 30% Glycerol 0.02% bromophenol blue, 5% BME) and boiled for 5 min. The samples were electrophoresed in 7.5% polyacrylamide gels containing 0.1% sodium dodecyl sulfate. Western transfer onto nitrocellulose membrane was carried out using semi-dry transfer at 25 V for 1 h. 10% nonfat dry milk in TBS-Tween (T) was used to block the membrane for 1 h and washed in TBS-T three times for 5 min each. The blots were incubated overnight at 4 °C with the appropriate amount of antibodies prepared in 1% milk (1:1000). After three washes, the membrane was incubated with HRP-conjugated secondary antibody for 60 min at room temperature. Following secondary incubation, the blot was washed three times in TBS-T and incubated with the substrate (Bio-Rad) according to the manufacturer's instruction. The blots were exposed to Fuji Super RX-U Half Speed Blue films (Brandywine Imaging Inc) in the dark room. All western blots were performed at least three times independently. Using the replicates, the data were analyzed using Image Lab™. This analysis is reported alongside all western blot images.

#### **4.2.8 Luciferase Reporter Assay**

An aliquot of 10 ng pGL4.32 (luc2P/NF-κB-RE/Hygro), 1 ng pRL *Renilla* luciferase reporter vector, 0.1 ng of Nod2-CMV vector were transfected to cells

(seeding density =  $5 \times 10^4$ ) in a 24 well dish using Lipofectamine LTX. Cells were pre-incubated with Thiamet-G for 4 h and then incubated with stimuli for 5 h, and the lysates were collected to perform the Dual-Luciferase Reporter Assay (Promega) and were normalized to *Renilla* activity. Relative luciferase activity of firefly to *Renilla* is plotted. Results shown are the means  $\pm$  S.D. of experiments.

#### **4.2.9 Half-life Determination**

Cycloheximide was used at a concentration of 100  $\mu\text{g/ml}$ , and the lysates were collected every 4 h. Thiamet-G (1  $\mu\text{M}$ ) was incubated 4 h prior to the addition of cycloheximide. Cells were treated, lysed, quantified for protein content and analyzed by Western blot.

The protein bands for Nod2 and Actin were quantified using Image Lab 5.0. Actin is used as the loading control and the ratio of the intensity of Nod2 to actin bands ( $I_r$ ) were used to analyze the half-life values as previously described (6). Briefly, relative Nod2 band intensities were plotted against time assuming first-order decay ( $\ln(I_r)$  vs. time). The rate constant was calculated using the negative slope of the line ( $k = -\text{slope}$ ), and the corresponding half-life was calculated ( $T_{1/2} = \ln(2)/k$ ). Each condition was performed in duplicates and the Student's t-tests were used to determine statistical significance.  $P < 0.05$  was considered as statistically significant.

#### **4.2.10 Cellular Thermal Shift Assay (CETSA)**

Cells were seeded ( $5\sim 6 \times 10^6$ ) in a 100-mm dish. The next day, cells were treated with Thiamet-G (1  $\mu\text{M}$ , 4 h) or DMSO. After 4 h, cells were rinsed with 1X PBS with protease inhibitors twice and then transferred the cells by using 4 mL of PBS with protease inhibitors into 15-mL tubes. The tubes were centrifuged at 150 g

for 5 min at room temperature and the cells were resuspended with 500  $\mu$ l of PBS with protease inhibitor. 27  $\mu$ l of cells were added in each PCR tube. The PCR tubes were heated at different temperature (40-70  $^{\circ}$ C) for 3 min in the thermocycler. After heating, the tubes were removed immediately and incubated at room temperature for 3 min. After 3 min, the samples were snap-frozen immediately with liquid nitrogen and kept at -80  $^{\circ}$ C overnight.

The next day, the samples were freeze-thawed twice with liquid nitrogen and a water bath at 25  $^{\circ}$ C. The tubes were vortexed after thawing and then centrifuged at 20,000 g for 20 min in the cold room (4  $^{\circ}$ C). After centrifugation, 24  $\mu$ l of supernatant was added a new microfuge tube and 6  $\mu$ l of 5X loading dye was added. Samples were heated at 100  $^{\circ}$ C for 8 min and then Western blot protocol was followed.

#### **4.2.11 Site-directed Mutagenesis**

The S933A mutation was introduced in Nod2 using GeneArt<sup>®</sup> Site-Directed Mutagenesis PLUS System kit on the Nod2/pBKCMV plasmid per the manufacturer's instructions. Primers for S933A of Nod2 are previously described (7). The presence of mutation in Nod2 was verified via sequencing. Nod2(S933A)/K2605 vector was constructed by digesting Nod2(S933A) from Nod2(S933A)/pBKCMV vector using BamH1 and Xho1 enzymes. The ligated products were transformed into competent cells. The presence of the insert within the construct was confirmed by DNA sequencing (GENEWIZ, Inc). The mutant Nod2(S933A)/K2605 was used to make a stable cell line.

### 4.3 Results

#### 4.3.1 Construction of Nod2 Mutants Expressing Stable Cell Lines via Lentiviral System

K2605 lentiviral vectors containing Nod2 mutants were constructed as described under methods. Stable cell lines of HEK293T cells (Nod2-R702W-Myc/K2605, Nod2-G908R-Myc/K2605, and Nod2-1007fs-Myc/K2605) that express Nod2 mutants with a Myc tag under the K2605 lentiviral system were constructed as previously described (Figure 4.1A) (8, 9). We successfully obtained these three Nod2 mutants expressing stable cell lines (Figure 4.1B) via lentiviral system.

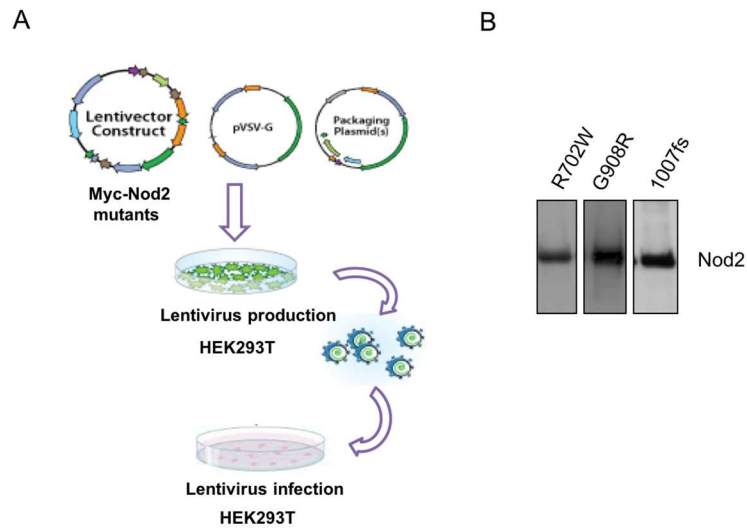


**Figure 4.1: HEK293T stable cell lines expressing Nod2 mutants.** (A) HEK293T cells are used to produce lentiviral particles containing Nod2 mutants with helper plasmid (pCMV $\Delta$ R8.2) and the envelope plasmid and then transduced into HEK293T cell. Stable cell lines were developed after puromycin selection. (B) Cell lysates from HEK293T-Nod2-R702W-Myc/K2605, HEK293T-Nod2-G908R-Myc/K2605, and HEK293T-Nod2-1007fs-Myc/K2605 were probed for Myc antibody (1:1000).

### 4.3.2 *O*-GlcNAcylation of Nod2 Variants (R702W, G908R, and 1007fs)

Nod2 variants correlated to Crohn's disease are R702W, G908R and 1007fs. R702W and G908R are point mutation from arginine to tryptophan at residue 702 and glycine to arginine at residue 908. 1007fs is a frame shift mutation translating a truncated protein (2, 10-12). These three variants are not mutated at serine or threonine residues where the *O*-GlcNAc modification occur (13, 14). We believe that these three major Nod2 mutants correlated to Crohn's disease are *O*-GlcNAcylated.

In order to prove this hypothesis, I performed a co-immunoprecipitation assay in the HEK293T-Nod2-R702W-Myc/K2605, HEK293T-Nod2-G908R-Myc/K2605, and HEK293T-Nod2-1007fs-Myc/K2605 cell lines that were treated with or without the *O*-GlcNAcase inhibitor, Thiamet-G (1  $\mu$ M, 4 h). Nod2 mutants were immunoprecipitated from cell lysates with an anti-Myc antibody and detected with CTD110.6. I confirmed these three Nod2 mutants are *O*-GlcNAcylated (Figure 4.2).

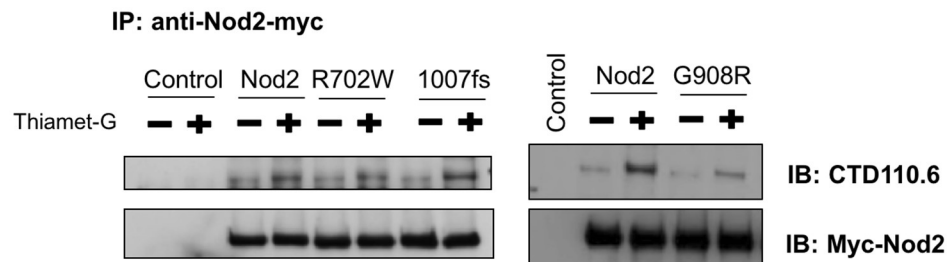


**Figure 4.2: OGT modifies Nod2 mutants.** Cell lysates HEK293T-Nod2-Myc/K2605, HEK293T-Nod2-R702W-Myc/K2605, HEK293T-Nod2-G908R-Myc/K2605, and HEK293T-Nod2-1007fs-Myc/K2605 cell lines were immunopurified with Myc antibody and blotted with CTD110.6. and Myc antibodies; Control cells do not express Myc-Nod2. Thiamet-G inhibits OGA, elevating *O*-GlcNAcylation.

### 4.3.3 Construction of Doxycycline Regulated Nod2 Mutants Expressing Stable Cell Lines

HRSp plasmids having Nod2 variants (HRSp-Nod2-R702W-Myc, HRSp-Nod2-G908R-Myc, and HRSp-Nod2-1007fs-Myc) were constructed as described in methods. Stable cell lines of HEK293T cells that express doxycycline inducible Nod2 mutants-Myc under the control of Retro-TET-ART system were developed via retroviral system. There are three plasmids involved in this system: HRSp-Nod2 mutants-Myc, transactivator (RTAb) and transrepressor (RTRg) (5, 15-17) (Figure 4.3).

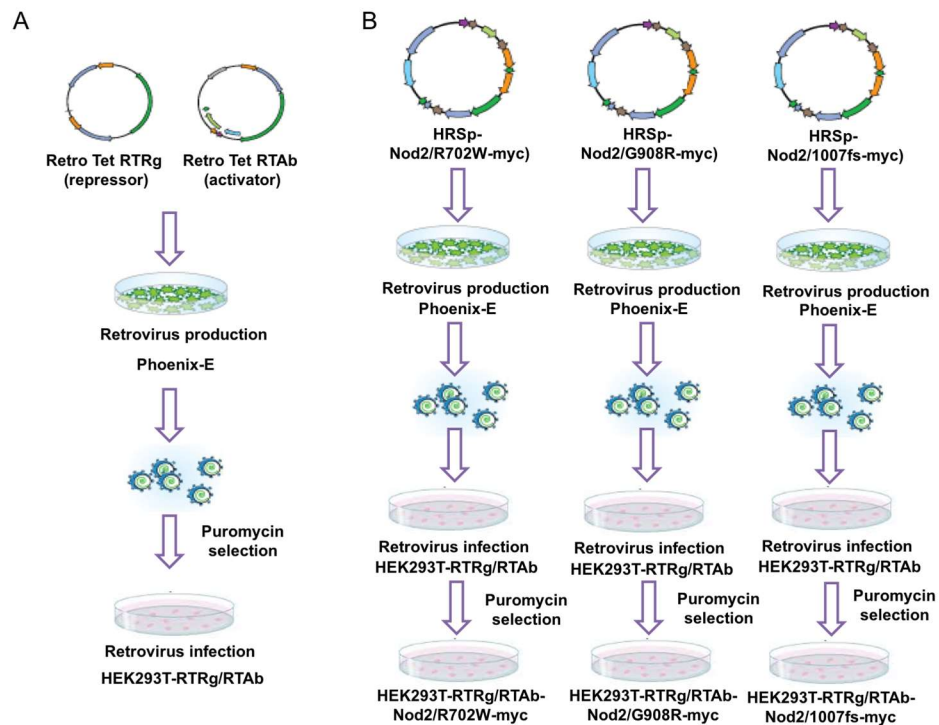


**Figure 4.3: Procedure of stable cell lines expressing doxycycline regulated Nod2 mutants.** (A) Phoenix-E cells are used to make retrovirus. First, retrovirus expressing containing RTRg and RTAb vectors is generated and transduced into HEK293T cells. (B) Second, retrovirus having HRSp-Nod2-R702W-Myc, HRSp-Nod2-G908R-Myc, or HRSp-Nod2-1007fs-Myc were generated by Phoenix-E cells individually and then transduced into HEK293T-RTRg/RTAb cells to create doxycycline regulated Nod2 mutants after puromycin.

#### 4.3.4 Doxycycline Regulated Nod2 Mutants Expression

Retro-TET-ART system was used to create stable cell lines expressing proteins. This system can control protein level by inducers, tetracycline or doxycycline, and is dose dependent (5). I successfully generated stable cell lines of Nod2 mutants having an N-terminal Myc tag in HEK293T cells (HEK293T-Nod2-R702W-Myc/Tet-op, HEK293T-Nod2-G908R-Myc/Tet-op, HEK293T-Nod2-1007fs-Myc/Tet-op cells) The data showed that Nod2 protein levels increased with an increasing concentration of doxycycline, a tetracycline derivative (Figure 4.4) (17, 18).

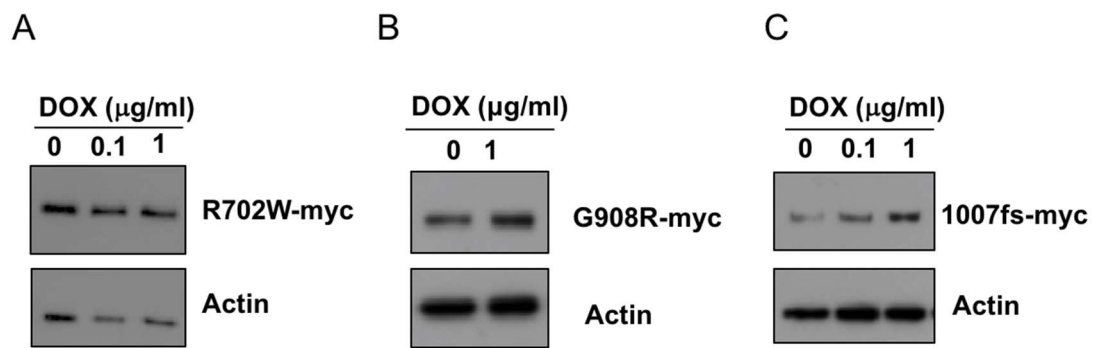


**Figure 4.4: Doxycycline regulated Nod2 mutants expression in HEK293T cells.** (A) Cell lysates from HEK293T-Nod2-R702W-Myc/Tet-op cell line induced at different concentration of doxycycline were probed for Myc antibody (1:1000) to detect the amount of Nod2 expressed. Actin antibody (1:1000) was a loading control. (B) Cell lysates from HEK293T-Nod2-G908R-Myc/Tet-op cell line induced at different concentration of doxycycline were probed for Myc antibody (1:1000) to detect the amount of Nod2 expressed. Actin antibody (1:1000) was a loading control. (C) Cell lysates from HEK293T-Nod2-1007fs-Myc/Tet-op cell line induced at different concentration of doxycycline were probed for Myc antibody (1:1000) to detect the amount of Nod2 expressed. Actin antibody (1:1000) was a loading control.



#### 4.3.5 *O*-GlcNAcylation Regulated the Stability of Nod2 Variant (R702W)

*O*-GlcNAcylation increased both the stability and activity of wild type Nod2, so we hypothesized that this modification had the same effect on the Crohn's disease associated Nod2 variants. When *O*-GlcNAcylation level is increased in HEK293T-RTRg/RTAb-Nod2-R702W-myc cell line by treating with Thiamet-G, an OGA inhibitor, the levels of Nod2 protein in cells is increased compared to DMSO treatment. Increasing the levels of the *O*-GlcNAcylation increased the half-life of the mutant Nod2 from  $8.1 \pm 1.7$  h to  $15.0 \pm 1.8$  h (Figure 4.5).

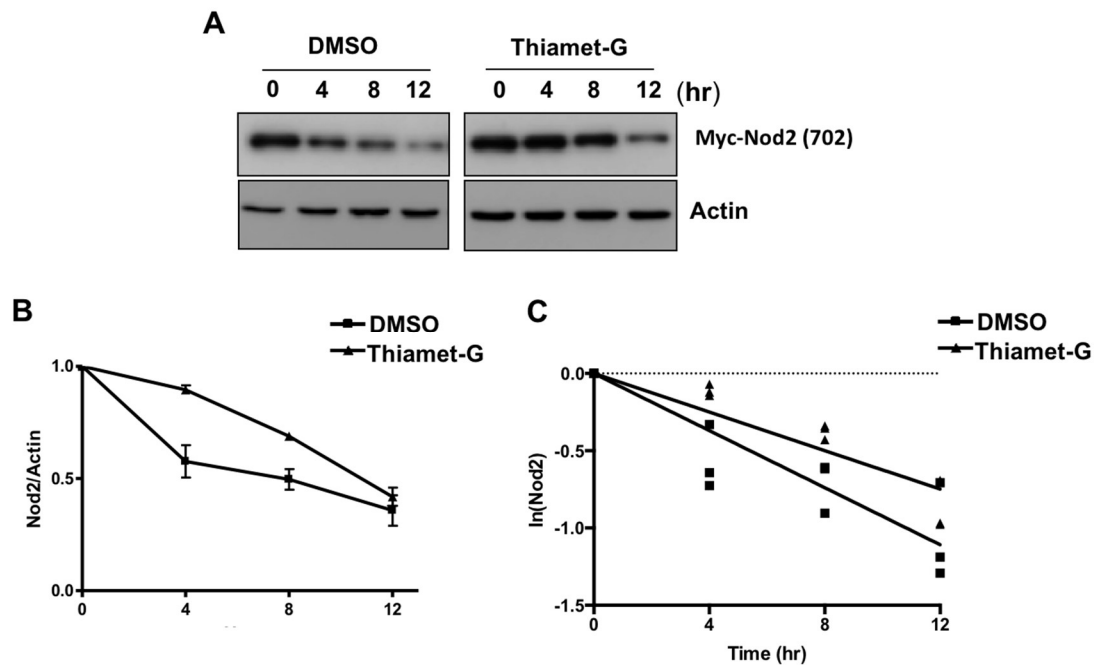


**Figure 4.5: *O*-GlcNAcylation regulated the stability of Nod2 mutant (R702W) in cells.** (A) HEK293T-Nod2-R702W-Myc/Tet-op cells were incubated with 1  $\mu$ M Thiamet-G or DMSO for 4 h, and before cycloheximide treatment (100  $\mu$ g/ml) at the indicated time intervals. Nod2 was detected by anti-Myc western blotting. (B) Relative amount of Nod2 Myc to actin was plotted from three independent experiments as the means  $\pm$  S.D. (C) The plot of the logarithm of Nod2 versus time for a first-order reaction. (Reprinted with permission from Hou et. al., Copyright 2017, Glycobiology)

#### 4.3.6 *O*-GlcNAcylation Regulated the Activity of Nod2 Variant (R702W)

In addition, when the level of the *O*-GlcNAcylation modification is increased with Thiamet-G, I observed that cells had a significant increase in MDP- induced NF- $\kappa$ B activity (Figure 4.6). These data indicated that *O*-GlcNAc modification is able to regulate the stability and activity of Nod2 mutant (R702W) in cells.

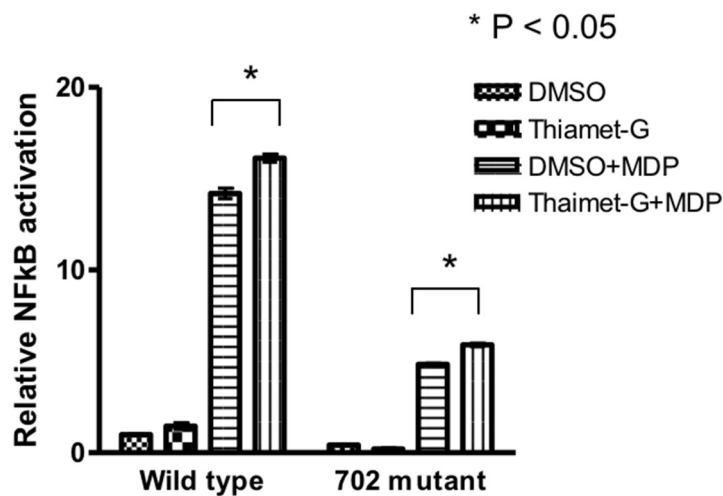


**Figure 4.6: *O*-GlcNAcylation regulated the activity of Nod2 mutant (R702W) in cells.** Dual-luciferase assay performed on HEK293T transfected with 0.1ng 702 plasmid in the presence of 100 nM Thiamet-G or DMSO for 4 h. After 4 h cells were incubated with 20  $\mu$ M MDP for 5h, harvested, and tested for luciferase activity. \* p < 0.05 was considered as significant. (Reprinted with permission from Hou et. al., Copyright 2017, Glycobiology)

#### 4.3.7 *O*-GlcNAcylation Did Not Regulate the Stability of Nod2 Variant (G908R)

A HEK293T cell line stably expressing a Nod2 mutant (G908R) was treated with Thiamet-G (1  $\mu$ M, 4 h); increasing the levels of *O*-GlcNAcylation in cells by Thiamet-G did not affect the half-life of the mutant Nod2 (Figure 4.7).

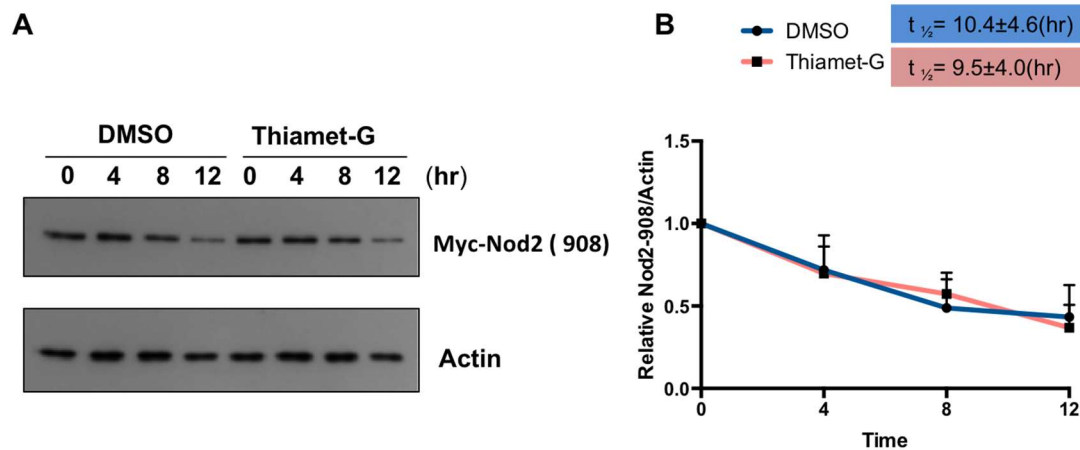


**Figure 4.7: *O*-GlcNAcylation did not affect the stability of Nod2 mutant (G908R) in cells.** (A) HEK293T-Nod2-G908R-Myc/Tet-op cells were incubated with 1  $\mu\text{M}$  Thiamet-G or DMSO for 4 h, and before cycloheximide treatment (100  $\mu\text{g/ml}$ ) at the indicated time intervals. Nod2 was detected by anti-Myc western blotting. (B) Relative amount of Nod2 Myc to actin was plotted from three independent experiments as the means  $\pm$  S.D.

#### 4.3.7.1 Cellular Thermal Shift Assay (CETSA)

In order to confirm the cellular half-life results, a secondary assay, cellular thermal shift assay (CETSA) (19, 20), was performed to investigate if *O*-GlcNAcylation regulates the stability of Nod2 mutant (G908R) (Figure 4.8).

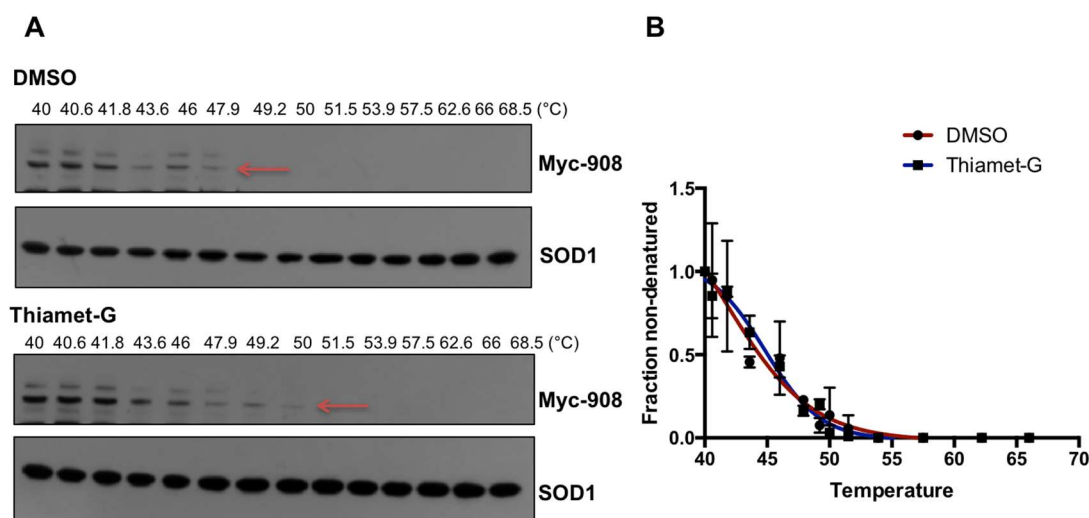


**Figure 4.8: *O*-GlcNAcylation did not affect the stability of Nod2 mutant (G908R) in cells using CETSA assay.** (A) HEK293T-Nod2-G908R-Myc/Tet-op cells were incubated with 1  $\mu$ M Thiamet-G or DMSO for 4 h, and performed CETSA assay and Western Blots (see materials and methods). Myc antibody (1:1000), SOD1 antibody (1:1000) (B) Relative amount of Nod2 Myc to SOD1 was plotted from three independent experiments as the means  $\pm$  S.D. by using GraphPad Prism (Boltzmann Sigmoidal model)

#### 4.3.8 *O*-GlcNAcylation Did Not Regulate the Activity of Nod2 Variant (G908R)

It is not surprising that when the level of the *O*-GlcNAcylation modification is increased with Thiamet-G, cells did not have an increase in MDP- induced NF- $\kappa$ B activity (Figure 4.9). These data indicated that *O*-GlcNAc modification is not able to regulate the stability and activity of Nod2 mutant (G908R) in cells.

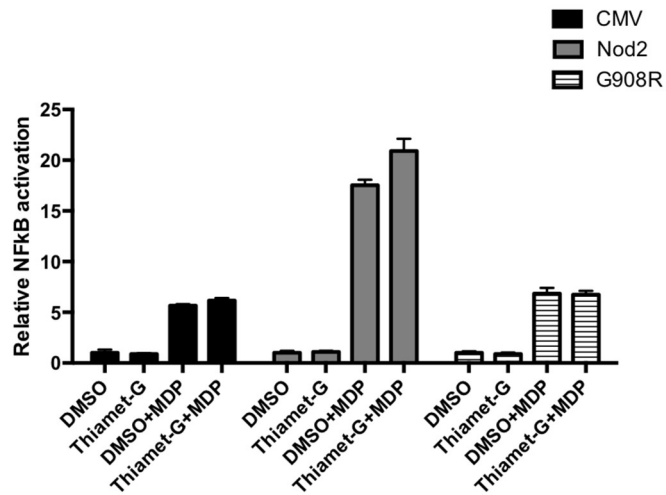


**Figure 4.9: *O*-GlcNAcylation did not regulate the activity of Nod2 mutant (G908R) in cells.** Dual-luciferase assay performed on HEK293T transfected with 0.1ng 908 plasmid in the presence of 100 nM Thiamet-G or DMSO for 4 h. After 4 h cells were incubated with 20  $\mu$ M MDP for 5h, harvested, and tested for luciferase activity. \*  $p < 0.05$  was considered as significant.

#### 4.3.9 The Global *O*-GlcNAcylation in HEK293T-Nod2-G908R-Myc/Tet-op Cell Line

In addition, I wondered if *O*-GlcNAcylation did not change the stability and activity of Nod2 mutant (G908R) due to cells not responding to Thiamet-G. To support this hypothesis, I treated cells with Thiamet-G (1  $\mu$ M, 4 h) to investigate the global *O*-GlcNAcylation. However, the global level of *O*-GlcNAcylation is increased in Nod2 mutant (G908R) cells, similar to wild type Nod2 (Figure 4.10).

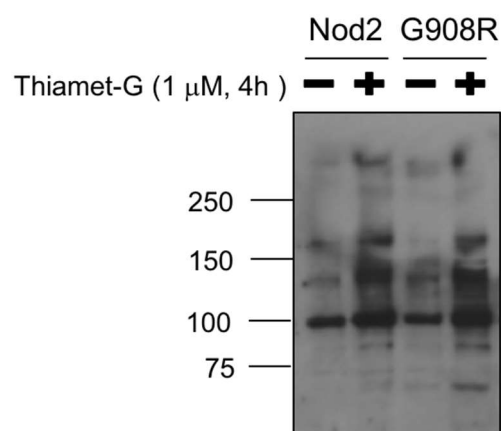


**Figure 4.10: Global *O*-GlcNAcylation is increased using Thiamet-G.** Cell lysates from HEK293T-Nod2-Myc/Tet-op cell line and HEK293T-Nod2-G908R-Myc/Tet-op cell line induced with Thiamet-G for 4 h and then were probed for CTD110.6 antibody (1:1000) to detect the global *O*-GlcNAcylation in cells.

#### 4.3.10 Construct a Point Mutation of Residue S933 of Full Length Nod2

Computation modeling suggests that residues R877, W931 and S933 are the critical binding sites for Nod2 ligand, MDP (7). In addition, Shimizu's group reported the crystal structure of an inactive form of Nod2 and constructed point mutants from the putative MDP-binding pocket in the LRR domain, including residue S933. They found most of these residues mutated affect NF- $\kappa$ B activation, especially residues R877A, G905A, W907A, W931A and S933A (21). When we looked at modeling of MDP in the Nod2 activate site (7), residue 908 is very close to residue 933. We hypothesized that serine at residue 933 might be *O*-GlcNAcylated by OGT. Mutation from glycine to arginine at residue 908 might affect *O*-GlcNAc modification at residue 933 since a huge difference in structure occurs.

To support this idea, a point mutation is made from serine to alanine of full length Nod2 at residue 933 using GeneArt® Site-Directed Mutagenesis PLUS System

kit. This plasmid was then used to produce a stable Nod2 cell line containing the 933 mutation.

#### **4.3.11 Create of Nod2 Mutants (S933A) Expressing Stable Cell Lines via Lentiviral System**

K2605 lentiviral vectors containing Nod2 mutants (S933A) were constructed as described under methods. Stable cell lines of HEK293T cells (Nod2-S933A-Myc/K2605) that express Nod2 mutants with Myc tag under the K2605 lentiviral system were constructed as previously described (Figure 4.1A) (8, 9). I successfully obtained this Nod2 mutant (S933A) expressing stable cell line (Figure 4.11) via lentiviral system.

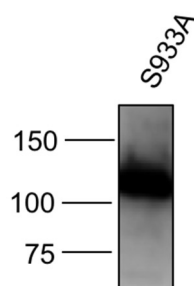


**Figure 4.11: HEK293T stable cell lines expressing Nod2 mutants (S933A).** Cell lysates from Nod2-S933A-Myc/K2605 was probed for Myc antibody (1:1000).

#### **4.3.12 O-GlcNAcylation of Nod2 Variants (S933A)**

In order to investigate if Nod2 mutant (S933A) is *O*-GlcNAcylated, I performed a co-immunoprecipitation assay in the K2605-Nod2/S933Amyc cell line that was treated with or without the *O*-GlcNAcase inhibitor, Thiamet-G (1  $\mu$ M, 4 h). The Nod2 mutant was immunoprecipitated from cell lysates with an anti-Myc

antibody and detected with CTD110.6. I confirmed this Nod2 mutant (S933A) is *O*-GlcNAcylated (Figure 4.12). However, these data do not rule out the possibility that the site is modified. *O*-GlcNAcylation is known to occur on more than one site of the client protein. In order to confirm, if S933 is modified by the *O*-GlcNAcylation, mass spectrometry experiments will need to be performed

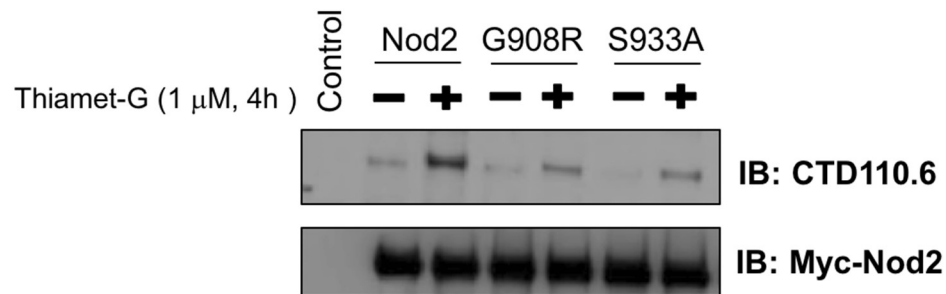


**Figure 4.12: OGT modifies Nod2 mutant (S933A).** (A) Cell lysates from Nod2-S933A-Myc/K2605 cell line was immunopurified with Myc antibody and blotted with CTD110.6. and Myc antibodies; Control cells do not express Myc-Nod2. Thiamet-G inhibits OGA, elevating *O*-GlcNAcylation.

#### 4.3.13 *O*-GlcNAcylation Rescued the Stability and Activity of Nod2 Variant (1007fs)

When HEK293T-Nod2-1007fs-Myc/Tet-op cells were treated with Thiamet-G (1  $\mu$ M, 4 h), I found that the melting temperature is shifted compared to DMSO treatment. This data indicates that Nod2 variant (1007fs) becomes slightly more stable upon Thiamet-G treatment (Figure 4.13).



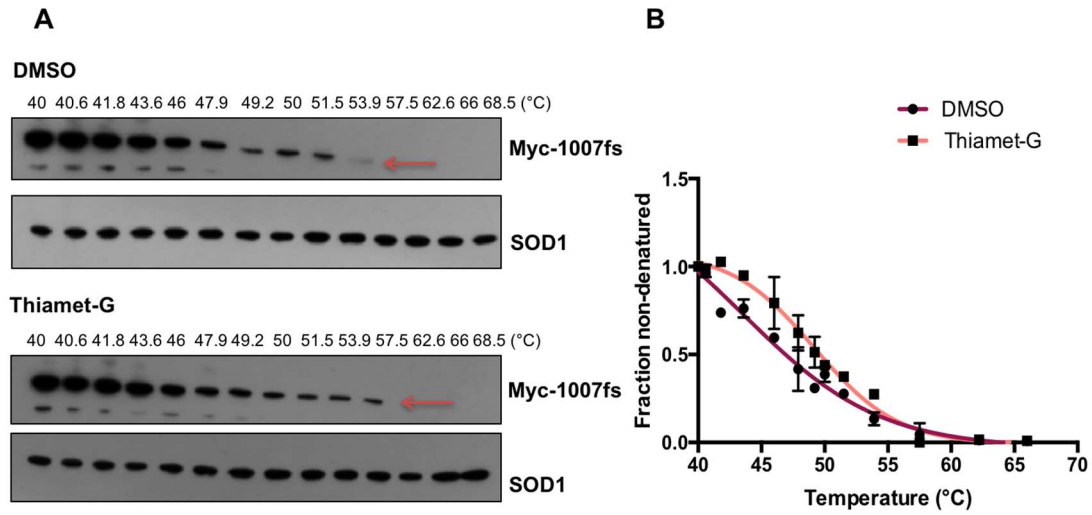


**Figure 4.13: *O*-GlcNAcylation affected the stability of Nod2 mutant (1007) in cells using CETSA assay.** (A) HEK293T-Nod2-1007fs-Myc/Tet-op cells were incubated with 1  $\mu$ M Thiamet-G or DMSO for 4 h, and performed CETSA assay and Western Blots (see materials and methods). Myc antibody (1:1000), SOD1 antibody (1:1000) (B) Relative amount of Nod2 Myc to SOD1 was plotted from three independent experiments as the means  $\pm$  S.D. by using GraphPad Prism (Boltzmann Sigmoidal model).

Finally, if *O*-GlcNAcylation levels in HEK293T-Nod2-1007fs-Myc/Tet-op cells increased, the cells' ability to signal the present of MDP also significantly increased (Figure 4.14).

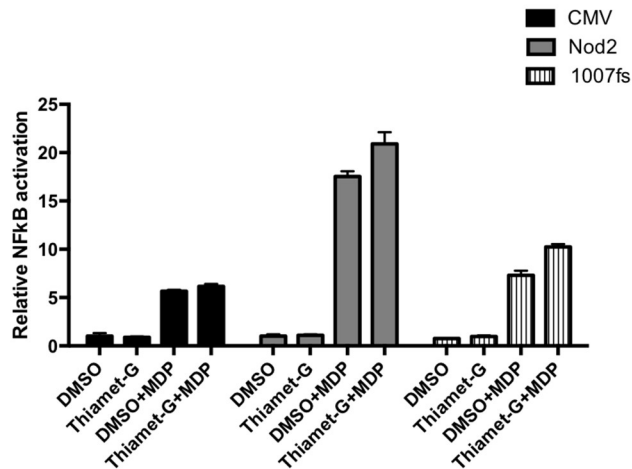


**Figure 4.14: *O*-GlcNAcylation regulated the activity of Nod2 mutant (1007fs) in cells.** Dual-luciferase assay performed on HEK293T transfected with 0.1ng 1007fs plasmid in the presence of 100 nM Thiamet-G or DMSO for 4 h. After 4 h cells were incubated with 20  $\mu$ M MDP for 5h, harvested, and tested for luciferase activity. \*  $p < 0.05$  was considered as significant.

#### 4.4 Discussion

Nod2 associated Crohn's diseases variants have shown to have a decreased NF-kB activation after MDP treatment (3, 4, 12). It will be important to understand why Crohn's-associated Nod2 variants have a low NF-kB activation at a molecular level and investigate the hypothesis that *O*-GlcNAcylation can rescue the stability and activity of Crohn's-associated Nod2 variants.

Previous studies have already shown the half-life of Crohn's mutants were lower than wild type Nod2 (4). In this thesis, I found that increasing *O*-GlcNAcylation can rescue not only the stability in these mutants (R702W and 1007fs) (Figure 4.5 and Figure 4.13), but also the activity (Figure 4.6 and Figure 4.14).

Interestingly, Crohn's-associated mutant (G908R) is *O*-GlcNAcylated (Figure 4.2), but this modification cannot regulate the stability and activity of Nod2-G908R

(Figure 4.7- 4.9). Residue S933 is known to be an important residue involved in MDP binding and NF- $\kappa$ B activation (7, 21). We proposed that residue S933 might be *O*-GlcNAcylated, and having a mutation at residue G908R may affect *O*-GlcNAc modification site at residue S933. To address this question, a single point mutation at residue S933A was constructed to investigate if this affects *O*-GlcNAcylation of full length wild type Nod2. The data indicated that mutant (S933A) is still *O*-GlcNAcylated, but this mutation decreased *O*-GlcNAcylation levels via the intensity of band by Western blots compared to wild type Nod2 (Figure 4.12). We hypothesized that Nod2 has multiple *O*-GlcNAcylation sites. In order to test this hypothesis, further studies need to be conducted to identify *O*-GlcNAcylation sites. I will discuss the preliminary data about how to identify the modification sites in the next chapter.

## REFERENCES

1. Hugot JP, Laurent-Puig P, Gower-Rousseau C, Olson JM, Lee JC, Beaugerie L, Naom I, Dupas JL, Van Gossum A, Orholm M, Bonaiti-Pellie C, Weissenbach J, Mathew CG, Lennard-Jones JE, Cortot A, Colombel JF, Thomas G. Mapping of a susceptibility locus for Crohn's disease on chromosome 16. *Nature*. 1996;379(6568):821-3. doi: 10.1038/379821a0. PubMed PMID: 8587604.
2. Hugot JP, Chamaillard M, Zouali H, Lesage S, Cezard JP, Belaiche J, Almer S, Tysk C, O'Morain CA, Gassull M, Binder V, Finkel Y, Cortot A, Modigliani R, Laurent-Puig P, Gower-Rousseau C, Macry J, Colombel JF, Sahbatou M, Thomas G. Association of NOD2 leucine-rich repeat variants with susceptibility to Crohn's disease. *Nature*. 2001;411(6837):599-603. Epub 2001/06/01. doi: 10.1038/35079107. PubMed PMID: 11385576.
3. Inohara N, Ogura Y, Fontalba A, Gutierrez O, Pons F, Crespo J, Fukase K, Inamura S, Kusumoto S, Hashimoto M, Foster SJ, Moran AP, Fernandez-Luna JL, Nunez G. Host recognition of bacterial muramyl dipeptide mediated through NOD2. Implications for Crohn's disease. *The Journal of biological chemistry*. 2003;278(8):5509-12. PubMed PMID: 12514169.
4. Mohanan V, Grimes CL. The molecular chaperone HSP70 binds to and stabilizes NOD2, an important protein involved in Crohn disease. *The Journal of biological chemistry*. 2014;289(27):18987-98. Epub 2014/05/03. doi: 10.1074/jbc.M114.557686. PubMed PMID: 24790089; PMCID: 4081938.
5. Rossi FM, Guicherit OM, Spicher A, Kringstein AM, Fatyol K, Blakely BT, Blau HM. Tetracycline-regulatable factors with distinct dimerization domains allow reversible growth inhibition by p16. *Nature genetics*. 1998;20(4):389-93. doi: 10.1038/3871. PubMed PMID: 9843215.
6. Belle A, Tanay A, Bitincka L, Shamir R, O'Shea EK. Quantification of protein half-lives in the budding yeast proteome. *Proc Natl Acad Sci U S A*. 2006;103(35):13004-9. Epub 2006/08/19. doi: 10.1073/pnas.0605420103. PubMed PMID: 16916930; PMCID: 1550773.

7. Lauro ML, D'Ambrosio EA, Bahnson BJ, Grimes CL. Molecular Recognition of Muramyl Dipeptide Occurs in the Leucine-rich Repeat Domain of Nod2. *ACS Infect Dis.* 2017;3(4):264-70. doi: 10.1021/acsinfecdis.6b00154. PubMed PMID: 27748583.
8. Chen C, Okayama H. High-efficiency transformation of mammalian cells by plasmid DNA. *Molecular and cellular biology.* 1987;7(8):2745-52. PubMed PMID: 3670292; PMCID: PMC367891.
9. Mohanan V, Temburni MK, Kappes JC, Galileo DS. L1CAM stimulates glioma cell motility and proliferation through the fibroblast growth factor receptor. *Clinical & experimental metastasis.* 2013;30(4):507-20. Epub 2012/12/06. doi: 10.1007/s10585-012-9555-4. PubMed PMID: 23212305.
10. Lesage S, Zouali H, Cezard JP, Colombel JF, Belaiche J, Almer S, Tysk C, O'Morain C, Gassull M, Binder V, Finkel Y, Modigliani R, Gower-Rousseau C, Macry J, Merlin F, Chamaillard M, Jannot AS, Thomas G, Hugot JP, Group E-I, Group E, Group G. CARD15/NOD2 mutational analysis and genotype-phenotype correlation in 612 patients with inflammatory bowel disease. *American journal of human genetics.* 2002;70(4):845-57. Epub 2002/03/05. doi: 10.1086/339432. PubMed PMID: 11875755; PMCID: 379113.
11. Hampe J, Cuthbert A, Croucher PJ, Mirza MM, Mascheretti S, Fisher S, Frenzel H, King K, Hasselmeyer A, MacPherson AJ, Bridger S, van Deventer S, Forbes A, Nikolaus S, Lennard-Jones JE, Foelsch UR, Krawczak M, Lewis C, Schreiber S, Mathew CG. Association between insertion mutation in NOD2 gene and Crohn's disease in German and British populations. *Lancet.* 2001;357(9272):1925-8. doi: 10.1016/S0140-6736(00)05063-7. PubMed PMID: 11425413.
12. Ogura Y, Bonen DK, Inohara N, Nicolae DL, Chen FF, Ramos R, Britton H, Moran T, Karaliuskas R, Duerr RH, Achkar JP, Brant SR, Bayless TM, Kirschner BS, Hanauer SB, Nunez G, Cho JH. A frameshift mutation in NOD2 associated with susceptibility to Crohn's disease. *Nature.* 2001;411(6837):603-6. PubMed PMID: 11385577.
13. Torres CR, Hart GW. Topography and polypeptide distribution of terminal N-acetylglucosamine residues on the surfaces of intact lymphocytes. Evidence for O-linked GlcNAc. *The Journal of biological chemistry.* 1984;259(5):3308-17. Epub 1984/03/10. PubMed PMID: 6421821.
14. Dong DL, Hart GW. Purification and characterization of an O-GlcNAc selective N-acetyl-beta-D-glucosaminidase from rat spleen cytosol. *The Journal of*

biological chemistry. 1994;269(30):19321-30. Epub 1994/07/29. PubMed PMID: 8034696.

15. Gossen M, Bujard H. Tight control of gene expression in mammalian cells by tetracycline-responsive promoters. *Proc Natl Acad Sci U S A*. 1992;89(12):5547-51. PubMed PMID: 1319065; PMCID: PMC49329.

16. Gossen M, Freundlieb S, Bender G, Muller G, Hillen W, Bujard H. Transcriptional activation by tetracyclines in mammalian cells. *Science*. 1995;268(5218):1766-9. PubMed PMID: 7792603.

17. Chi TY, Chen GG, Ho LK, Lai PB. Establishment of a doxycycline-regulated cell line with inducible, doubly-stable expression of the wild-type p53 gene from p53-deleted hepatocellular carcinoma cells. *Cancer Cell Int*. 2005;5:27. doi: 10.1186/1475-2867-5-27. PubMed PMID: 16117829; PMCID: PMC1224858.

18. Benabdellah K, Cobo M, Munoz P, Toscano MG, Martin F. Development of an all-in-one lentiviral vector system based on the original TetR for the easy generation of Tet-ON cell lines. *PloS one*. 2011;6(8):e23734. doi: 10.1371/journal.pone.0023734. PubMed PMID: 21876765; PMCID: PMC3158098.

19. Jafari R, Almqvist H, Axelsson H, Ignatushchenko M, Lundback T, Nordlund P, Martinez Molina D. The cellular thermal shift assay for evaluating drug target interactions in cells. *Nat Protoc*. 2014;9(9):2100-22. doi: 10.1038/nprot.2014.138. PubMed PMID: 25101824.

20. Martinez Molina D, Jafari R, Ignatushchenko M, Seki T, Larsson EA, Dan C, Sreekumar L, Cao Y, Nordlund P. Monitoring drug target engagement in cells and tissues using the cellular thermal shift assay. *Science*. 2013;341(6141):84-7. doi: 10.1126/science.1233606. PubMed PMID: 23828940.

21. Maekawa S, Ohto U, Shibata T, Miyake K, Shimizu T. Crystal structure of NOD2 and its implications in human disease. *Nature communications*. 2016;7:11813. doi: 10.1038/ncomms11813. PubMed PMID: 27283905; PMCID: PMC4906405.

## Chapter 5

### NBD DOMAIN IS REQUIRED FOR *O*-GLCNACYLATION

#### 5.1 Introduction

*O*-linked N-acetylglucosamine (*O*-GlcNAc) was first discovered by Torres and Hart in 1984 (1). It is a dynamic post-translational modification of serine/threonine residues of proteins and is involved in many signal pathways, such as transcription and translation regulation, protein interactions, localization, protein stability, cell cycle regulation, and stress and survival (2-4). Therefore, misregulation of this modification will lead to many diseases, for example, cancer, neurodegenerative diseases, diabetes, and chronic diseases (5-8).

Nowadays over a thousand proteins are identified to be *O*-GlcNAcylated (9, 10). However, there are several reasons that this modification was not discovered until 1984. First, there are a lot of enzymes, such as lysosomal hexosaminidases and nucleocytoplasmic- $\beta$ -*N*-acetylglucosaminidases, that remove *O*-GlcNAc from proteins in cells. Second, it does not affect the molecular weight changes after adding or removing of *O*-GlcNAc on SDS-PAGE gels. Third, it is difficult to detect *O*-GlcNAc by mass spectrometry (11).

Luckily, monoclonal antibodies that detect *O*-GlcNAc were discovered (12-15) and an OGA ( $\beta$ -*N*-acetylglucosaminidase) inhibitor, Thiamet-G, was developed (16), leading to an improved ability to detect this modification in cells.

Even though some proteins can be identified directly from full proteome digests through liquid chromatography tandem mass spectrometry (LC-MS/MS) (17), identification of residues that are *O*-GlcNAcylated is still a challenge.

In this Chapter, we examined a range of Nod2 domain truncations (Figure 5.2A) and created stable cell lines (Figure 5.2B) to narrow down which domain is required for *O*-GlcNAcylation.

## **5.2 Materials and Methods**

### **5.2.1 Cell Culture**

HEK293T-Nod2-Myc cell line (18), HEK293T-Nod2-CARD-Myc/K2605 cell line, HEK293T-Nod2-NBD-Myc/K2605 cell line, HEK293T-Nod2-LRR-Myc/K2605 cell line, HEK293T-CARD-NBD-Myc/K2605 cell line, and HEK293T-NBD-LRR-Myc/K2605 cell line were cultured in DMEM, 10% FBS (Atlantic Biologicals), 2 mM l-glutamine, penicillin-streptomycin and grown in a humidified incubator at 37 °C and 5% CO<sub>2</sub>.

### **5.2.2 Antibodies and Materials**

The mouse monoclonal anti-*O*-GlcNAc antibody, CTD110.6 was produced and purified by Core C4 (Dept. Biological Chemistry, JHU). All other antibodies were purchased from Cell Signaling Technology. Thiamet-G was purchased from Sigma-Aldrich. 10 X PBS was purchased from Lonza (cat, no: 17-517Q). Myc peptide was purchased from Sigma-Aldrich.



### 5.2.3 Plasmid Construction

The following primers (Table 1.1) were used to amplify the CARD, NBD, LRR, CARD-NBD, NBD-LRR domains of Nod2 and mutation (T424A) of Nod2.

**Table 1.1: Primer DNA sequences used for molecular cloning.**

Construct	Primer
<b>CARD forward</b>	5'CGCGGATCCGCCACCATGGAGCAGAACTCATCTCTGAAGAG GATCTGATGGGGGAAGAGGGTTCA3'
<b>CARD reverse</b>	5'CCGCCGCTCGAGTCACTGAGGAAGCGAGACTGAGCAGACACC GTGGTCCTCAG3'
<b>NBD forward</b>	5'CGCGGATCCGCCACCATGGAGCAGAACTCATCTCT GAA GAG GAT CTGATGGCCAAGCTGAGGACC3'
<b>NBD reverse</b>	5'CCGCCGCTCGAGTCACCCGGTGCAGCTGGCGGGGATGG3'
<b>LRR forward</b>	5'CGCGGATCCGCCACCATGGAGCAGAACTCATCTCTGAA GAG GAT CTGATGCCCGGGTTCATC3'
<b>LRR reverse</b>	5'CCGCCGCTCGAGTCAAAGCAAGAGTCTGGTGTCCCT3'
<b>CARD-NBD forward</b>	5'CGCGGATCCGCCACCATGGAGCAGAACTCATCTCTGAAGAG GATCTGATGGGGGAAGAGGGTTCA3'
<b>CARD-NBD reverse</b>	5'CCGCCGCTCGAGTCACCCGGTGCAGCTGGCGGGGATGG3'
<b>NBD-LRR forward</b>	5'CGCGGATCCGCCACCATGGAGCAGAACTCATCTCT GAA GAG GAT CTGATGGCCAAGCTGAGGACC3'
<b>NBD-LRR reverse</b>	5'CCGCCGCTCGAGTCAAAGCAAGAGTCTGGTGTCCCT3'
<b>T424A forward</b>	5'AATGCCCGCAAGGTGGTGGCCAGCCGTCCGGCCGCTGTG3'
<b>T424A reverse</b>	5'CACAGCGGCCGGACGGCTGGCCACCACCTTGCGGGCATT3'

#### **5.2.4 Site-directed Mutagenesis**

The T424A mutation was introduced in Nod2 using GeneArt® Site-Directed Mutagenesis PLUS System kit on the Nod2/pBKCMV plasmid per the manufacturer's instructions. Primers for T424A of Nod2 are previously described (Table 1.1). The presence of mutation in Nod2 was verified via sequencing. Nod2(T424A)/K2605 vector was constructed by digesting Nod2(T424A) from Nod2(T424A)/pBKCMV vector using BamH1 and Xho1 enzymes. The ligated products were transformed into competent cells. The presence of the insert within the construct was confirmed by DNA sequencing (GENEWIZ, Inc). The mutant Nod2(T424A)/pBKCMV was used to make a stable cell line.

#### **5.2.5 Cell Transfection and Lentiviral Transduction**

HEK293T cells were seeded in a 6-well plate (seeding density =  $5 \times 10^5$ ). The next day, cells were transfected with K2605-Nod2-T424A-myc lentiviral vector along with helper plasmid (pCMVΔR8.2) and the envelope plasmid in the proportion of 4:3:1 (2: 1.5: 0.5 μg for cells in a 6-well plate). DNA was transfected into cells using Lipofectamine LTX (500 μl of Opti-MEM and 6 μl of LTX). Medium was changed the next day after transfection. After 8 h, medium containing the viral vector particles was collected and then filtered (0.45 μM). The packaged vectors were added to the cell line to be stably transduced along with polybrene (10 μg/ml final concentration). The vector transduced cells were selected by puromycin (12 μg/ml final concentration).

#### **5.2.6 Protein Purification from HEK293T-Nod2Myc Cells**

Cells were seeded in 150 mm dish ( $2.5 \times 10^6$ ) for 3 days. After 3 days, cells were rinsed with 1X PBS and the lysates were collected using freshly prepared lysis

buffer (1% triton X-100, 2 mM EDTA, 4 mM Na<sub>3</sub>PO<sub>4</sub>, 100 mM NaCl, 10 mM MES pH 5.8, 10 mM NaF, 1 protease inhibitor cocktail tablet (Roche)) and lysed by passing through a 20-gauge needle. 1.2 mg of lysates were mixed with 2 µl of antibody and incubated overnight at 4 °C. Lysate-antibody mixture was incubated with 40 µl of Dynabeads protein A (Life Technologies) beads (prewashed in 0.1M sodium phosphate pH8.0 and lysis buffer) for 3 h at 4 °C. After 3 h, lysate-antibody-bead mixture was washed four times using 200 µL of lysis buffer containing varying concentrations of NaCl as follows: Wash 1– 100 mM NaCl, wash 2-300 mM NaCl, wash 3-500 mM NaCl, wash 4-100 mM NaCl. Proteins were eluted with 2 µl of Myc peptide (5 µg/ml, Sigma-Aldrich) in Tris buffer saline (TBS) overnight at 4 °C.

#### **5.2.7 Co- Immunoprecipitation**

Cells were rinsed with 1X PBS and the lysates were collected using freshly prepared lysis buffer (1% triton X-100, 2 mM EDTA, 4 mM Na<sub>3</sub>PO<sub>4</sub>, 100 mM NaCl, 10 mM MES pH 5.8, 10 mM NaF, 1 protease inhibitor cocktail tablet (Roche)) and lysed by passing through a 20-gauge needle. 1.2 mg of lysates were mixed with 2 µl of antibody and incubated overnight at 4 °C. Lysate-antibody mixture was incubated with 40 µl of Dynabeads protein A (Life Technologies) beads (prewashed in 0.1M sodium phosphate pH8.0 and lysis buffer) for 3 h at 4 °C. After 3 h, lysate-antibody-bead mixture was washed four times using 200 µL of lysis buffer containing varying concentrations of NaCl as follows: Wash 1– 100 mM NaCl, wash 2- 300 mM NaCl, wash 3- 500 mM NaCl, wash 4- 100 mM NaCl. Proteins were eluted at 100 °C for 5 min with 2X reaction buffer (100 mM TrisHCl pH 6.8, 4% SDS, 12% Glycerol, 0.008% bromophenol blue, 2% BME (β-mercaptoethanol)).

### 5.2.8 Western Blot

Cells were rinsed with 1X PBS and appropriate amount of lysis buffer (1% triton X-100, 2 mM EDTA, 4 mM  $\text{Na}_3\text{PO}_4$ , 100 mM NaCl, 10 mM MES pH 5.8, 10 mM NaF, 1 protease inhibitor tablet) was added and lysed using a 20-gauge needle. Protein quantification was performed by a Bradford assay using Bio-Rad Protein Assay Dye Reagent Concentrate according to the manufacturer's instruction. Samples were prepared using 5X loading buffer (250 mM TrisHCl pH 6.8, 10% SDS, 30% Glycerol 0.02% bromophenol blue, 5% BME) and boiled for 5 min. The samples were electrophoresed in 7.5% polyacrylamide gels containing 0.1% sodium dodecyl sulfate. Western transfer onto nitrocellulose membrane was carried out using semi-dry transfer at 25 V for 1 h. 10% nonfat dry milk in TBS-Tween (T) was used to block the membrane for 1 h and washed in TBS-T three times for 5 min each. The blots were incubated overnight at 4 °C with the appropriate amount of antibodies prepared in 1% milk (1:1000). After three washes, the membrane was incubated with HRP-conjugated secondary antibody for 60 min at room temperature. Following secondary incubation, the blot was washed three times in TBS-T and incubated with the substrate (Bio-Rad) according to the manufacturer's instruction. The blots were exposed to Fuji Super RX-U Half Speed Blue films (Brandywine Imaging Inc) in the dark room. All western blots were performed at least three times independently. Using the replicates, the data were analyzed using Image Lab<sup>TM</sup>. This analysis is reported alongside all western blot images.

### 5.2.9 Prediction of *O*-GlcNAc-modified Sites

The complete Nod2 amino acid sequence (obtained from NCBI, GeneBank: AAG33677.1) was upload into YinOYang program (19) template and submitted to prediction (<http://www.cbs.dtu.dk/services/YinOYang/>).

## 5.3 Results

### 5.3.1 Purification of Nod2 from HEK293T-Nod2-Myc/K2605 Cells

A HEK293T stable cell line expressing Nod2 with a Myc tag was used to purify Nod2 protein. As explained under materials and methods, Nod2 protein was expressed with a Myc tag and purified using Myc tag under different concentration of beads and Myc tag (Figure 5.1). From the data, there was no difference of band intensity between using 40  $\mu$ l and 60  $\mu$ l of beads (30 mg/ml). In addition, there was no difference of band intensity between using 2  $\mu$ l and 4  $\mu$ l of Myc peptide (5  $\mu$ g/ml). Finally, I decided to use this condition (40  $\mu$ l of beads (30 mg/ml) and 2  $\mu$ l of Myc peptide (5  $\mu$ g/ml)) to purify Nod2 protein.

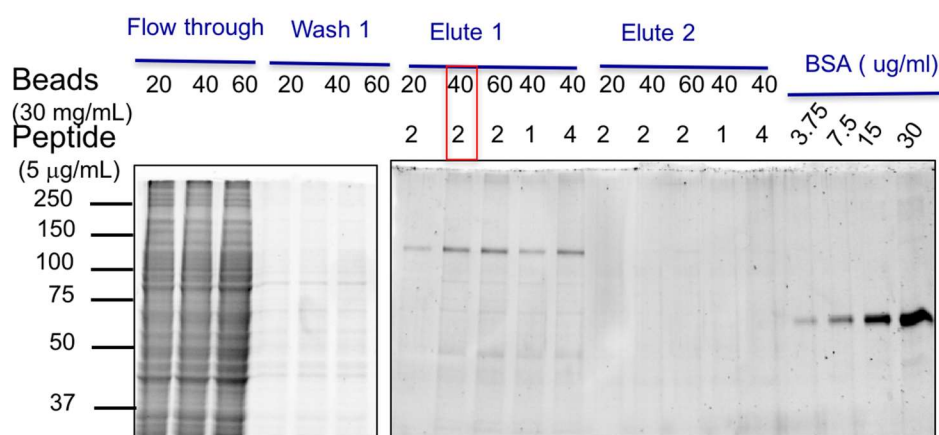


**Figure 5.1: SDS-Page analysis of Nod2 protein purification.** SDS-gel was stained using coomassie brilliant blue. Expected MW of Nod2 is 110 kDa.

### **5.3.2 Mapping of *O*-GlcNAc-modified Sites of Nod2**

2 µg of Nod2 protein was purified from HEK293T-Nod2-Myc/K2605 cell line after treating with Thiamet-G (1 µM, 4 h) using a Myc tag (Figure 5.1) and then sent to a collaborator Dr. Natasha Zachara's lab from John Hopkins University for mapping of *O*-GlcNAc-modified sites. However, they only achieved around 22 % sequence coverage of Nod2 using electron transfer dissociation (ETD). Therefore, I decided to truncate Nod2 to different domains and see which domain could be *O*-GlcNAcylated in cells, as it is easier to map small regions of Nod2 instead of full length of Nod2.

### **5.3.3 Construction of Different Nod2 Domains Expressing Stable Cell Lines via Lentiviral System**

K2605 lentiviral vectors containing different Nod2 domains were constructed as described under methods. Stable cell lines of HEK293T cells (HEK293T-Nod2-CARD-Myc/K2605 cell, HEK293T-Nod2-NBD-Myc/K2605 cell, HEK293T-Nod2-LRR-Myc/K2605 cell, HEK293T-CARD-NBD-Myc/K2605 cell, and HEK293T-NBD-LRR-Myc/K2605 cell) that express different Nod2 domains with a Myc tag under the K2605 lentiviral system as previously described (Figure 4.1A) (18, 20). I successfully obtained these different Nod2 domains expressing stable cell lines (Figure 5.2) via lentiviral system.

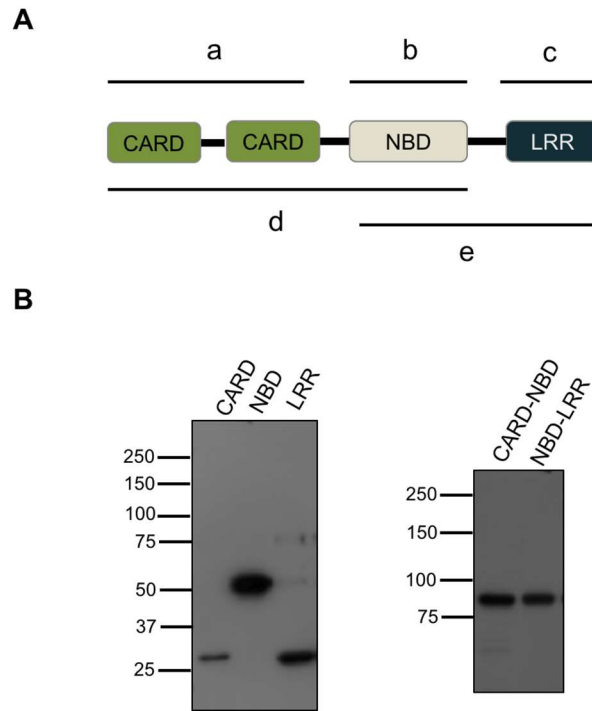


**Figure 5.2: HEK293T stable cell lines expressing Nod2 domains.** (A) The constructs of Nod2: a) CARD b) NBD c) LRR d) CARD-NBD e) NBD-LRR. (B) Cell lysates from HEK293T-Nod2-CARD-Myc/K2605 cell, HEK293T-Nod2-NBD-Myc/K2605 cell, HEK293T-Nod2-LRR-Myc/K2605 cell, HEK293T-CARD-NBD-Myc/K2605 cell, and HEK293T-NBD-LRR-Myc/K2605 cells were probed for Myc antibody (1:1000).

#### 5.3.4 Individual Nod2 Domain Is Not *O*-GlcNAcylated

Nod2 is a 110 kDa cytosolic protein that has two N-terminal CARD domains (Caspase recruitment domain), one C-terminal LRR domain (leucine-rich repeats), and one central NBD domain (nucleotide-binding domain). In order to narrow down the regions of *O*-GlcNAcylation, I truncated Nod2 into individual domains and created stable cell lines to detect *O*-GlcNAcylation.

I performed a co-immunoprecipitation assay in the HEK293T-Nod2-CARD-Myc/K2605 cell line, HEK293T-Nod2-NBD-Myc/K2605 cell line, and HEK293T-

Nod2-LRR-Myc/K2605 cell lines that were treated with or without the *O*-GlcNAcase inhibitor, Thiamet-G (1  $\mu$ M, 4 h). Nod2 domains were immunoprecipitated from cell lysates with an anti-Myc antibody and detected with CTD110.6. There was no band showing up at the corresponding size after probing with CTD110.6. I confirmed that no individual domain of Nod2 is *O*-GlcNAcylated (Figure 5.3).

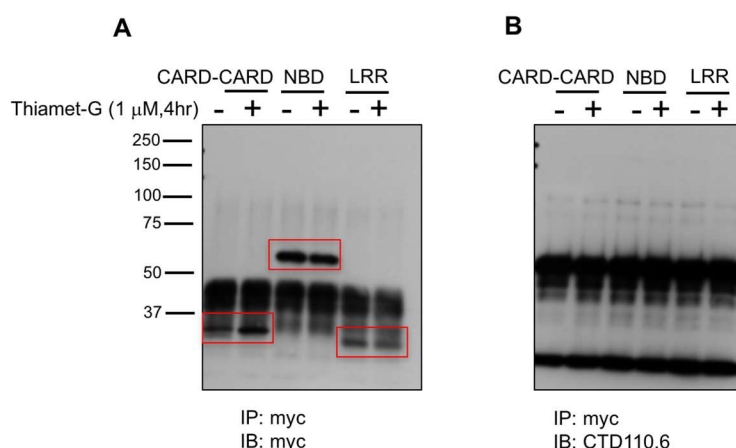


**Figure 5.3: OGT did not modify Nod2 individual domain.** Cell lysates from HEK293T-Nod2-CARD-Myc/K2605 cell line, HEK293T-Nod2-NBD-Myc/K2605 cell line, and HEK293T-Nod2-LRR-Myc/K2605 cell lines were immunopurified with Myc antibody and blotted with (A) Myc and (B) CTD110.6 antibodies; Control cells do not express Myc-Nod2. Thiamet-G inhibits OGA, elevating *O*-GlcNAcylation. Boxed area in each lane is the different domain of Nod2.

### 5.3.5 Two Domains Combined of Nod2 Are *O*-GlcNAcylated

Individual domains of Nod2 are not *O*-GlcNAcylated (Figure 5.3). Therefore, I decided to investigate if *O*-GlcNAcylation can happen in two domains combined of Nod2 (CARD-NBD or NBD-LRR). I performed a co-immunoprecipitation assay in the HEK293T-Nod2-CARD-NBD-Myc/K2605 cell line, and HEK293T-Nod2-NBD-



LRR-Myc/K2605 cell lines that were treated with or without the *O*-GlcNAcase inhibitor, Thiamet-G (1  $\mu$ M, 4 h). Nod2 domains were immunoprecipitated from cell lysates with an anti-Myc antibody and detected with CTD110.6. There was band showing up at the corresponding size after probing with CTD110.6. (Figure 5.4).

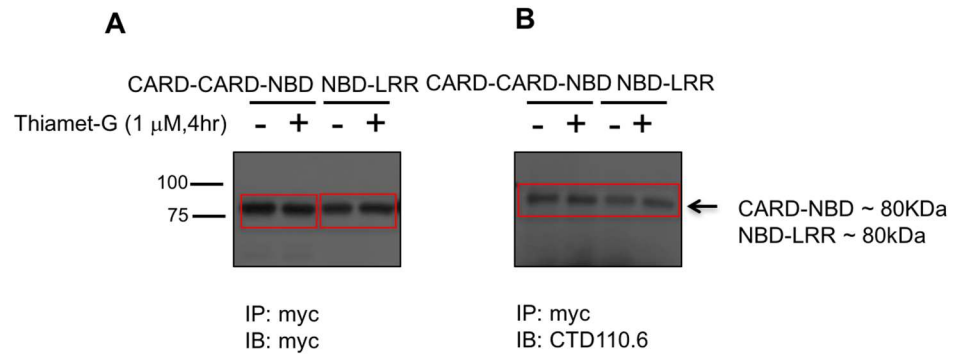


**Figure 5.4: OGT modified two domains combined of Nod2.** Cell lysates from HEK293T-Nod2-CARD-NBD-Myc/K2605 cell and HEK293T-Nod2-NBD-LRR-Myc/K2605 cell lines were immunopurified with Myc antibody and blotted with (A) Myc and (B) CTD110.6 antibodies; Control cells do not express Myc-Nod2. Thiamet-G inhibits OGA, elevating *O*-GlcNAcylation. Boxed area in each lane is the two domains combined of Nod2.

In order to make sure this modification is real, when free GlcNAc was preincubated with CTD110.6 in this experiment, the band for *O*-GlcNAcylation decreased (Figure 5.5). I confirmed at least two domains of Nod2 are need for *O*-GlcNAcylation, and the NBD domain of Nod2 is particular importance.

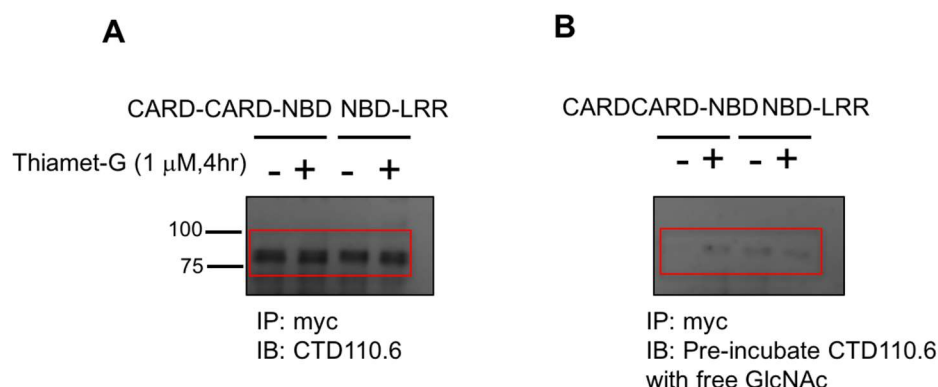


**Figure 5.5: OGT modified two domains combined of Nod2.** Cell lysates from HEK293T-NOD2-CARD-NBD-Myc/K2605 cell and HEK293T-NOD2-NBD-LRR-Myc/K2605 cell lines were immunopurified with Myc antibody and blotted with (A) CTD110.6 and (B) CTD110.6 antibody that preincubated with free GlcNAc; Control cells do not express Myc-Nod2. Thiamet-G inhibits OGA, elevating *O*-GlcNAcylation. Boxed area in each lane is the two domains combined of Nod2.

### 5.3.6 Prediction of *O*-GlcNAc- modified Sites Program

while *O*-GlcNAcylation does not have a consensus amino acid sequence, PVST (Proline-Valine-Serine-Threonine) sequences are preferred, as well as other common motifs (21). Some prediction tools have been developed, (19, 21) including YinOYang.

The YinOYang program is based on *O*-GlcNAc acceptor sites of proteins that are already determined. The prediction sites depend on the surface accessibility of the sites and the sequence context. This program depends on the *O*-GlcNAc prediction strength and the threshold, from low (+) to high (+++++) (22). Using the YinOYang prediction program, 10 residues are predicated to be *O*-GlcNAcylation, especially residue at T424 (+++) (Figure 5.6).

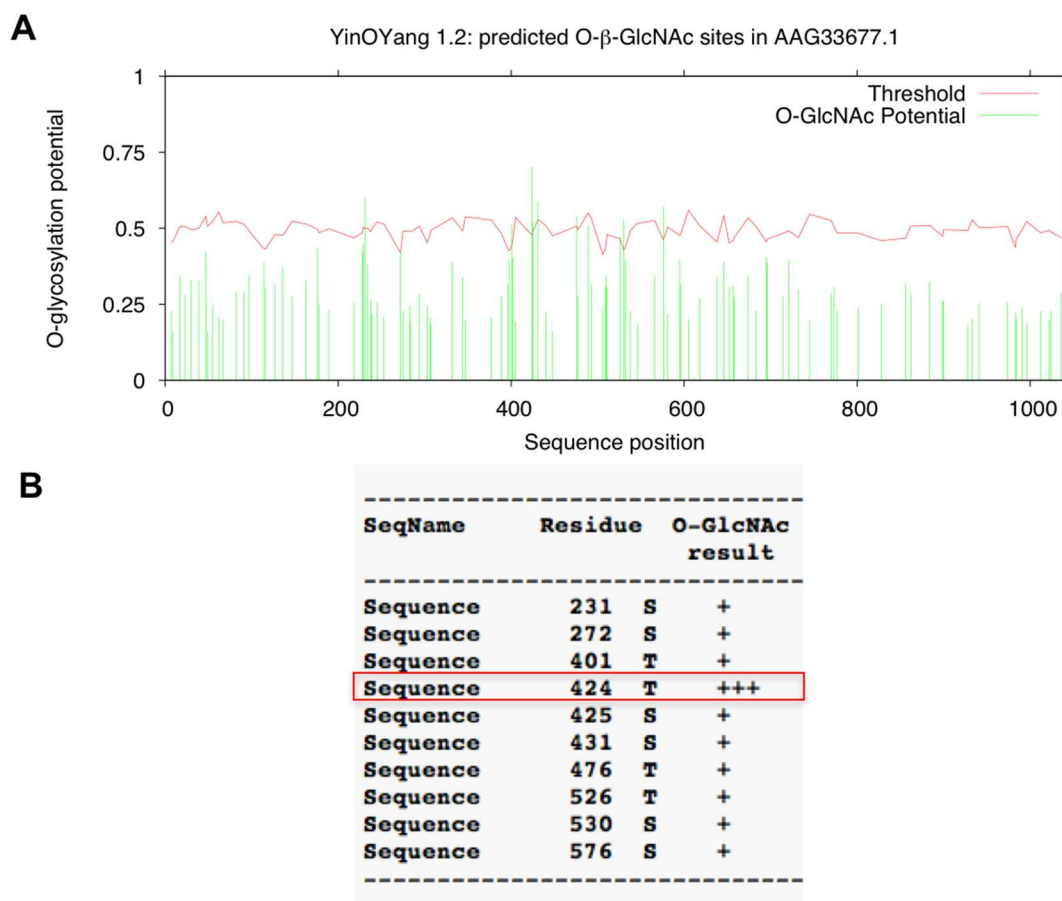


**Figure 5.6: Prediction of *O*-GlcNAc –modified sites of Nod2.** (A) The result of the *O*-GlcNAc prediction strength and the threshold. (B) The prediction indicated that residue T424 is highly recommended to be in *O*-GlcNAc-modified site.

### 5.3.7 Mutation of T424A of Nod2

According to the YinOYang prediction program, residue at T424 is a highly-preferred site for *O*-GlcNAcylation (Figure 5.7). Therefore, we decided to mutate this residue from Threonine to Alanine to determine if this residue is critical for *O*-GlcNAcylation.

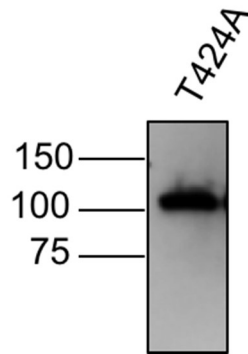


**Figure 5.7: HEK293T stable cell lines expressing Nod2 mutant (T424A).** Cell lysates from HEK293T-Nod2-T424A-Myc/K2605 were probed for Myc antibody (1:1000).

### 5.3.8 Nod2 Mutant (T424A) Is *O*-GlcNAcylated

In order to examine if the residue at 424 is critical for *O*-GlcNAcylation, I performed a co-immunoprecipitation assay in the HEK293T-Nod2-T424A-Myc/K2605 cell line that was treated with or without the *O*-GlcNAcase inhibitor, Thiamet-G (1  $\mu$ M, 4 h). Nod2 mutant (T424A) was immunoprecipitated from cell lysates with an anti-Myc antibody and detected with CTD110.6. I confirmed this Nod2 mutant is still *O*-GlcNAcylated (Figure 5.8).

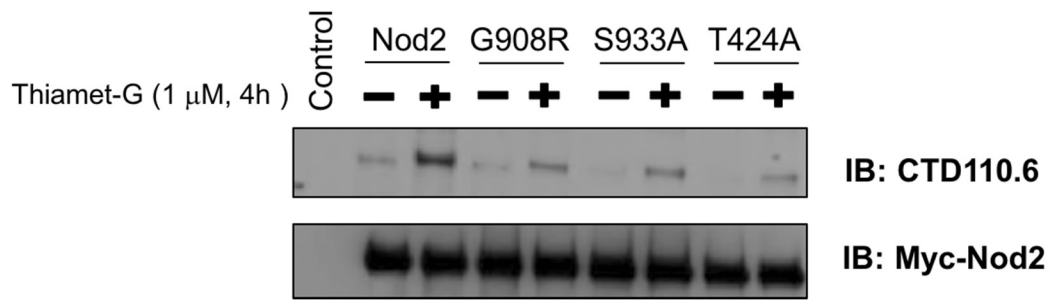


**Figure 5.8: Nod2 mutant (T424A) is *O*-GlcNAcylated.** Cell lysates from HEK293T -Nod2-T424A-Myc/K2605 cell line was immunopurified with Myc antibody and blotted with Myc and CTD110.6 antibodies; Control cells do not express Myc-Nod2. Thiamet-G inhibits OGA, elevating *O*-GlcNAcylation.

#### 5.4 Discussion

*O*-GlcNAcylation is involved in many biological pathways (2-4). Therefore, mapping of *O*-GlcNAcylation is crucial to reveal the mechanisms of different biological events. However, it is still challenging to characterize *O*-GlcNAcylation of proteins.

When trying to map *O*-GlcNAc modified sites of Nod2 via ETD, however, we only got about 22 % sequence coverage of Nod2 from collaborator Dr. Natasha Zachara's lab. In order to discover the sites of *O*-GlcNAcylation, I truncated Nod2 into different domains and used them to make stable cell lines (Figure 5.2). I performed a co-immunoprecipitation assay in these stable cell lines and found that two domains combined of Nod2 (CARD-NBD or NBD-LRR) are *O*-GlcNAcylated (Figure 5.4-5.5), but not individual domains of Nod2 (Figure 5.3). In addition, the prediction of *O*-GlcNAc- modified sites of Nod2 are all in the NBD domain via the YinOYang prediction program (Figure 5.6). Therefore, it seems that NBD domain is critical for *O*-GlcNAcylation.

Furthermore, the residue at T424 is a highly-preferred site for *O*-GlcNAcylation based on the YinOYang prediction program. Thus, I mutated the amino acid from threonine to alanine at residue 424 to examine if this residue could affect *O*-GlcNAcylation in cells (Figure 5.7). Our data showed this mutant (T424A) is still *O*-GlcNAcylated by OGT in cells, but the band intensity in Western blot was decreased dramatically (Figure 5.8). It indicated either this residue may affect modification indirectly or that Nod2 has many modification sites. Further studies need to be conducted to identify *O*-GlcNAc-modified sites of Nod2.

## REFERENCES

1. Torres CR, Hart GW. Topography and polypeptide distribution of terminal N-acetylglucosamine residues on the surfaces of intact lymphocytes. Evidence for O-linked GlcNAc. *The Journal of biological chemistry*. 1984;259(5):3308-17. Epub 1984/03/10. PubMed PMID: 6421821.
2. Love DC, Hanover JA. The hexosamine signaling pathway: deciphering the "O-GlcNAc code". *Sci STKE*. 2005;2005(312):re13. doi: 10.1126/stke.3122005re13. PubMed PMID: 16317114.
3. Hart GW, Housley MP, Slawson C. Cycling of O-linked beta-N-acetylglucosamine on nucleocytoplasmic proteins. *Nature*. 2007;446(7139):1017-22. Epub 2007/04/27. doi: 10.1038/nature05815. PubMed PMID: 17460662.
4. Hart GW, Slawson C, Ramirez-Correa G, Lagerlof O. Cross talk between O-GlcNAcylation and phosphorylation: roles in signaling, transcription, and chronic disease. *Annual review of biochemistry*. 2011;80:825-58. doi: 10.1146/annurev-biochem-060608-102511. PubMed PMID: 21391816; PMCID: PMC3294376.
5. Banerjee PS, Lagerlof O, Hart GW. Roles of O-GlcNAc in chronic diseases of aging. *Mol Aspects Med*. 2016;51:1-15. doi: 10.1016/j.mam.2016.05.005. PubMed PMID: 27259471.
6. Ferrer CM, Sodi VL, Reginato MJ. O-GlcNAcylation in Cancer Biology: Linking Metabolism and Signaling. *J Mol Biol*. 2016;428(16):3282-94. doi: 10.1016/j.jmb.2016.05.028. PubMed PMID: 27343361; PMCID: PMC4983259.
7. Wright JN, Collins HE, Wende AR, Chatham JC. O-GlcNAcylation and cardiovascular disease. *Biochem Soc Trans*. 2017;45(2):545-53. doi: 10.1042/BST20160164. PubMed PMID: 28408494.
8. Ma X, Li H, He Y, Hao J. The emerging link between O-GlcNAcylation and neurological disorders. *Cell Mol Life Sci*. 2017. doi: 10.1007/s00018-017-2542-9. PubMed PMID: 28534084.

9. Wells L, Vosseller K, Hart GW. Glycosylation of nucleocytoplasmic proteins: signal transduction and O-GlcNAc. *Science*. 2001;291(5512):2376-8. PubMed PMID: 11269319.
10. Ma J, Hart GW. O-GlcNAc profiling: from proteins to proteomes. *Clin Proteomics*. 2014;11(1):8. doi: 10.1186/1559-0275-11-8. PubMed PMID: 24593906; PMCID: PMC4015695.
11. Hart GW, Akimoto Y. The O-GlcNAc Modification. In: Varki A, Cummings RD, Esko JD, Freeze HH, Stanley P, Bertozzi CR, Hart GW, Etzler ME, editors. *Essentials of Glycobiology*. 2nd ed. Cold Spring Harbor (NY)2009.
12. Comer FI, Vosseller K, Wells L, Accavitti MA, Hart GW. Characterization of a mouse monoclonal antibody specific for O-linked N-acetylglucosamine. *Anal Biochem*. 2001;293(2):169-77. doi: 10.1006/abio.2001.5132. PubMed PMID: 11399029.
13. Snow CM, Senior A, Gerace L. Monoclonal antibodies identify a group of nuclear pore complex glycoproteins. *J Cell Biol*. 1987;104(5):1143-56. PubMed PMID: 2437126; PMCID: PMC2114474.
14. Turner JR, Tartakoff AM, Greenspan NS. Cytologic assessment of nuclear and cytoplasmic O-linked N-acetylglucosamine distribution by using anti-streptococcal monoclonal antibodies. *Proc Natl Acad Sci U S A*. 1990;87(15):5608-12. PubMed PMID: 2116002; PMCID: PMC54376.
15. Teo CF, Ingale S, Wolfert MA, Elsayed GA, Not LG, Chatham JC, Wells L, Boons GJ. Glycopeptide-specific monoclonal antibodies suggest new roles for O-GlcNAc. *Nature chemical biology*. 2010;6(5):338-43. doi: 10.1038/nchembio.338. PubMed PMID: 20305658; PMCID: PMC2857662.
16. Yuzwa SA, Macauley MS, Heinonen JE, Shan X, Dennis RJ, He Y, Whitworth GE, Stubbs KA, McEachern EJ, Davies GJ, Vocadlo DJ. A potent mechanism-inspired O-GlcNAcase inhibitor that blocks phosphorylation of tau in vivo. *Nature chemical biology*. 2008;4(8):483-90. doi: 10.1038/nchembio.96. PubMed PMID: 18587388.
17. Hahne H, Gholami AM, Kuster B. Discovery of O-GlcNAc-modified proteins in published large-scale proteome data. *Mol Cell Proteomics*. 2012;11(10):843-50. doi: 10.1074/mcp.M112.019463. PubMed PMID: 22661428; PMCID: PMC3494142.
18. Mohanan V, Grimes CL. The molecular chaperone HSP70 binds to and stabilizes NOD2, an important protein involved in Crohn disease. *The Journal of*



biological chemistry. 2014;289(27):18987-98. Epub 2014/05/03. doi: 10.1074/jbc.M114.557686. PubMed PMID: 24790089; PMCID: 4081938.

19. Gupta R, Brunak S. Prediction of glycosylation across the human proteome and the correlation to protein function. *Pac Symp Biocomput.* 2002:310-22. PubMed PMID: 11928486.

20. Chen C, Okayama H. High-efficiency transformation of mammalian cells by plasmid DNA. *Molecular and cellular biology.* 1987;7(8):2745-52. PubMed PMID: 3670292; PMCID: PMC367891.

21. Wang J, Torii M, Liu H, Hart GW, Hu ZZ. dbOGAP - an integrated bioinformatics resource for protein O-GlcNAcylation. *BMC Bioinformatics.* 2011;12:91. doi: 10.1186/1471-2105-12-91. PubMed PMID: 21466708; PMCID: PMC3083348.

22. Hart GW, Greis KD, Dong LY, Blomberg MA, Chou TY, Jiang MS, Roquemore EP, Snow DM, Kreppel LK, Cole RN, et al. O-linked N-acetylglucosamine: the "yin-yang" of Ser/Thr phosphorylation? Nuclear and cytoplasmic glycosylation. *Adv Exp Med Biol.* 1995;376:115-23. PubMed PMID: 8597237.

## Chapter 6

### CONCLUTIONS AND FUTURE DIRECTIONS

The human innate immune system is the first line of defense against pathogens. This system is critical in distinguishing the “good” vs “bad” bacteria that populate the human body by using innate immune receptors or pathogen recognition receptors (PRRs) (1, 2). These PRRs will recognize microorganism-associated molecular patterns (MAMPs) and then trigger an immune response to help the human body against invading pathogens (Figure 1.1).

There are two major types of PRRs: Toll-like receptors (TLRs) and nucleotide-binding oligomerization domain (NOD)-like receptors (NLRs) (3, 4). Nod2 is one well characterized NLR which can recognize MDP from bacterial peptidoglycan and then trigger an inflammatory reaction, including the NF- $\kappa$ B pathway (5, 6). However, if Nod2 is mutated, it is linked to the development of Crohn’s disease. There are three major mutations of Nod2 correlated to Crohn’s disease are R702W, G908R, and 1007fs (7-9). In addition, previous studies showed that these three Crohn-associated Nod2 mutants decrease NF- $\kappa$ B activation upon MDP, bacterial cell wall fragment, stimulation (10). The primary reason for this is due to these mutants are very unstable and leads to decrease their stability and activity (11). The objective of my thesis was to understand a molecular level of Crohn’s diseases. I sought to identify a post-translational modification, *O*-GlcNAcylation, of Nod2 in the signaling cascade.

Biochemically, the Nod2 protein remains to be fully characterized due to the lack of tools to study this inherently unstable protein. For the first time, I show that Nod2 is

post-translationally modified by a small carbohydrate, GlcNAc. I identified this by using antibody that specifically detects *O*-GlcNAc linkage, by perform co-immunoprecipitation using GlcNAc antibody and probing for Nod2 and vice-versa (Figure 2.2-2.3). In addition, in order to initially probe the role of *O*-GlcNAcylation on the Crohn's-associated mutants, I performed experiments with Crohn's-associated mutants; I demonstrated three major Crohn's-associated Nod2 mutants are *O*-GlcNAcylated (Figure 4.2). Further characterization of this modification, revealed that increasing the level of *O*-GlcNAc in cells increases the half-life of Nod2. Maintaining the stability of proteins is one of primary effects of the GlcNAc modification on proteins (12, 13). We have previously shown that Crohn's-associated Nod2 mutants have a decreased half-life compared to the wild-type (11). R702W and 1007fs Nod2 Crohn's mutants expressed in cells incubated with Thiamet-G displayed an increased the stability compared to control (Figure 4.5 & Figure 4.13). Further I determined that increasing *O*-GlcNAc levels using a small molecular inhibitor of OGA, Thiamet-G can affect the MDP induced NF- $\kappa$ B activity via Nod2 (Figure 4.6 & Figure 4.14). However, *O*-GlcNAcylation did not affect the stability and activity of G908R Nod2 mutant even it is *O*-GlcNAc-modified by OGA (Figure 4.2 & Figure 4.7-4.9). The data showed that *O*-GlcNAcylation is not enough to rescue its stability and there may be other mechanisms to regulate Nod2 stability in G908R Nod2 mutant. These data demonstrated that increasing *O*-GlcNAcylation not only stabilizes Nod2 and its mutants, but also increases its activity. Thus, this finding could have an impact on the development of novel treatments of Crohn's disease where the mutants lack their stability and fail to respond to bacterial cell wall fragments.

In conclusion of this dissertation, I have discovered that Nod2 is post-

transnationally modified by the enzyme, OGT and this modification has an ability to alter its stability and cellular response.

The future of this project is to map of *O*-GlcNAc-modified sites of Nod2 even it is still a challenge. Characterization of *O*-GlcNAcylation is difficult due to no consensus amino acid sequences and general enzyme which can cleave *O*-linked glycan (14, 15). We can either purify the small regions of Nod2 that are *O*-GlcNAcylated (Figure 5.4-5.5) instead of full length of Nod2 to increase the sequence coverage of Nod2 and identify the mapping sites or perform other approaches.

Previous studies showed that *O*-GlcNAcylated peptides can be enriched by enzymatic coupling of an azide-GalNAc to *O*-GlcNAc using an engineered galactosyl transferase (16). The azide-*O*-GlcNAc can be enriched by photocleavage tag having alkynyl beads or the alkynyl biotin (17, 18). *O*-GlcNAc-modified sites could be identified by MS using this strategy(19).

Another approach to identify *O*-GlcNAc sites is to use the alkyne-modified resin for metabolic azide-labeled *O*-GlcNAcylated proteins to immobilize. *O*-GlcNAc proteins were identified by LC-MS/MS after digestion of resin (20). I believed that using the enzymatic or metabolic labeling methods would help us to identify modified sites of Nod2 in the future.

## REFERENCES

1. Janeway CA, Jr., Medzhitov R. Innate immune recognition. Annual review of immunology. 2002;20:197-216. Epub 2002/02/28. doi: 10.1146/annurev.immunol.20.083001.084359. PubMed PMID: 11861602.
2. Tosi MF. Innate immune responses to infection. The Journal of allergy and clinical immunology. 2005;116(2):241-9; quiz 50. Epub 2005/08/09. doi: 10.1016/j.jaci.2005.05.036. PubMed PMID: 16083775.
3. Franchi L, Warner N, Viani K, Nunez G. Function of Nod-like receptors in microbial recognition and host defense. Immunol Rev. 2009;227(1):106-28. PubMed PMID: 19120480.
4. Takeda K, Akira S. Roles of Toll-like receptors in innate immune responses. Genes Cells. 2001;6(9):733-42. PubMed PMID: 11554921.
5. McCarthy JV, Ni J, Dixit VM. RIP2 is a novel NF-kappaB-activating and cell death-inducing kinase. The Journal of biological chemistry. 1998;273(27):16968-75. PubMed PMID: 9642260.
6. Nembrini C, Kisielow J, Shamshiev AT, Tortola L, Coyle AJ, Kopf M, Marsland BJ. The kinase activity of Rip2 determines its stability and consequently Nod1- and Nod2-mediated immune responses. The Journal of biological chemistry. 2009;284(29):19183-8. Epub 2009/05/29. doi: 10.1074/jbc.M109.006353. PubMed PMID: 19473975; PMCID: 2740541.
7. Ogura Y, Bonen DK, Inohara N, Nicolae DL, Chen FF, Ramos R, Britton H, Moran T, Karaliuskas R, Duerr RH, Achkar JP, Brant SR, Bayless TM, Kirschner BS, Hanauer SB, Nunez G, Cho JH. A frameshift mutation in NOD2 associated with susceptibility to Crohn's disease. Nature. 2001;411(6837):603-6. PubMed PMID: 11385577.
8. Hugot JP, Chamaillard M, Zouali H, Lesage S, Cezard JP, Belaiche J, Almer S, Tysk C, O'Morain CA, Gassull M, Binder V, Finkel Y, Cortot A, Modigliani R, Laurent-Puig P, Gower-Rousseau C, Macry J, Colombel JF, Sahbatou M, Thomas G. Association of NOD2 leucine-rich repeat variants with susceptibility to Crohn's

disease. *Nature*. 2001;411(6837):599-603. Epub 2001/06/01. doi: 10.1038/35079107. PubMed PMID: 11385576.

9. Lesage S, Zouali H, Cezard JP, Colombel JF, Belaiche J, Almer S, Tysk C, O'Morain C, Gassull M, Binder V, Finkel Y, Modigliani R, Gower-Rousseau C, Macry J, Merlin F, Chamaillard M, Jannot AS, Thomas G, Hugot JP, Group E-I, Group E, Group G. CARD15/NOD2 mutational analysis and genotype-phenotype correlation in 612 patients with inflammatory bowel disease. *American journal of human genetics*. 2002;70(4):845-57. Epub 2002/03/05. doi: 10.1086/339432. PubMed PMID: 11875755; PMCID: 379113.

10. Inohara N, Ogura Y, Fontalba A, Gutierrez O, Pons F, Crespo J, Fukase K, Inamura S, Kusumoto S, Hashimoto M, Foster SJ, Moran AP, Fernandez-Luna JL, Nunez G. Host recognition of bacterial muramyl dipeptide mediated through NOD2. Implications for Crohn's disease. *The Journal of biological chemistry*. 2003;278(8):5509-12. PubMed PMID: 12514169.

11. Mohanan V, Grimes CL. The molecular chaperone HSP70 binds to and stabilizes NOD2, an important protein involved in Crohn disease. *The Journal of biological chemistry*. 2014;289(27):18987-98. Epub 2014/05/03. doi: 10.1074/jbc.M114.557686. PubMed PMID: 24790089; PMCID: 4081938.

12. Chu CS, Lo PW, Yeh YH, Hsu PH, Peng SH, Teng YC, Kang ML, Wong CH, Juan LJ. O-GlcNAcylation regulates EZH2 protein stability and function. *P Natl Acad Sci USA*. 2014;111(4):1355-60. doi: DOI 10.1073/pnas.1323226111. PubMed PMID: ISI:000330231100042.

13. Zhu Y, Liu TW, Cecioni S, Eskandari R, Zandberg WF, Vocadlo DJ. O-GlcNAc occurs cotranslationally to stabilize nascent polypeptide chains. *Nature chemical biology*. 2015;11(5):319-25. Epub 2015/03/17. doi: 10.1038/nchembio.1774. PubMed PMID: 25774941.

14. Ma J, Hart GW. O-GlcNAc profiling: from proteins to proteomes. *Clin Proteomics*. 2014;11(1):8. doi: 10.1186/1559-0275-11-8. PubMed PMID: 24593906; PMCID: PMC4015695.

15. Tran DT, Ten Hagen KG. Mucin-type O-glycosylation during development. *The Journal of biological chemistry*. 2013;288(10):6921-9. doi: 10.1074/jbc.R112.418558. PubMed PMID: 23329828; PMCID: PMC3591602.

16. Khidekel N, Ficarro SB, Clark PM, Bryan MC, Swaney DL, Rexach JE, Sun YE, Coon JJ, Peters EC, Hsieh-Wilson LC. Probing the dynamics of O-GlcNAc

glycosylation in the brain using quantitative proteomics. *Nature chemical biology*. 2007;3(6):339-48. doi: 10.1038/nchembio881. PubMed PMID: 17496889.

17. Wang Z, Udeshi ND, O'Malley M, Shabanowitz J, Hunt DF, Hart GW. Enrichment and site mapping of O-linked N-acetylglucosamine by a combination of chemical/enzymatic tagging, photochemical cleavage, and electron transfer dissociation mass spectrometry. *Mol Cell Proteomics*. 2010;9(1):153-60. doi: 10.1074/mcp.M900268-MCP200. PubMed PMID: 19692427; PMCID: PMC2808261.

18. Wang Z, Udeshi ND, Slawson C, Compton PD, Sakabe K, Cheung WD, Shabanowitz J, Hunt DF, Hart GW. Extensive crosstalk between O-GlcNAcylation and phosphorylation regulates cytokinesis. *Sci Signal*. 2010;3(104):ra2. doi: 10.1126/scisignal.2000526. PubMed PMID: 20068230; PMCID: PMC2866299.

19. Alfaro JF, Gong CX, Monroe ME, Aldrich JT, Clauss TR, Purvine SO, Wang Z, Camp DG, 2nd, Shabanowitz J, Stanley P, Hart GW, Hunt DF, Yang F, Smith RD. Tandem mass spectrometry identifies many mouse brain O-GlcNAcylated proteins including EGF domain-specific O-GlcNAc transferase targets. *Proc Natl Acad Sci U S A*. 2012;109(19):7280-5. doi: 10.1073/pnas.1200425109. PubMed PMID: 22517741; PMCID: PMC3358849.

20. Hahne H, Sobotzki N, Nyberg T, Helm D, Borodkin VS, van Aalten DM, Agnew B, Kuster B. Proteome wide purification and identification of O-GlcNAc-modified proteins using click chemistry and mass spectrometry. *J Proteome Res*. 2013;12(2):927-36. doi: 10.1021/pr300967y. PubMed PMID: 23301498; PMCID: PMC4946622.

## Appendix A

### METABOLIC LABELING OF THE CARBOHYDRATE CORE IN BACTERIAL PEPTIDOGLYCAN AND ITS APPLICATION

I also collaborated with Hai Liang and Kristen E. DeMeester's project during my Ph.D. Hai Liang contributed to the design of AmgK and MurU utility, performed in vitro protein characterization and bacterial cell wall labelling. Kristen contributed to NAM probe and synthetic designs, and performed all syntheses, purifications, compound characterization, and bacterial cell wall labelling work. My role in the project was macrophage invasion study and assisted Hai and Kristen with cell imaging. Ultimately this work was published in *Nature Communications*, **8**, 15015 (2017). Here I present the main macrophage invasion assays and associated data from my part of the collaboration. This method will be useful in identifying immunostimulatory fragments and then investigating the effect these fragments have on *O*-GlcNAcylation, the main focus of my thesis.

#### Introduction

Bacterial cells are surrounded by a polymer known as peptidoglycan (PG), which protects the cell from changes in osmotic pressure and small molecule insults. A component of this material, *N*-acetyl-muramic acid (NAM), serves as a core structural element for innate immune recognition of PG fragments. We report the synthesis of modifiable NAM carbohydrate derivatives and the installation of these building blocks into the backbone of Gram-positive and Gram-negative bacterial PG utilizing



metabolic cell wall recycling and biosynthetic machineries. Whole cells were labeled via click chemistry and visualized using super-resolution microscopy, revealing higher resolution PG structural details and allowing the cell wall biosynthesis, as well as its destruction in macrophage cells, to be tracked.

**Method (Infection and immunostaining):**

The day before seeding the cells, sterile cover glasses (Fischer Scientific, Cat. # 12-545-80) were coated with 500  $\mu$ L of 0.1 mg/mL poly-L-ornithine (Sigma-Aldrich) in 24-well plates overnight. One day before infection, the poly-L-ornithine was removed and the cover glasses were washed with Dulbecco's modified eagle medium (DMEM) medium without antibiotics twice. J774 macrophages (provided by M.Parent, purchased ATCC catalog number TIB-67) were seeded on these cover glasses in 24-well plates with DMEM medium (Methods) without antibiotics (pen-strep) at a density of  $1 \times 10^5$  cells per well. For infection with remodeled *E. coli*  $\Delta$ MurQ-KU cells, bacteria were grown and remolded with modified NAM derivative **3** as described above. The bacteria ( $5 \times 10^5$  cells) were added to the macrophage for different time lengths 20, 40, 60 and 80 min. After incubation, the medium was removed and fresh medium with gentamicin (1:1000) was added to kill extracellular bacteria for 30 min at 37 °C. After 30 min, the medium was removed and cells were rinsed twice with 1 X PBS at room temperature. Cells were fixed with 4% formaldehyde in 1 X PBS for 10 min at room temperature. Cells were rinsed with 1 X PBS and then permeabilized with 1% Triton X-100 for 10 min at room temperature. Fixed cells were then rinsed in 1 X PBS containing 3% BSA and 0.1% Triton X-100 (1 X PBSTB) for 3 X 5 min. After rinsing cells in 1 X PBS, the click reaction was performed as described above in 1 X

PBS with 0.01% BSA and 0.1% Triton X-100 for 30 min. After 30 min, the cells were rinsed in 1 X PBS and then washed in PBSTB for 5 X 8 min. The cells were mounted on glass slides with DAPI (Invitrogen) and ready for imaging.

### **Result (Tracking of bacterial invasion and breakdown in macrophages):**

To determine if this method would be useful in studying the interaction between NAM-based PG fragments and the innate immune system, NAM labeled bacterial invasion of mammalian cells was studied. Bioorthogonally modified *E. coli*  $\Delta$ MurQ-KU cells were used to infect J774 macrophage cells and were then subsequently labeled via click chemistry. SIM images confirm that the invasion of modified bacteria into the macrophage cytosol was successfully tracked while unlabeled bacterial cells were not visualized (Figure A.1. A). A population of macrophage cells contained deformed bacterial cells with released fluorescent fragments (Fig. A.1. B). As time increased, less whole bacterial cells were present inside the macrophage while more fragments appeared (Figure A.2). This labeling method allows selective tracking of the bacterial cell consumption and specific visualization of glycan units of PG upon macrophage infection, which can be used in future studies toward the identification and characterization of naturally occurring immunostimulatory NAM-containing PG fragments.

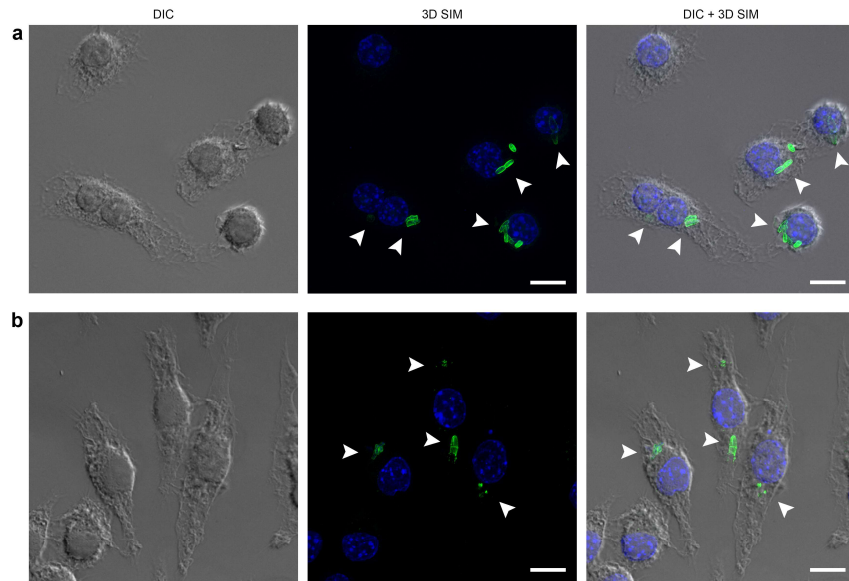


**Figure A.1: J774 mouse macrophage cells infected with labeled *E. coli*  $\Delta$ MurQ-KU cells.** (A) *E. coli*  $\Delta$ MurQ-KU cells pre-treated with **3** for 45 min were then used to infect J774 cells for 1 h. Cells were fixed and Az488 was clicked into remodeled bacterial peptidoglycan (green). Whole bacterial cells were visualized as shown with white arrows. Cellular DNA was labeled with DAPI (blue) (scale bar, 10  $\mu$ m). (B) Cells treated as in (a) in which deformed bacterial cells with released fluorescent fragments were visualized as shown with white arrows. Fluorescent images are maximum intensity projections of z-stacks. Three-dimensional renderings are provided in Supplementary Videos S6 and S8. Images are representative of a minimum of 3 fields viewed per replicate with at least 2 technical replicates and infection experiments were conducted in at least 3 biological replicates. (Reprinted with permission from Liang and DeMeester et. al., Copyright 2017, Nature Communications)

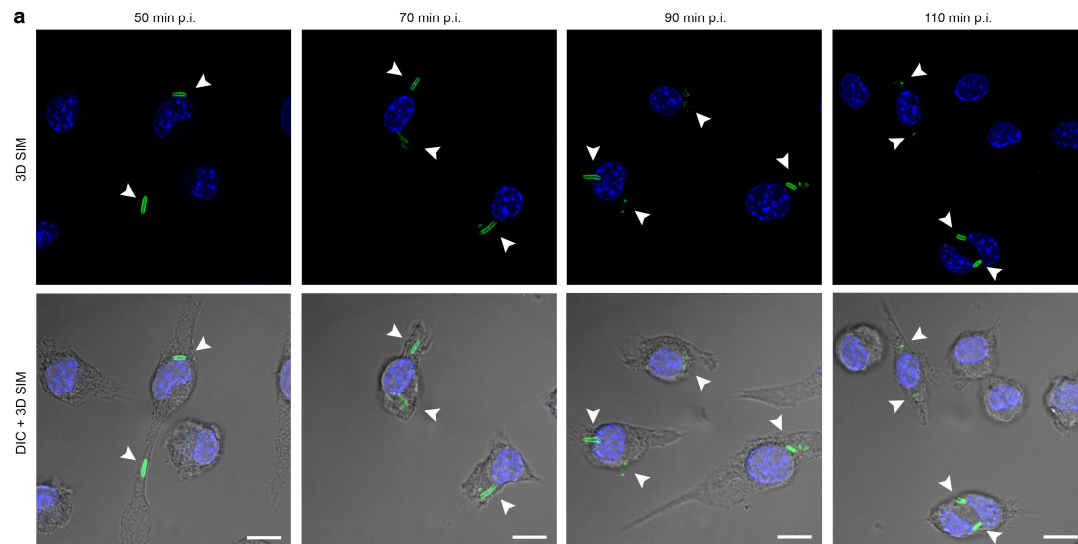


**Figure A.2: Time course study of J774 macrophage invasion.** *E. coli*  $\Delta$ MurQ KU cells pre-treated with **3** for 45 min were then used to infect J774 cells for 20, 40, 60 or 80 minutes. Macrophage cells were treated with gentamycin for an additional 30 min. then collected at total time points 50, 70, 90 and 110 min post infection (p.i.). Cells were fixed and Az488 was clicked into remodeled bacterial peptidoglycan (green). DAPI (blue) was used for cellular DNA staining. Three-dimensional SIM imaging (top) and DIC + 3-D SIM overlay (bottom) are shown. Arrowheads point to corresponding labeled bacterial cells or fragments. Images shown are one representative field for each time point (scale bars, 10  $\mu$ m). Fluorescent images are maximum intensity projections of z-stacks. Images are representative of a minimum of 3 fields viewed per replicate with at least 2 technical replicates and the experiment was conducted in at least 3 biological replicates. (Reprinted with permission from Liang and DeMeester et. al., Copyright 2017, Nature Communications)

**Appendix B**  
**PERMISSION LETTERS**



# RightsLink®

[Home](#)
[Account Info](#)
[Help](#)


**Title:** Identification and biological consequences of the *O*-GlcNAc modification of the human innate immune receptor, Nod2

**Author:** Hou, Ching-Wen; Mohanan, Vishnu

Logged in as:  
Ching-Wen Hou  
Account #:  
3001172728

[LOGOUT](#)

**Publication:** Glycobiology  
**Publisher:** Oxford University Press  
**Date:** 2015-09-14

Copyright © 2015, Oxford University Press

## Order Completed

Thank you for your order.

This Agreement between Ching-Wen Hou ("You") and Oxford University Press ("Oxford University Press") consists of your license details and the terms and conditions provided by Oxford University Press and Copyright Clearance Center.

Your confirmation email will contain your order number for future reference.

### [Printable details.](#)

License Number	4147800591463
License date	Jul 14, 2017
Licensed Content Publisher	Oxford University Press
Licensed Content Publication	Glycobiology
Licensed Content Title	Identification and biological consequences of the <i>O</i> -GlcNAc modification of the human innate immune receptor, Nod2
Licensed Content Author	Hou, Ching-Wen; Mohanan, Vishnu
Licensed Content Date	Sep 14, 2015
Licensed Content Volume	26
Licensed Content Issue	1
Type of Use	Thesis/Dissertation
Requestor type	Author of this OUP content
Format	Print and electronic
Portion	Abstract
Will you be translating?	No
Order reference number	
Title of your thesis / dissertation	THE SWEET MODIFICATION OF NOD2, AN INNATE IMMUNE RECEPTOR INVOLVED IN CROHN'S DISEASE
Expected completion date	Aug 2017
Estimated size(pages)	130
Requestor Location	Ching-Wen Hou

	<div>Attn: Ching-Wen Hou</div>
Publisher Tax ID	GB125506730
Billing Type	Invoice
Billing address	Ching-Wen Hou
	<div>Attn: Ching-Wen Hou</div>
Total	0.00 USD

[ORDER MORE](#)

[CLOSE WINDOW](#)

Copyright © 2017 [Copyright Clearance Center, Inc.](#) All Rights Reserved. [Privacy statement.](#) [Terms and Conditions.](#)  
Comments? We would like to hear from you. E-mail us at [customercare@copyright.com](mailto:customercare@copyright.com)



# RightsLink®

[Home](#)
[Account Info](#)
[Help](#)


**Title:** Identification and biological consequences of the *O*-GlcNAc modification of the human innate immune receptor, Nod2

**Author:** Hou, Ching-Wen; Mohanan, Vishnu

**Publication:** Glycobiology

**Publisher:** Oxford University Press

**Date:** 2015-09-14

Copyright © 2015, Oxford University Press

Logged in as:  
Ching-Wen Hou  
Account #:  
3001172728

[LOGOUT](#)

## Order Completed

Thank you for your order.

This Agreement between Ching-Wen Hou ("You") and Oxford University Press ("Oxford University Press") consists of your license details and the terms and conditions provided by Oxford University Press and Copyright Clearance Center.

Your confirmation email will contain your order number for future reference.

### [Printable details.](#)

License Number	4147800808462
License date	Jul 14, 2017
Licensed Content Publisher	Oxford University Press
Licensed Content Publication	Glycobiology
Licensed Content Title	Identification and biological consequences of the <i>O</i> -GlcNAc modification of the human innate immune receptor, Nod2
Licensed Content Author	Hou, Ching-Wen; Mohanan, Vishnu
Licensed Content Date	Sep 14, 2015
Licensed Content Volume	26
Licensed Content Issue	1
Type of Use	Thesis/Dissertation
Requestor type	Author of this OUP content
Format	Print and electronic
Portion	Text Extract
Number of pages requested	5
Will you be translating?	No
Order reference number	
Title of your thesis / dissertation	THE SWEET MODIFICATION OF NOD2, AN INNATE IMMUNE RECEPTOR INVOLVED IN CROHN'S DISEASE
Expected completion date	Aug 2017
Estimated size(pages)	130



Requestor Location	Ching-Wen Hou [REDACTED]
	[REDACTED]
	United States Attn: Ching-Wen Hou
Publisher Tax ID	GB125506730
Billing Type	Invoice
Billing address	Ching-Wen Hou [REDACTED]
	[REDACTED]
	United States Attn: Ching-Wen Hou
Total	0.00 USD

[ORDER MORE](#)[CLOSE WINDOW](#)

Copyright © 2017 [Copyright Clearance Center, Inc.](#) All Rights Reserved. [Privacy statement](#). [Terms and Conditions](#).  
Comments? We would like to hear from you. E-mail us at [customercare@copyright.com](mailto:customercare@copyright.com)



# RightsLink®

[Home](#)
[Account Info](#)
[Help](#)


**Title:** Identification and biological consequences of the O-GlcNAc modification of the human innate immune receptor, Nod2

**Author:** Hou, Ching-Wen; Mohanan, Vishnu

**Publication:** Glycobiology

**Publisher:** Oxford University Press

**Date:** 2015-09-14

Copyright © 2015, Oxford University Press

Logged in as:  
Ching-Wen Hou  
Account #:  
3001172728

[LOGOUT](#)

## Order Completed

Thank you for your order.

This Agreement between Ching-Wen Hou ("You") and Oxford University Press ("Oxford University Press") consists of your license details and the terms and conditions provided by Oxford University Press and Copyright Clearance Center.

Your confirmation email will contain your order number for future reference.

### [Printable details.](#)

License Number	4147800726768
License date	Jul 14, 2017
Licensed Content Publisher	Oxford University Press
Licensed Content Publication	Glycobiology
Licensed Content Title	Identification and biological consequences of the O-GlcNAc modification of the human innate immune receptor, Nod2
Licensed Content Author	Hou, Ching-Wen; Mohanan, Vishnu
Licensed Content Date	Sep 14, 2015
Licensed Content Volume	26
Licensed Content Issue	1
Type of Use	Thesis/Dissertation
Requestor type	Author of this OUP content
Format	Print and electronic
Portion	Figure/table
Number of figures/tables	4
Will you be translating?	No
Order reference number	
Title of your thesis / dissertation	THE SWEET MODIFICATION OF NOD2, AN INNATE IMMUNE RECEPTOR INVOLVED IN CROHN'S DISEASE
Expected completion date	Aug 2017
Estimated size(pages)	130
Requestor Location	Ching-Wen Hou

Publisher Tax ID  
Billing Type  
Billing address

United States  
Attn: Ching-Wen Hou  
GB125506730  
Invoice  
Ching-Wen Hou

Total

NEWARK, DE 19713  
United States  
Attn: Ching-Wen Hou  
0.00 USD

[ORDER MORE](#)

[CLOSE WINDOW](#)

Copyright © 2017 [Copyright Clearance Center, Inc.](#) All Rights Reserved. [Privacy statement](#). [Terms and Conditions](#).  
Comments? We would like to hear from you. E-mail us at [customer@copyright.com](mailto:customer@copyright.com)



RightsLink®

[Home](#)[Account Info](#)[Help](#)ACS Publications  
Most Trusted. Most Cited. Most Read.**Title:** Redefining the Defensive Line:  
Critical Components of the  
Innate Immune System**Author:** Ching-Wen Hou, Mackenzie L.  
Lauro, Catherine Leimkuhler  
Grimes**Publication:** ACS Infectious Diseases**Publisher:** American Chemical Society**Date:** Nov 1, 2016

Copyright © 2016, American Chemical Society

Logged in as:  
Ching-Wen Hou[LOGOUT](#)**PERMISSION/LICENSE IS GRANTED FOR YOUR ORDER AT NO CHARGE**

This type of permission/license, instead of the standard Terms & Conditions, is sent to you because no fee is being charged for your order. Please note the following:

- Permission is granted for your request in both print and electronic formats, and translations.
- If figures and/or tables were requested, they may be adapted or used in part.
- Please print this page for your records and send a copy of it to your publisher/graduate school.
- Appropriate credit for the requested material should be given as follows: "Reprinted (adapted) with permission from (COMPLETE REFERENCE CITATION). Copyright (YEAR) American Chemical Society." Insert appropriate information in place of the capitalized words.
- One-time permission is granted only for the use specified in your request. No additional uses are granted (such as derivative works or other editions). For any other uses, please submit a new request.

[BACK](#)[CLOSE WINDOW](#)

Copyright © 2017 [Copyright Clearance Center, Inc.](#) All Rights Reserved. [Privacy statement.](#) [Terms and Conditions.](#)  
Comments? We would like to hear from you. E-mail us at [customercare@copyright.com](mailto:customercare@copyright.com)



RightsLink®

Home

Create  
Account

Help



**Title:** Metabolic labelling of the carbohydrate core in bacterial peptidoglycan and its applications

**Author:** Hai Liang, Kristen E. DeMeester, Ching-Wen Hou, Michelle A. Parent, Jeffrey L. Caplan et al.

**Publication:** Nature Communications

**Publisher:** Nature Publishing Group

**Date:** Apr 20, 2017

Copyright © 2017, Rights Managed by Nature Publishing Group

LOGIN

If you're a [copyright.com](#) user, you can login to RightsLink using your copyright.com credentials. Already a [RightsLink](#) user or want to [learn more?](#)

### Creative Commons

The article for which you have requested permission has been distributed under a Creative Commons CC-BY license (please see the article itself for the license version number). You may reuse this material without obtaining permission from Nature Publishing Group, providing that the author and the original source of publication are fully acknowledged, as per the terms of the license. For license terms, please see <http://creativecommons.org/>

CLOSE WINDOW

Are you the [author](#) of this NPG article?

To order reprints of this content, please contact Springer Healthcare by e-mail: [reprintswarehouse@springer.com](mailto:reprintswarehouse@springer.com), and you will be contacted very shortly with a quote.

Copyright © 2017 [Copyright Clearance Center, Inc.](#) All Rights Reserved. [Privacy statement](#). [Terms and Conditions](#). Comments? We would like to hear from you. E-mail us at [customer@copyright.com](mailto:customer@copyright.com)